DIGITAL DENTISTRY:
Simplifying the Workflow via 3D Modeling and Artificial Intelligence Assistance

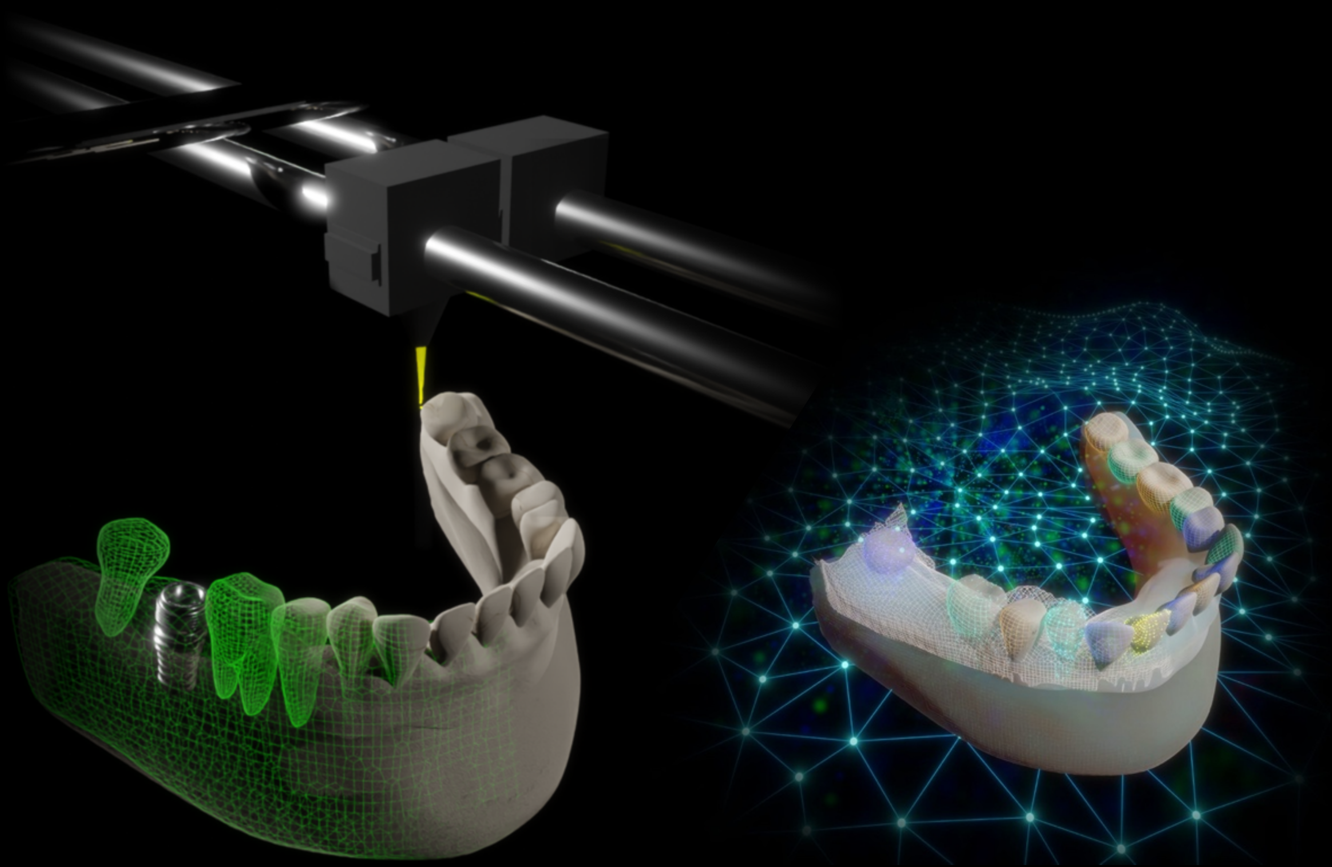

Xiaotong Wang

2023

KU Leuven
Biomedical Sciences Group
Faculty of Medicine
Department of Imaging and Pathology

KU LEUVEN

DOCTORAL SCHOOL
BIOMEDICAL SCIENCES

DIGITAL DENTISTRY:

SIMPLIFYING THE WORKFLOW VIA 3D MODELING AND ARTIFICIAL INTELLIGENCE ASSISTANCE

Xiaotong Wang

Dissertation presented in partial fulfilment of the requirements for the degree of Doctor in Biomedical Sciences

Jury:

Supervisor: Prof. dr. Reinhilde Jacobs
Co-supervisor: Dr. Eman Shaheen
Dr. Sohaib Shujaat
Chair examining committee: Prof. dr. Steven Dymarkowski
Chair public defence: Prof. dr. Philippe Demaerel
Jury members: Prof. dr. Andy Temmerman
Dr. Kostas Syriopoulos
Prof. dr. Kathrin Becker
Dr. Charbel Bou Serhal

May 2023

KU Leuven
Groep Biomedische Wetenschappen
Faculteit Geneeskunde
Departement Beeldvorming en Pathologie

DOCTORAL SCHOOL
BIOMEDICAL SCIENCES

DIGITALE TANDHEELKUNDE:

VEREENVOUDIGING VAN DE WORKFLOW VIA 3D MODELLERING EN KUNSTMATIGE INTELLIGENTIE ONDERSTEUNING

Xiaotong Wang

Proefschrift voorgedragen tot het behalen van de graad van Doctor in de Biomedische Wetenschappen

Jury:

Promotor: Prof. dr. Reinhilde Jacobs
Co-promotor: Dr. Eman Shaheen
Dr. Sohaib Shujaat
Voorzitter leescommissie: Prof. dr. Steven Dymarkowski
Voorzitter openbare verdediging: Prof. dr. Philippe Demaerel
Juryleden: Prof. dr. Andy Temmerman
Dr. Kostas Syriopoulos
Prof. dr. Kathrin Becker
Dr. Charbel Bou Serhal

Mei 2023

Preface

This PhD thesis is composed of 6 research articles, preceded with a general introduction and summarized with a general discussion. The articles follow the standard IMRAD format (Introduction, Materials and Methods, Results and Discussion) and were based on peer-reviewed publications:

Article 1

Wang X, Shujaat S, Shaheen E, Jacobs R. Accuracy of desktop versus professional 3D printers for maxillofacial model production. A systematic review and meta-analysis. J Dent. 2021 Sep;112:103741. doi: 10.1016/j.jdent.2021.103741.

Article 2

Wang X, Shujaat S, Shaheen E, E Ferraris, Jacobs R. Trueness of cone-beam computed tomography-derived skull models fabricated by different technology-based three-dimensional printers. BMC Oral Health. (Accepted)

Article 3

Wang X, Shujaat S, Shaheen E, Jacobs R. Quality and haptic feedback of three-dimensionally printed models for simulating dental implant surgery. J Prosthet Dent. 2022 May;S0022-3913(22)00201-3. doi: 10.1016/j.prosdent.2022.02.027.

Article 4

Wang X, Shaheen E, Shujaat S, Meeus J, Legrand P, Lahoud P, Gerhardt M, Politis C, Jacobs R. Influence of experience on dental implant placement. An in vitro comparison of freehand, static guided and dynamic navigation approaches. Int. J. Implant Dent. 2022 Oct;8(1):42. doi: 10.1186/s40729-022-00441-3.

Article 5

Wang X, Shujaat S, Meeus J, Shaheen E, Legrand P, Lahoud P, Gerhardt M, Jacobs R. Performance of novice versus experienced surgeons for dental implant placement with freehand, static guided and dynamic navigation approaches. Sci Rep. 2023 Feb;13(1):2598.

Article 6

Wang X, Alqahtani K, Bogaert T, Shujaat S, Jacobs R, Shaheen E. Convolutional neural network for automated tooth segmentation on intraoral scans. Clin. Oral Investig. (Accepted)

Personal acknowledgements

First and foremost, I'd like to sincerely thank my supervisor, **Prof. Reinhilde Jacobs**, for her invaluable support, guidance, and encouragement throughout my PhD journey. Her expertise and vast knowledge have been invaluable in shaping my research and professional development.

Second, I'd like to express my deep gratitude to my co-promoters, **Dr. Eman Shaheen** and **Dr. Sohaib Shujaat**, for their support and mentorship throughout my academic life. Their guidance and support have been instrumental in the completion of my research.

Further, I would like to show my thankfulness to all of those who supported and helped me during my PhD life, especially **Prof. Paul Legrand**, **Dr. Jan Meeus**, **Prof. Eleonora Ferraris**, and **the ReLu team** for their expertise and assistance in my research. Their contributions have been crucial in the success of my project.

In addition, I'd like to thank my friends and colleagues in the OMFS-IMPATH Research Group as well as all the friends I made in Belgium for their friendship, support, and encouragement throughout my PhD journey.

Special thanks to my supervisor **Prof. Xiaohui Jiao** from Harbin Medical University, his guidance and support throughout my research journey and clinical practice have been invaluable.

Most of all, I wish to express my thankfulness to my mom and dad (**Zhenjuan** & **Fengqi**), and my loving husband (**Yongyu**) for their love and support throughout the past four years. They have been my constant source of motivation and inspiration, and their belief in me has been the driving force for my achievement.

Lastly, I am grateful that **China Scholarship Council (CSC)** offered me the financial assistance to complete my studies during these challenging times of COVID-19.

'The best way to predict the future is to create it' - Abraham Lincoln

Table of Contents

List of Abbreviations

2D	Two-dimensional
3D	Three-dimensional
3DP	Three-dimensional printing
A-AI	Automated artificial intelligence
AI	Artificial intelligence
ABS	Acrylonitrile-butadiene-styrene
AM	Additive manufacturing
ANOVA	One-way analysis of variance
BJ	Binder jetting
CAD-CAM	Computer aided design/Computer aided manufacturing
CBCT	Cone-beam computed tomography
CNN	Convolutional neural network
DICOM	Digital imaging and communications in medicine
DL	Deep learning
DN	Dynamic navigation
DSC	Dice similarity coefficient
FDM	Fused filament fabrication
FH	Freehand
FOV	Field of view
FN	False negatives
FP	False positives
HU	Hounsfield units
JBI	Joanna Briggs Institute
MAE	Mean absolute error
MJ	Material jetting
ML	Machine learning
OR	Odds ratio
PC	Poly-carbonate
PEEK	Polyether ether ketone
PETG	Polyethylene terephthalate
PLA	Polylactic acid
PMMA	Polymethylmethacrylate
PPG	Pilot drill-based partial guidance
ICC	Intra-class correlation coefficient
IOS	Intraoral scanned

IoU	Intersection over union
R-AI	Refined artificial intelligence
RMS	Root mean square
RP	Rapid prototyping
RVD	Relative volume difference
SA	Semi-automatic
SD	Standard deviation
SDL	Selective deposition lamination
SLA	Stereolithography
SLM	Selective laser melting
SLS	Selective laser sintering
STL	Standard tessellation language
TN	True negatives
TP	True positives
UDMA	Urethane dimethacrylate
UV	Ultraviolet
V	Vertical

General Introduction

Aims & Hypotheses

Digital technology is an innovative approach to dentistry. Digital dentistry is the computerization of the dental treatment process, which includes digitizing patient management, Computer aided design/computer aided manufacturing (CAD-CAM), three-dimensional printing (3DP), computer-assisted surgery, artificial intelligence (AI), augmented and virtual reality, robotics, and other technologies (**Fig. 1**). The advancements in technology allow for accurate and efficient performance, which benefits patients and clinicians. Due to the rise of digital technologies in the field of dentistry, dental practices have transitioned their workflow from using conventional treatment methods to one that uses digital technology [1, 2].

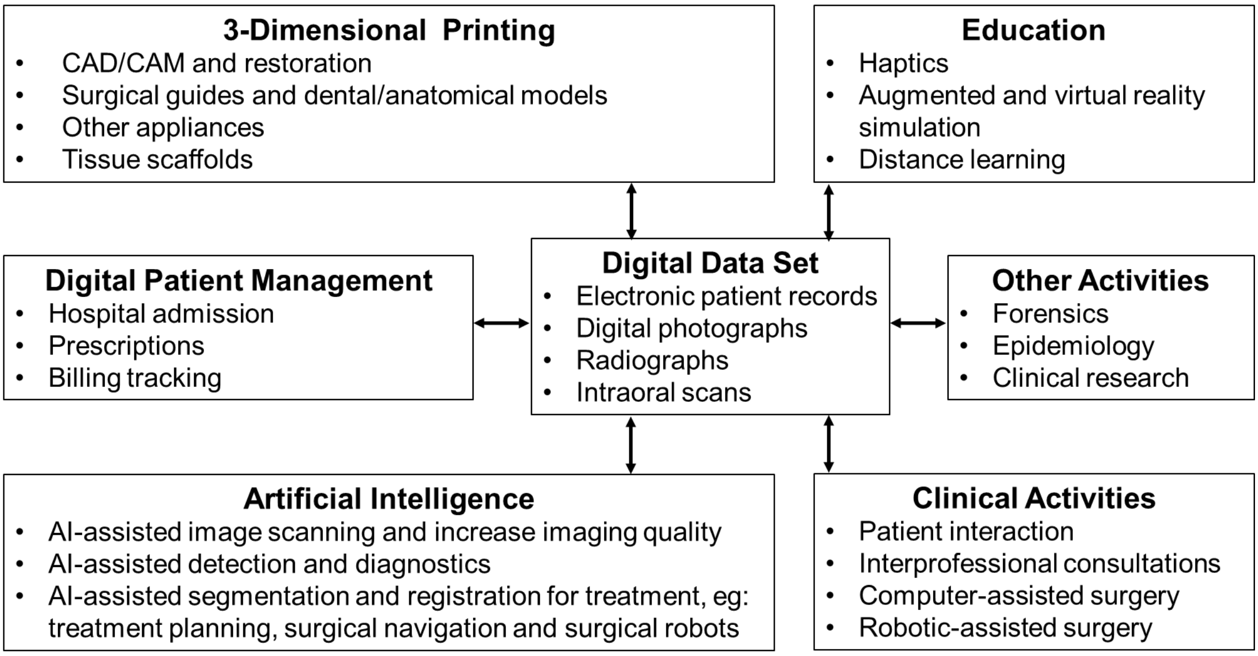

Figure 1. The reach of digital dentistry.

Digital workflows have been mostly employed in the dentistry field ranging from implantology, prosthodontics and orthodontics to oral and maxillofacial surgery. This enables accurate diagnostics, functionally driven planning, computer-assisted treatment execution and follow-up examination [3, 4].

Digital patient management includes, but is not limited to, hospital admission, electronic patient medical records, prescriptions, and billing tracking.

CAD/CAM system have revolutionized the design and manufacture of restorations. CAD/CAM technology enables faster manufacturing times and customized production with high precision. It consists of three phases: data acquisition, computer data processing and manufacturing using 3DP or milling [5, 6].

1. 3DP

3DP, also known as rapid prototyping (RP) or additive manufacturing (AM) , is a manufacturing technique that uses CAD software to reconstruct a 3D digital model, created layer by layer on a 3D printer [7]. This revolutionary technology enables the production of working models, implant surgical guides, orthodontic appliances, prosthodontic restorations, and maxillofacial prostheses [8].

1.1 3DP applications

1.1.1 Applications in Prosthodontics

3D printing technology has drawn a substantial amount of attention in the prosthodontic dentistry field due to its personalized, digital and high precision features. It enables the creation of a range of dental restorations, including temporary restorations, complete and partial dentures, crowns, and bridges [9]. It is expected to replace most of the conventional restorative techniques and has a promising application in the fields of restorative manufacturing and aesthetic restoration [10, 11].

1.1.2 Applications in Oral and Maxillofacial Surgery

3DP enables the creation of anatomical models and surgical guides for reconstructive surgery. The biggest advantage of using 3DP for jaw reconstruction is that it completely eliminates the disadvantages of conventional surgery, which depends on the surgeon's expertise. The digital design, precise excision and personalized repair can contribute to more accurate surgery and satisfactory surgical outcomes. In addition, the time of the surgical operation is decreased when 3DP is used instead of conventional procedures. A 3D printed model of the patient's anatomy can be utilized for preoperative reconstructive plate bending, surgical simulation, and patient communication [12].

In maxillofacial surgery, soft and hard tissue deformities caused by congenital diseases, trauma, and tumors are common. 3D printing technology offers a more personalized approach to jaw and facial rehabilitation compared to conventional techniques. This technology enables the creation of custom-fit prostheses for defects in the jaw, nasal bone, and maxillofacial region [13].

Osteotomy guides and occlusal splints, which enable more precise jaw positions in accordance with the virtual planning and reduce complications, are two orthognathic surgery devices that benefit from 3D printing [14].

1.1.3 Applications in Dental Implantology

3D printing has numerous applications in dental implantology, including surgical guides, implants, and bone augmentation procedures. The surgical guides enhance accuracy and reduce variability due to the surgeon's skill. Customized 3D printed implants improve stability through stronger osseointegration with the alveolar bone and more closely replicate the stress distribution of natural teeth. The success rate of implant surgery for people with insufficient bone volume in the implant location is significantly increased by the utilization of 3D printed personalized bone grafts, customized titanium mesh, and bone reconstruction guides [14].

1.1.4 Applications in Orthodontics

3D printing technology has met the increasing demand for precision, comfort, and personalized orthodontic care by allowing the fabrication of dental casts, customized brackets, bonding trays, and appliances that are tailored to the patient's specific intraoral condition. Guides for orthodontic mini implants are created using techniques similar to those used in implant dentistry. While the traditional method for making aligners involves thermoforming based on 3D-printed casts, there is now the option to directly print aligners using 3D printing technology [5, 14].

1.1.5 Applications in Endodontics

In endodontics, 3D printing is widely used for pulp access guidance, calcified root canal positioning, creating extra-apical guide plates, etc [15].

1.1.6 Applications in dental education

The realistic 3D printed models have been applied in dental anatomy theoretical teaching or clinical training. Anatomical models can be used for educational purposes to improve understanding of organ structure. Additionally, 3D-printed models are produced for surgical training and simulation. 3D-printed teeth are used for preclinical training such as caries excavation, root canal therapy and crown preparation, and have resolved the issue of insufficient extracted natural teeth [7, 16].

1.2 Cost of 3DP

Due to financial limitations, installing dental 3D printing equipment may not be practical for small and medium-sized dental clinic. As the majority of dental clinics are small to medium sized, this poses a significant challenge for the market. For advanced image processing and 3D modeling in medical and engineering fields, Mimics, a widely used FDA-approved software is relatively expensive, while less expensive solutions, like the FDA-approved OsiriX is available. Free software, like 3D Slicer, can only be used with properly approved study protocols. On the other hand, the commercial software designed for digital workflow in dental practices are generally reasonably priced, such as Onyx-Ceph for orthodontics and implant studio for guided implant placement. A wide variety of 3D printers exist on the market, which can be further classified as desktop and professional 3D printers. While professional printers are priced between $20,000 and $200,000, desktop printers ranged in price from $1500 to $7,000 [17, 18]. In terms of cost, it is also necessary to take labor costs, material costs, and 3D printer maintenance into account. Due to budgetary constraints, many smaller dental practices may choose to outsource manufacturing to a commercial external printing service center. In this instance, however, the speed offered by 3D printing might be significantly reduced as delivery time increase, with parts taking days or weeks to arrive at their destination. Therefore, for small and medium-sized end users, the expenses generally outweigh the benefits of 3D printing, however certain large clinics and hospitals may be able to purchase 3D printers at reasonable prices and receive the full benefits of mass production [19]. Nowadays, the accessibility and affordability of equipment and software for printing of casts and CAD-CAM design have improved with technological advancements. As a result, many dental offices are now utilizing this technology to produce precise and customized restorations in-house, instead of outsourcing to a dental laboratory. This approach provides greater control over the final product, faster turnaround times, and cost savings for both the dental office and the patient. Nevertheless, if the objective of printing surpasses the printer's capacities, such as producing intricate dental products, 3D printing with metals, or fabricating specialized anatomical structures, outsourcing may still be indispensable.

Lack of trained operators is another main obstacle to the widespread use of 3D printing. To effectively integrate additive manufacturing into design and production, trained operators are necessary. Employees with 3D printing expertise are pretty scarce, and this is further exacerbated by the rapid technological and material advancements in the market for dental 3D printing. Training programs available for additive manufacturing are scarce, and the large gap between academia and practical applications is pervasive in the medical field and difficult to bridge [19].

With the technological advancements of 3DP, low-cost desktop 3D printers may be an alternative [20]. They can produce clinical acceptable temporary crowns [21], trays and prototypes for denture try-ins [22], dental models [23], and anatomical models, such as mandible [24, 25], orbital wall [26] and maxilla [27]. Therefore, it is important to assess whether the low-cost printers could offer comparable accuracy to that of high-cost printers.

1.3 Accuracy of 3DP

1.3.1 Factors affecting accuracy of 3DP

Both accuracy and precision are important factors to consider when assessing the quality of a 3D printed model. Precision refers to how consistent multiple 3D printed models are with each other. Precision is influenced by various factors, such as the 3D printer's resolution, the quality of the printing material, and the repeatability of the printing process. The accuracy of a printed object refers to how closely its size and form correspond to the original design model. Accuracy can be impacted by accuracy assessment technique and every step of the 3DP procedure, including data collection, computer data processing (including segmentation and standard tessellation language (STL) processing), model fabrication, and post-processing (**Fig. 2**) [28].

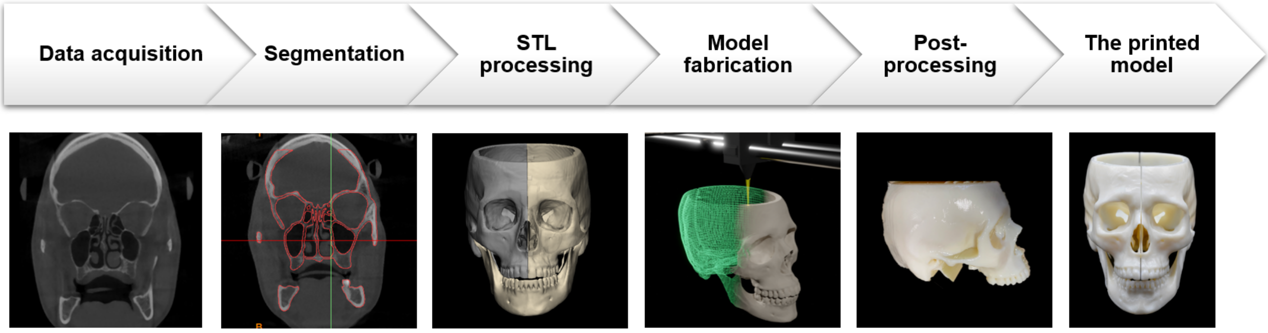

Figure 2. 3D printing of maxillofacial skeletal models

Data acquisition is the first and critical step of 3D printing. The succeeding steps of 3D reconstruction and printing can only be carried out successfully if accurate data information is collected. Spatial resolution, contrast to noise ratio, and artifact all have an impact on image data quality; for example, a thick slice thickness that is unable to capture fine feature details results in low spatial resolution. Accurate segmentation depends on the image's quality; for example, high contrast between regions makes segmentation relatively easy, while metal artifacts make it difficult [29].

Medical image segmentation and STL post-processing are components of computer data processing in 3D printing. The goal is to separate the desired organ from surrounding anatomy and prepare the 3D object for printing. Segmentation starts with the patient's Digital Imaging and Communications in Medicine (DICOM) images. Based on the method used, segmentation is categorized into three types: automatic, manual, and semi-automatic. Threshold-based segmentation is the most common approach, however, it has the potential to produce inaccurate results due to errors related to the selected threshold and the usage of manual segmentation when necessary [28]. Following segmentation, the data is frequently recorded in the STL file format, which converts all surfaces and curves into a mesh consisting of a series of triangles. The STL files are then optimized to be prepared for printing, such as by removing undesirable edges or the design of specialized molds. The wrapping and smoothing processes may affect accuracy while perhaps improving the model's appearance. Therefore, it is essential to verify the accuracy before printing by superimposing the finished STL file over the original image [30].

Model fabrication is the process of choosing the appropriate material for the product requirements and setting the printing parameters. The STL file model will be "sliced" into a number of cross-sectional files by 3D printing software, which will then save them and establish the print volume and path for the 3D printer. After the object is printed, a series of post-processing steps are required, such as cleaning with chemical solutions, removing the support material and sanding. Since some of these operations are typically performed manually, human error is always a possibility [28].

The accuracy of a 3D printed product is influenced by multiple factors in the modeling process, including the 3D printing technique used, printing parameter settings, material choice, and model design [16]. Accuracy varies dependent on the 3D printing technique (**Fig. 3**).

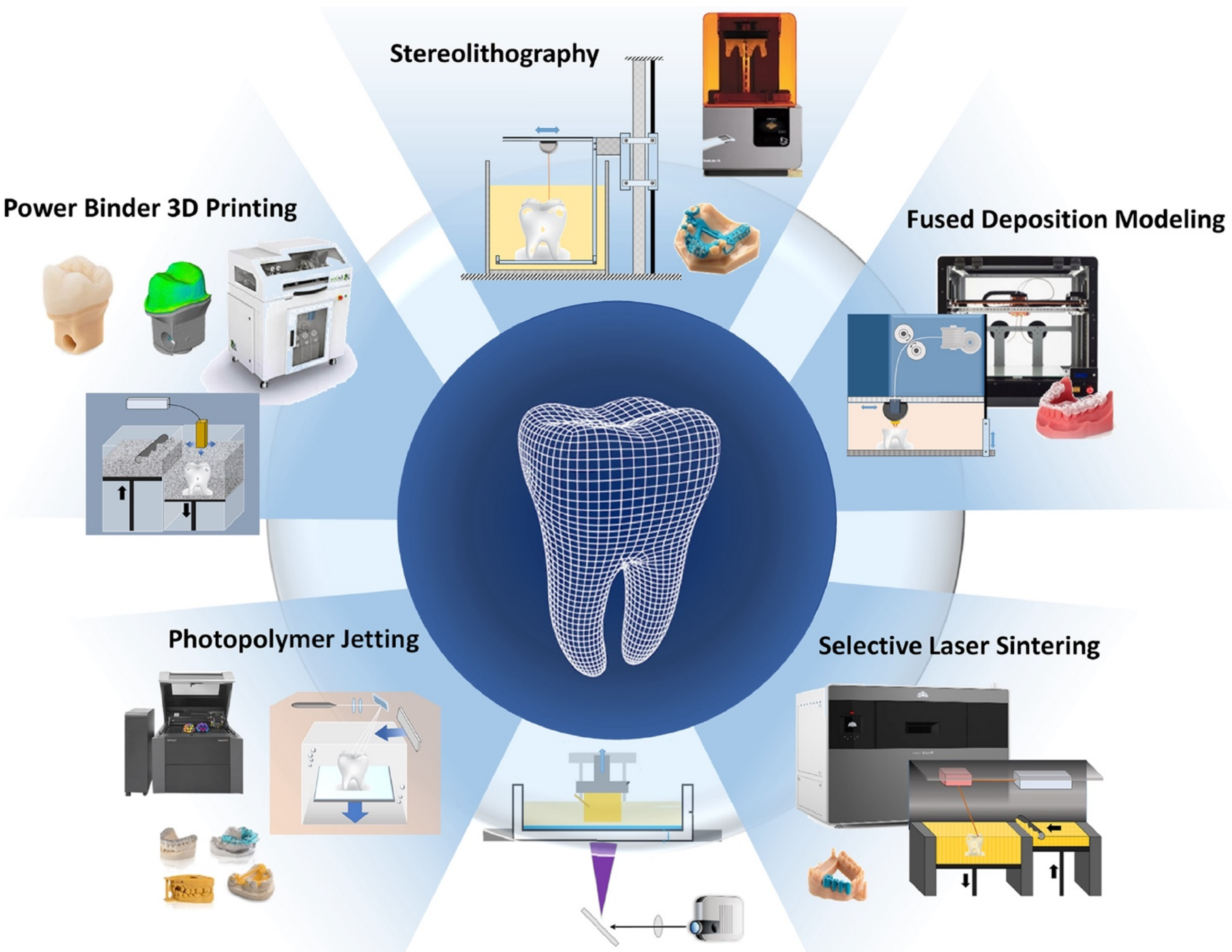

Figure 3. Current 3D printing techniques used in dentistry. Images are reproduced from [8] with permission from Elsevier.

The first 3D printing technology utilized for commercial purposes was Stereolithography (SLA), which uses an ultraviolet (UV) laser to polymerize a photo-sensitive liquid resin. The build platform is submerged in the resin and each layer is cured, causing it to move a distance equivalent to its layer thickness and form the next layer, leading to the complete printing of an object. Digital Light Processing (DLP) is similar to SLA as it also uses curing, polymerization, and building processes, but instead of a laser, a digital projector serves as the light source [31]. In comparison to DLP, the differential curing technique of SLA results in greater accuracy and better quality, while the DLP method speeds up production. Photopolymer printing technologies such as SLA and DLP have an accuracy of approximately ±0.15 mm. The amount of detail increases as laser beam diameter decreases. The speed of printing decreases with the diameter of the laser beam increases, but the workpiece's accuracy and fineness suffer [5].

The second most common 3D printing technology, fused filament fabrication (FFF) or fused deposition modeling (FDM), is an affordable option. A strand of thermoplastic material is fed into an extruder, heated and melted material is squeezed out of a nozzle and layered to build a final product. Some of the most frequently used filaments in FDM are polylactic acid (PLA), acrylonitrile-butadiene-styrene (ABS), polycarbonate, and polyamide. Its typical accuracy is about ±0.5 mm. The processing time is slightly longer since the nozzle's mechanical movement has a speed limit [32]. The width of the extruded filament in FFF 3D printing is determined by the diameter of the nozzle, with a range of 0.1-0.4 mm affecting the precision of the final product. The printing temperature involves the temperature of the printhead and the bed temperature. The bonding, stacking, and flowability characteristics of the material are primarily impacted by the extrusion head heating temperature. Excessive temperature during 3D printing can cause the material to come out as a liquid instead of a controlled filament form, whereas a low temperature may hinder the material from adhering to the bed or separating between layers, leading to nozzle blockage [33- 35].

Selective laser sintering (SLS) utilizes a laser to fuse powders, including metal, ceramic, and polymer, into a solid object. The powder spreader spreads the powder layer by layer on the working table, and then the powder is flattened and compacted by the roller. The thickness of each layer of powder corresponds to the thickness of the slice of the CAD model. Each layer of powder is selectively sintered onto the substrate by the CO_2 laser, while the powder not scanned and sintered by the laser remains in place for support until the entire part is sintered [14]. SLS has an accuracy of approximately ±0.2 mm.

Binder Jetting, also known as powder binder printing, ColorJet by 3D Systems, Multi Jet by HP, or 3DP by Z Corporation, involves using print heads to apply a liquid bonding agent to a bed of powder to form a solid layer [8].

Material Jetting or termed Photopolymer jetting (PolyJet) can allow objects to be printed using print heads to jet liquid resin droplets that can be cured by UV light. It is capable of printing with multi-material and multi-colour. The size of the jetted droplet determines the minimum feature size, which is 0.1-0.3 mm [1, 8].

According to the printer's setting range, users can customize the printing settings, including layer resolution, printing speed, filler, etc. These factors will have an effect on the accuracy; for instance, a quicker printing speed will result in a lower accuracy. In general, a thinner layer thickness is preferable because it produces a higher resolution [1].

The accuracy of 3D printing is impacted by the precision of movement of the printer's mechanical controls, which may deviate if they do not move as instructed by the software. Factors affecting this include the quality of the printer's components, how well it's assembled, manufacturing accuracy, and operational vibrations. In general, desktop 3D printers are less expensive and the mechanical performance of the controls differs between high-end and entry-level printers depending on the quality of the mechanical components [28, 30].

1.3.2 Accuracy of 3DP model

In 1994, a study was conducted by Barker et al. to evaluate the accuracy of an SLA 3D-printed skull [36]. The researchers compared the measurements of anatomical landmarks on cadaveric bones to those on 3D printed models and found an absolute difference of 0.85 mm, with a range from 0.1 mm to 4.62 mm [37]. Since then, similar experiments have been carried out to compare the accuracy of 3D printed models in various fields, including craniomaxillofacial and orthopedic, cardiac and vascular. The dimensional difference is generally smaller than 1 mm, although in some regions of the model or tissue segmentation, it can reach 4–6 mm [28, 30, 33].

Precise measurement techniques are necessary to determine the size of the 3D printed model. One way to do this is by comparing locations of landmarks on both the original and printed models, either manually with a caliper or using automated coordinate measurement. Manual measures with calipers are difficult to perform accurately due to operator variability, the distinct measured landmark locations, and the inability to measure non-linear anatomical structures. Automated coordinate-measuring can be programmed to measure landmark positions more accurately. However, only external measurements of the model can be made using either manual or automatic measurements [23, 38].

The alternative measurement technique involves scanning a printed model with a laser or optical device, using a CT scan, etc. to create a digitized STL model, and then aligning it with the original STL model [38]. The accuracy of a printed model is assessed by a color-coded comparison of the parts with the original model. This allows for the calculation of the mean error or mean absolute error (MAE) between the printed and original models [39]. The MAE quantifies the overall magnitude of the error, while the mean error shows the direction of the error: distinguishing between areas where the printed model is inside the original model (negative error) and areas where the printed model is outside the original model (positive error). George et al. recommend using MAE instead of mean error to avoid skewing the average difference due to the positive and negative errors in the original model [28].

1.4 Haptic feedback of 3DP training models

Dental hands-on training is essential for teaching dental students the skills and knowledge they need to succeed in their careers. Through hands-on practice, dental students can learn and refine complex procedures, such as tooth extraction and filling, without the risks and constraints of working on real patients [40].

Haptic feedback is a valuable tool for improving the effectiveness of hands-on training in dental education. Haptic feedback provides a safe and controlled learning environment for dental students to practice complex procedures by simulating realistic touch and force sensations [41]. Dental teaching models include cadavers, animals, synthetic models, virtual reality systems, and patient-specific 3D printed models. Each type of training model has advantages and disadvantages. Cadavers offer a realistic and detailed representation of human anatomy, but they are scarce and costly. Although animal models can provide similar haptic feedback to that of real bone, they could not be accurate representations of human anatomy and physiology. Synthetic models fabricated by manufactures are easily accessible, but they lack the realism and detail of cadavers and animals. Complex procedures can be simulated using virtual reality systems, but they could not provide the same level of haptic feedback as hands-on practice with physical models [42, 43]. Virtual reality surgical platform has potential to create independent learning management, independent simulation practice, and independent assessment functions, and the platform can become a new generation of virtual-reality integration of clinical skills teaching system. However, there are still many technical challenges in realizing a naturally interactive, highly immersive and easily accessible virtual reality medical system [44].

Patient-specific 3D printed models offer a customizable and affordable option, a training model providing both anatomy and haptics can enhance not only students' comprehension of dental anatomy, but also helps them develop manual dexterity and improve their clinical skills [45, 46]. Models that precisely mimic both the biomechanical and visual properties of human tissue are not currently available [47]. However, 3D printing of biomaterials is developing in the fields of tissue engineering, like degradable tissue engineering scaffolds, 3D printed in vitro bionic 3D biostructures, organs and organ regeneration [48]. Personalized biodegradable tissue engineering scaffolds will provide a new way to repair bone/ cartilage tissue, skin tissue, etc.; the development of bio-3D printed in vitro biomimetic bio-structures will be of great value for short time and high throughput screening of new drugs; bio-3D printed organ regeneration, if realized, will have profound implications for organ transplantation. However, due to the limitations of 3D printers, suitable 3D printed biomaterials are currently limited, and the quality needs to be further improved. This work may help discover materials that can be used to create products for anatomical teaching or surgical simulation [47].

Currently, many researchers are attempting to visually and haptically construct replicas that resemble real organs in the field of education. Each tissue and organ in the human body has distinct physical and mechanical characteristics. Different tissues and organs of the human body have their own unique physical and mechanical properties. From skin, muscle, cartilage to hard bone, the selection of materials corresponding to the tissue properties during 3D printing is required [47].

Depending on the usage, different materials can be employed for 3D printing manufacturing. The most commonly used 3DP materials are liquid, filament or powder based and consist of metals, ceramics, polymers, resins, and plastics. The main metallic materials include stainless steel alloys, cobalt-based alloy, titanium and its alloys. Zirconia and alumina are the two ceramic materials that are most frequently utilized. The most popular polymers are polycarbonate (PC), acrylonitrile-butadiene-styrene (ABS), polylactic acid (PLA), polymethylmethacrylate (PMMA) and polyether ether ketone (PEEK) [8].

Haffner et al. researched the 3D printed materials that best replicate the visual and tactile properties of the human temporal bone. They found that polyethylene terephthalate (PETG) had the most realistic feel, followed by polylactic acid (PLA), acrylonitrile butadiene styrene (ABS), poly-carbonate (PC), and nylon [49].

The mechanical properties (e.g. tensile strength and elastic modulus) of the 3D printed material should be in accordance with the biomechanical characteristics of the tissue [16, 37]. For 3D printed bones, there are two types: cortical bone and trabecular or cancellous bone, with different mechanical properties due to their different structures. Cancellous bone forms the inner part of the bone, while cortical bone is the outermost denser boundary. The mechanical characteristics of the tissue are impacted by each level of bone structure. One of the challenges of replicating bone for surgical teaching is to mimic trabecular bone [47]. The structure of bone would have to be replicated in order to mimic its haptic feedback and mechanical characteristics, particularly its elastic modulus and hardness, has not been achieved in dentistry yet [50].

2. Computer-assisted surgery

The demand for implant surgery has increased as it becomes more and more popular for oral rehabilitation. The complications of implant surgery have emerged as a significant factor influencing the implant long-term stability. The "standardized and accurate" implant treatment is essential for reducing complications and ensuring long-term stability, especially for inexperienced practitioners.

CT scans offer high resolution and are increasingly being used for preoperative diagnosis and implant planning. Cone-beam computed tomography (CBCT) is a cost-effective option that exposes patients to lower radiation levels compared to conventional CT scans. Implant planning software allows doctors to create 3D reconstructions of a patient's soft and hard tissues. The digital information data, such as CBCT scan data in DICOM format and intraoral scanned (IOS) data in STL format, is uploaded for 3D virtual reconstruction [51]. Thereafter, the surgeon can plan the implant placement by considering the restorative needs, using 3D models reconstructed from axial, coronal, and sagittal views. This helps the surgeon understand the anatomy of the jaws and determine the height and width of the alveolar bone at the edentate area. Computer-assisted surgery enables a precise transfer of the surgical planning for the virtual implant to the actual clinical surgical operation and assisting in the achievement of the expected accurate and aesthetically pleasing implant restoration results. The computer-assisted surgery is typically classified into static surgical guide and dynamic navigation system. The former acquires data from CBCT and converts it into a surgical guide that statically guides the implant surgery. The latter is a virtual implant planning design that dynamically realizes real-time position and navigates during implant surgery [52].

Computer-assisted surgery offers the following benefits:

1) Increased safety by preventing damage to important structures such as the maxillary sinus and mandibular canal, avoiding adjacent teeth, and enhancing operation safety. Computer-assisted implant surgery makes flapless implant placement possible, which lowers the risk of bleeding and postoperative morbidity, permits immediate loading to fulfill the patient's functional needs, shortens post-operative duration of discomfort, and improves the patient's satisfaction.
2) Precise placement of implants through preoperative planning and 3D positioning, leading to better aesthetic outcomes and improved superstructure fabrication.
3) In some cases, it may allow the use of existing bone, reducing the need for additional bone augmentation surgery and reducing operation time and follow-up visits [51].

2.1 Static surgical guide

Surgical guides are physical templates that are custom-made to fit the patient's jaw. The surgical guide helps in accurately transferring the virtual position of the planned implant to the actual surgical location during the procedure. They can be used to guide the drill and ensure that the implant is placed in the correct location. In addition to the benefits of computer-assisted surgery, there are also disadvantages to surgical guides:

1) Production of static surgical guides is costly and labor-intensive.
2) The guide's stability during the implant placement depends on the way the guide is supported (Bone-, Tooth- or Mucosa- Supported) and is directly impacted by the mucosa or bone protrusion.
3) When the implant site is close to the adjacent teeth, the conduit of the guide tends to interfere with the implant placement.
4) The implant plan cannot be temporarily adjusted, the guide prevents rinsing, and the guide is prone to heat generation during drilling.
5) The limited operable space in the area of molar makes it challenging to do the operation with direct vision, which reduces the operator's tactile sensitivity and leads to more angular deviation [52].

2.2 Dynamic navigation system

The navigation system provides real-time guidance by monitoring the movement of the drills and implant in line with the pre-planned virtual design. It utilizes pre-operative imaging data obtained from CT or CBCT scans to create a 3D representation of the patient's jaw and teeth. This information is then used to create a surgical plan. During the surgery, the navigation tracing mark is attached to the patient's jaw. An essential part of using a dynamic navigation system is calibration. It involves registering the navigation system with the patient's jaw using a series of landmarks, enabling the system to precisely align the jaw's position and provide accurate guidance. In order to use optical tracking to track the position of the surgical instruments, each instrument's navigation tracing mark must be calibrated prior to use. This information is then used to provide real-time guidance, showing the surgeon the precise location and angle for implant placement [53].

Numerous studies have shown that dynamic navigation can achieve good clinical results in solitary implants, implants in edentulous jaws, pterygomaxillary and zygomatic implants, etc [54, 56]. The benefits of using a dynamic navigation technique include:

1) Improved safety and predictability of the surgical procedure through real-time navigation during surgery.
2) Surgical plans can be adjusted and changed at any time during surgery.
3) Different implant systems can be used universally.
4) Thermal damage is less likely with more sufficient cooling than static guides.
5) Reduced requirements for mouth opening [51].

Limitations of the dynamic navigation system include:

1) The complex preoperative registration and calibration steps which can prolong the surgical time, and may require specialized training to use effectively.
2) To enable the acquisition of signals from various angles and to simplify operator operation, the design of the navigation handpiece marker and bone tracing marker should be more lightweight.
3) To prevent the need for recalibration owing to changes in handpiece angles during surgery, it is important to improve the tracking method to achieve all-around capture of the implant handpiece and dental position information.
4) The cost of purchasing and maintaining navigation systems can be high, and insurance may not cover it [55].

2.3 Accuracy of computer-assisted surgery

Currently, there are three methods for performing dental implant surgery: manual (freehand), static guide, and dynamic navigation. Although the three methods have very different clinical protocols, numerous studies have proven that all of them may successfully insert dental implants [51, 57]. Accuracy is an important reference for the clinician to evaluate a particular method [58].

Tahmaseb's meta-analysis on implant placement found that the surgical guide group had an error of 1.2 mm and 1.4 mm in the deviation at the entry and apex, and a 3.5° angular deviation. When using the freehand method, a 9.9° angular deviation and errors of 2.7 mm and 2.59 mm were observed at the coronal and apical parts of the implants, respectively [51, 58]. A meta-analysis of dynamic implant placement showed linear deviations of 0.81 mm and 1.30 mm for the implant entry point and the apical point respectively, and 3.8° angular deviations [55]. The literature indicates that guided implant placement accuracy in edentulous jaws is considered clinically acceptable, with angular deviations ranging from 2.4° to 4.9°, entry deviations from 0.5 mm to 1.4 mm, and apical deviations from 0.76 mm to 1.6 mm [59].

The static surgical guide consists of two components: a resin base and a metal sleeve. The sleeve height and the distance from the alveolar ridge can significantly affect the static guide's precision [60]. Errors in a surgical guide can result from several factors, including the design and manufacturing of the guide. The surgical guide's tolerance for the sleeve and drill and the digital workflow that was used to create it—including data acquisition, software processing, and template production—can lead to deviation [61].

Dynamic navigation systems' clinical accuracy can be impacted by various factors like CBCT acquisition, calibration and registration, and the operator's performance, all of which can affect the precision of the final implantation [57]. Systematic errors such as those resulting from the software and hardware of the navigation system, as well as the CBCT imaging equipment, are challenging to minimize in practical use. The most significant impact on navigation accuracy is the registration error and calibration error, such as whether the distribution of calibration marker points is reasonable, whether the calibration and tracking device are stable, and whether the registration image is clear [52, 62]. The operator's experience also greatly affects the accuracy of guided surgery. Although guided surgery can assist novice practitioners in placing implants with improved accuracy and results similar to experienced practitioners, surgical experience still has a significant impact on the accuracy of the guided procedure [63].

2.4 Experience of operators

Most implant surgeries are performed using the freehand method in clinical settings. The clinician usually relies on anatomical landmarks of adjacent and contralateral teeth to prepare the implant osteotomy and complete the implant placement. Freehand implant insertion relies mostly on the surgeon's surgical experience for implant placement safety and final restorative outcomes [59].

Compared to conventional implant techniques, the static and dynamic guided approaches provide novice practitioners with improved accuracy in implant placement [63-65]. Although dynamic navigation techniques may shorten the learning curve for clinicians, they still require the operator to practice repeatedly and gain experience in its use [62, 65, 66]. There is not enough evidence to evaluate the accuracy and efficacy of novice versus experienced surgeons when placing dental implants utilizing guided and freehand techniques. It's important to evaluate whether navigation and surgical guide methods can enhance novice surgeons' surgical performance as compared to freehand surgery, with the performance of experienced surgeons serving as a reference.

3. Artificial intelligence

3.1 Artificial intelligence in medical imaging

Medical imaging is a crucial source of information for disease screening, diagnosis, and treatment, encompassing various fields such as medical imaging, image processing, visualization, early disease screening, risk prediction, disease detection and diagnosis, surgery planning, assisted navigation during surgery, postoperative tracking, and rehabilitation planning [67]. As a result, the use of artificial intelligence and big data-based technologies in medical imaging has become a focus of interest for medical organizations and research [68, 69].

Medical imaging consists of two parts: imaging and image mining. Firstly, the quality of medical imaging equipment is critical to the success of detection, diagnosis, and treatment of diseases, as it provides the information used. AI-optimized scanning workflow can greatly increase scanning efficiency and standardize imaging quality [70]. Secondly, a crucial step in the diagnostic and treatment process is understanding medical images and extracting key information that might help with treatment and diagnosis decisions. The interpretation of a large amount of image information increases the demand on physicians' medical imaging knowledge and increases their time to review the images. Artificial intelligence-assisted diagnostics can automate the time-consuming task of screening for lesions, quickly extracting important diagnostic information from large amounts of data and reducing the risk of misdiagnosis or missed diagnoses by minimizing human subjectivity in the review process. The use of AI in medical imaging can speed up complex image processing tasks, such as segmentation and registration, providing precise structural information about lesions for medical devices used in treatment like surgical navigation systems and robots [71- 73].

In recent years, artificial intelligence has gained popularity as a research topic in computer-assisted diagnosis, due to its capability to automate tasks in a way that mimics human intelligence [74]. Machine learning (ML), which is the most prevalent AI technology, uses large datasets to train mathematical models, allowing computers to learn without being explicitly programmed [71]. Among them, deep learning algorithms, a subcategory of ML, are even more widely studied and used at this stage, being applied in tasks such as image segmentation, image feature extraction, classification, and target detection [68]. The scenarios applied are the segmentation of human structure and lesion areas, early diagnosis of diseases, detection of anatomical structures and lesion areas [72]. Deep learning (DL) is called "deep" because it is organized in layers on multiple levels and can automatically extract meaningful features from big data [75].

Currently, convolutional neural network (CNN), a subset of DL, is extensively utilized in medical image processing. CNNs are now considered as the most advanced method for image segmentation, classification, prediction, image enhancement and treatment planning. U-Net is a well-known deep learning structure commonly utilized for semantic segmentation tasks. As shown in **Fig. 4**, it was introduced in 2015 by Ronneberger et al, and has since become a widely adopted model for image analysis and medical imaging applications[76-79]. The architecture of this model includes a contracting path that captures the contextual information from an input image, and a symmetric expanding path that maps the low-level features to the desired output. The unique U-shaped architecture of the model allows it to effectively capture both local and global information, making it well-suited for dental image analysis. In dentistry, the U-Net algorithm has been utilized for tasks such as segmentation of teeth [77, 78], oral lesions [79] and metal artifact reduction [80] in dental images, enabling more accurate and automated diagnoses [81, 82].

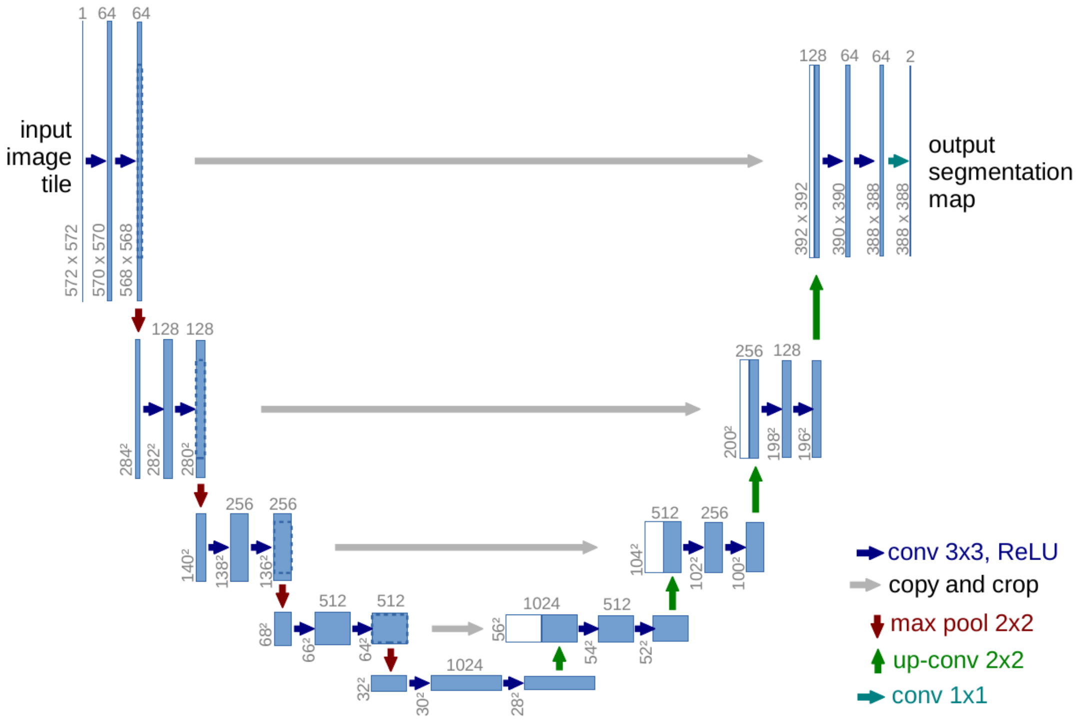

Figure 4. U-net model for biomedical image segmentation. Images are reproduced from [79] with permission from Springer Nature

Pros of U-Net for dental applications:

1) Good at handling complex and small structures in medical imaging: U-Net architecture, with its symmetrical design, is especially suited for image segmentation tasks where small objects need to be distinguished and located within larger structures. This makes it ideal for dental applications where teeth and other small structures need to be accurately segmented from surrounding tissue.
2) U-Net has a strong capability for segmentation tasks: The U-Net model is based on a fully convolutional network and was originally developed for biomedical image segmentation. This makes it well-suited for dental image analysis tasks that require segmentation, such as tooth detection and extraction, and root canal segmentation [83].
3) Good performance in reconstructing fine details in images: U-Net has a strong ability to reconstruct fine details in images by using skip connections [84] that allow the network to propagate high-resolution information from earlier layers to later layers. This makes it useful for dental applications where fine structures, such as tooth cracks [85] and fissures [86], need to be accurately segmented and analyzed.

Cons of U-Net for dental applications:

1) May be computationally expensive to train and use: U-Net's large number of parameters, as well as

its use of multiple convolutional and up-sampling layers, can make it computationally expensive to train and use [87]. This may limit its utility in resource-limited environments, such as mobile devices and low-power hardware.

2) U-Net may not be suitable for tasks requiring large amounts of context information: U-Net is designed for image segmentation tasks, where local context is important. For tasks that require a larger context [88, 89], such as tooth classification and diagnosis, other architectures may be more appropriate.
3) May be vulnerable to overfitting if the amount of training data is limited: Due to its large number of parameters, U-Net may have a risk of overfitting if the training data is limited [90, 91]. This can lead to poor performance on new, unseen data.

Recently, a 3D U-Net was introduced for segmenting biomedical images and has gained widespread usage in dentomaxillofacial radiology [68, 92- 99].

3.2 Challenges of AI application in healthcare

3.2.1 Data sources and quality problems

Big data, algorithms, and computing power are the three cornerstones of artificial intelligence. Among them, "massive, accurate, high-quality" big data is the basis for the realization of artificial intelligence. Medical data involving ethics, on the one hand, are difficult to obtain in a way that the data are numerous and complicated, and the fragmentation of information is still a problem; on the other hand, there is little data of high quality, and after getting the data, they have to be precisely labeled by experts, and the quantity and quality of labeling also directly affect the whole data set. In addition, each unit has its own database, and the data of each disease and its form are different, and there is no unified standard to integrate them, and there is also a lack of a large public database system [100]. High-quality data is the primary prerequisite for AI development. Errors or biases in the training database are often directly reflected in model behavior and have a significant impact on both model performance and clinical outcomes, so data quality is essential to unlocking the value of big data in healthcare [70].

3.2.2 Problems with AI algorithms

The complexity of the clinical problem requires a deepening of the neural network layers, and the complexity of the model does not match the amount of data corresponding to it. The model is too complex and the learning capability is so powerful that it learns the features of the data itself in the training set, which leads to overfitting of the algorithm; the complexity of the model is much lower than the amount of data that matches it, which leads to low learning capability of the model and produces underfitting. While underfitting can be solved by increasing the amount of data and the number of training sessions, overfitting is more difficult to solve and is a problem often encountered in deep learning. Especially in

practical medical applications, AI algorithms must be rigorously tested and evaluated, otherwise they can lead to medical errors and disputes and trigger large-scale medical risks [100].
In addition, the subjectivity of the algorithm and the "black box" of the algorithm cannot be ignored [75]. Currently, the most widely used deep learning algorithms in medical AI utilize extensive neural networks, with many hidden layers, that have strong self-learning and self-programming capabilities. However, this complexity leads to a lack of interpretability and transparency in the AI system, making it a "black box" that is difficult to understand the relationship between inputs and outputs. The consequence of the "black box" is that it's challenging to assess AI's errors and it cannot be effectively monitored [100]. If the data used for algorithm training is incomplete, inaccurate, or contains some subjective bias or discrimination, it is possible to replicate and amplify these "flaws" in algorithm training, and finally obtain biased or even wrong prediction results. As a result, certain groups of people are treated in a discriminatory manner in medical assessments, which may even lead to medical safety incidents. At the same time, the medical industry is concerned with human life and health. Lack of understanding of the decision-making process of the model will make it challenging for people to trust medical AI [70].

4. Aims and hypotheses

The purpose of the PhD project was to study the impact of digital technologies on dentistry and to explore how digital dentistry can simplify workflow through the use of 3D modeling and AI assistance.

This doctoral thesis is divided into three parts, each with its respective objectives.

Part I：3D modeling

(A) Accuracy assessment

Numerous studies have shown that creating patient-specific skeletal models using affordable desktop printers is clinically acceptable. However, there isn't enough evidence to compare the accuracy of desktop and professional printers in producing maxillofacial skeletal models.

The objectives were:

- To report the current evidence on the accuracy of maxillofacial skeletal models produced by desktop and professional 3D printers, and to investigate any potential contributing factors that may impact the accuracy of 3D printed models.
- To investigate the efficacy of CBCT-derived skull models produced by 3D printers at different cost levels.

The hypothesis was that:

Maxillofacial skeletal models produced by low-cost desktop printers could offer comparable accuracy to that of high-cost professional printers.

(B) Haptic feedback

3DP has been successfully employed in the production of the patient-specific skeletal model with anatomical replication, however it is unknown if these models can provide the optimal haptic feedback for simulating dental implant surgery. Therefore, it is crucial to investigate the haptic feedback of these models for hands-on dental implant training.

The objective was:

- To analyze the haptic feedback of different 3D-printed models for simulating dental implant surgery.

The hypothesis was that:

The haptic feedback of different 3D-printed models using various technologies and materials would be similar.

Part II: Computer-assisted surgery on 3D-printed models

Recently, computer-assisted surgery has demonstrated to enhance implant placement accuracy for novice surgeons. However, no evidence has been proposed in the literature for assessing the performance of novice compared to experienced surgeons for dental implant placement with freehand, static and dynamic guided approaches. The guided approaches may be beneficial in training novice surgeons for successful dental implant surgery.

The objective was:

- To investigate the accuracy and efficacy of novice versus experienced surgeons for dental implant placement with freehand, static guided and dynamic navigation approaches.

The hypothesis was that:

Considering the performance of experienced surgeons as a clinical reference, the use of dynamic navigation and static guided approaches could improve the surgical performance of novice surgeons compared to freehand approach.

Part III: Artificial intelligence

The existing application of deep learning is mostly focused on a single task. Building an online platform, which integrates data from multiple imaging modalities, may create the digital virtual patient for automatic anatomy detection, treatment planning and surgical simulation. In addition, the efficient, accurate and consistent result of automatic anatomical segmentation can be used for 3D printing. The online cloud-based platform has been constructed to detect teeth, nerve and bone structure in CBCT. Intraoral scans (IOS) are taken as an essential aid for providing more precise information of teeth morphology. IOS data is a vital part for creating virtual patient by integration with CBCT data.

The objective was:

To propose a deep learning-based convolutional neural network for automated tooth segmentation on intraoral scanned images.

The hypothesis was that:

A deep CNN approach would provide a segmentation of teeth on intraoral scanned images that is more accurate, consistent, and time-efficient compared to semi-automatically assisted segmentation.

5. References

[1] E.D. Rekow, Digital dentistry: The new state of the art — Is it disruptive or destructive? Dent. Mater. 36 (2020) 9–24.

[2] F. Schwendicke, Digital dentistry: Advances and challenges, J. Clin. Med. 9 (2020) 1–2.

[3] T. Nejatian, S. Almassi, A. Farhadi Shamsabadi, G. Vasudeva, Z. Hancox, A.S. Dhillon, F. Sefat, Digital dentistry, in: Adv. Dent. Biomater. (2019) 507–540.

[4] M. Tallarico, Computerization and digital workflow in medicine: Focus on digital dentistry, Materials (Basel). (2020)13.

[5] M. Javaid, A. Haleem, Current status and applications of additive manufacturing in dentistry: A literature-based review, J. Oral Biol. Craniofacial Res. 9 (2019) 179–185.

[6] T.F. Alghazzawi, Advancements in CAD/CAM technology: Options for practical implementation, J. Prosthodont. Res. 60 (2016) 72–84.

[7] D. Hoang, D. Perrault, M. Stevanovic, A. Ghiassi, Today surgical applications of three-dimensional printing: A review of the current literature & how to get started, Ann. Transl. Med. 4 (2016).

[8] D. Khorsandi, A. Fahimipour, P. Abasian, S.S. Saber, M. Seyedi, S. Ghanavati, A. Ahmad, A.A. De Stephanis, F. Taghavinezhaddilami, A. Leonova, R. Mohammadinejad, M. Shabani, B. Mazzolai, V. Mattoli, F.R. Tay, P. Makvandi, 3D and 4D printing in dentistry and maxillofacial surgery: Printing techniques, materials, and applications, Acta Biomater. 122 (2021) 26–49.

[9] E. Anadioti, B. Kane, E. Soulas, Current and Emerging Applications of 3D Printing in Restorative Dentistry, Curr. Oral Heal. Reports. 5 (2018) 133–139.

[10] J. Schweiger, D. Edelhoff, J.F. Güth, 3D printing in digital prosthetic dentistry: An overview of recent developments in additive manufacturing, J. Clin. Med. 10 (2021).

[11] M.E. Prendergast, J.A. Burdick, Recent Advances in Enabling Technologies in 3D Printing for Precision Medicine, Adv. Mater. 32 (2020) 1–14.

[12] M. G Noureldin, N. Y Dessoky, 3D Printing: Towards the Future of Oral and Maxillofacial Surgery, Acta Sci. Dent. Scienecs. 4 (2020) 107–112.

[13] T.D. Ngo, A. Kashani, G. Imbalzano, K.T.Q. Nguyen, D. Hui, Additive manufacturing (3D printing): A review of materials, methods, applications and challenges, Compos. Part B Eng. 143 (2018) 172–196.

[14] S. Pillai, A. Upadhyay, P. Khayambashi, I. Farooq, H. Sabri, M. Tarar, K.T. Lee, I. Harb, S. Zhou, Y. Wang, S.D. Tran, Dental 3d-printing: Transferring art from the laboratories to the clinics, Polymers (Basel). 13 (2021) 1–25.

[15] A. Sinha, C. Osnes, A.J. Keeling, Pilot study assessing 3D-printed teeth as a caries removal teaching tool, Eur. J. Dent. Educ. 26 (2022) 329–336.

[16] Y. Tian, C.X. Chen, X. Xu, J. Wang, X. Hou, K. Li, X. Lu, H.Y. Shi, E.S. Lee, H.B. Jiang, A Review of 3D Printing in Dentistry: Technologies, Affecting Factors, and Applications, Scanning. (2021) 9950131.

[17] T. Kamio, K. Hayashi, T. Onda, T. Takaki, T. Shibahara, T. Yakushiji, T. Shibui, H. Kato, Utilizing a low-cost desktop 3D printer to develop a “one-stop 3D printing lab” for oral and maxillofacial surgery and dentistry fields, 3D Print. Med. 4 (2018) 1–2.

[18] X. Wang, S. Shujaat, E. Shaheen, R. Jacobs, Accuracy of desktop versus professional 3D printers for maxillofacial model production. A systematic review and meta-analysis, J. Dent. (2021) 103741.

[19] R.H. Khonsari, J. Adam, M. Benassarou, H. Bertin, B. Billotet, J. Bouaoud, P. Bouletreau, R. Garmi, T. Gellée, P. Haen, S. Ketoff, G. Lescaille, A. Louvrier, J.C. Lutz, M. Makaremi, R. Nicot, N. Pham-Dang, M. Praud, F. Saint-Pierre, T. Schouman, L. Sicard, F. Simon, T. Wojcik, C. Meyer, In-house 3D printing: Why, when, and how? Overview of the national French good practice guidelines for in-house 3D-printing in maxillo-facial surgery, stomatology, and oral surgery, J. Stomatol. Oral Maxillofac. Surg. 122 (2021) 458–461.

[20] C.R. Hatz, B. Msallem, S. Aghlmandi, P. Brantner, F.M. Thieringer, Can an entry-level 3D printer create high-quality anatomical models? Accuracy assessment of mandibular models printed by a desktop 3D printer and a professional device, Int. J. Oral Maxillofac. Surg. 49 (2020) 143–148.

[21] A. Tahayeri, M.C. Morgan, A.P. Fugolin, D. Bompolaki, A. Athirasala, C.S. Pfeifer, J.L. Ferracane, L.E. Bertassoni, 3D printed versus conventionally cured provisional crown and bridge dental materials, Dent. Mater. 34 (2018) 192–200.

[22] J. Lüchtenborg, F. Burkhardt, J. Nold, S. Rothlauf, C. Wesemann, S. Pieralli, G. Wemken, S. Witkowski, B.C. Spies, Implementation of fused filament fabrication in dentistry, Appl. Sci. 11 (2021).

[23] A.B.N. Pereira, R.C. Almeida, C. Marassi, C.C. Abdo Quintão, F. de A.R. Carvalho, Do low-cost 3-dimensional printers produce suitable dental models?, Am. J. Orthod. Dentofac. Orthop. 161 (2022) 858–865.

[24] I. Velasco, S. Vahdani, H. Ramos, Low-cost method for obtaining medical rapid prototyping using desktop 3D printing: A novel technique for mandibular reconstruction planning, J. Clin. Exp. Dent. 9 (2017) e1103–e1108.

[25] B. Msallem, N. Sharma, S. Cao, F.S. Halbeisen, H.-F. Zeilhofer, F.M. Thieringer, Evaluation of the Dimensional Accuracy of 3D-Printed Anatomical Mandibular Models Using FFF, SLA, SLS, MJ, and BJ Printing Technology, J. Clin. Med. 9 (2020) 817.

[26] L.A. Dvoracek, J.Y. Lee, J. V. Unadkat, Y.H. Lee, D. Thakrar, J.E. Losee, J.A. Goldstein, Low-Cost, Three-Dimensionally-Printed, Anatomical Models for Optimization of Orbital Wall Reconstruction, Plast. Reconstr. Surg. (2021) 162–166.

[27] S. Kumar Malyala, R.Y. Kumar, A.M. Alwala, A 3D-printed osseointegrated combined jaw and dental implant prosthesis – A case study, Rapid Prototyp. J. 23 (2017) 1164–1169.

[28] E. George, P. Liacouras, F.J. Rybicki, D. Mitsouras, Measuring and establishing the accuracy and reproducibility of 3D printed medical models, Radiographics. 37 (2017) 1424–1450.

[29] S. Leng, K. McGee, J. Morris, A. Alexander, J. Kuhlmann, T. Vrieze, C.H. McCollough, J. Matsumoto, Anatomic modeling using 3D printing: quality assurance and optimization, 3D Print. Med. 3 (2017).

[30] I.W.W. Lau, Z. Sun, Dimensional accuracy and clinical value of 3d printed models in congenital heart disease: A systematic review and meta-analysis, J. Clin. Med. 8 (2019).

[31] W. Piedra-Cascón, V.R. Krishnamurthy, W. Att, M. Revilla-León, 3D printing parameters, supporting structures, slicing, and post-processing procedures of vat-polymerization additive manufacturing

technologies: A narrative review, J. Dent. 109 (2021).

[32] D. Mitsouras, P. Liacouras, A. Imanzadeh, A.A. Giannopoulos, T. Cai, K.K. Kumamaru, E. George, N. Wake, E.J. Caterson, B. Pomahac, V.B. Ho, G.T. Grant, F.J. Rybicki, Medical 3D printing for the radiologist, Radiographics. 35 (2015) 1965–1988.

[33] P. Ravi, L.L. Chepelev, G. V. Stichweh, B.S. Jones, F.J. Rybicki, Medical 3D Printing Dimensional Accuracy for Multi-pathological Anatomical Models 3D Printed Using Material Extrusion, J. Digit. Imaging. 35 (2022) 613–622.

[34] C.A. Jacobs, A.Y. Lin, A new classification of three-dimensional printing technologies: Systematic review of three-dimensional printing for patient-specific craniomaxillofacial surgery, in: Plast. Reconstr. Surg., Lippincott Williams and Wilkins. (2017)1211–1220.

[35] A. Zolfagharian, A. Kaynak, M. Bodaghi, A.Z. Kouzani, S. Gharaie, S. Nahavandi, Control-based 4D printing: Adaptive 4D-printed systems, Appl. Sci. 10 (2020).

[36] T.M. BARKER, W.J.S. EARWAKER, D.A. LISLE, Accuracy of stereolithographic models of human anatomy, Australas. Radiol. 38 (1994) 106–111.

[37] M. Meglioli, A. Naveau, G.M. Macaluso, S. Catros, 3D printed bone models in oral and cranio-maxillofacial surgery: a systematic review, 3D Print. Med. 6 (2020).

[38] M. Odeh, D. Levin, J. Inziello, F. Lobo Fenoglietto, M. Mathur, J. Hermsen, J. Stubbs, B. Ripley, Methods for verification of 3D printed anatomic model accuracy using cardiac models as an example, 3D Print. Med. 5 (2019) 1–12.

[39] S. Shujaat, E. Shaheen, F. Novillo, C. Politis, R. Jacobs, Accuracy of cone beam computed tomography–derived casts: A comparative study, J. Prosthet. Dent. (2020) 1–8.

[40] S.G. Maliha, J.R. Diaz-Siso, N.M. Plana, A. Torroni, R.L. Flores, Haptic, Physical, and Web-Based Simulators: Are They Underused in Maxillofacial Surgery Training?, J. Oral Maxillofac. Surg. 76 (2018) 2424.e1-2424.e11.

[41] F.G. Hamza-Lup, K. Bergeron, D. Newton, Haptic systems in user interfaces – State of the art survey, in: ACMSE 2019 - Proc. 2019 ACM Southeast Conf., Association for Computing Machinery, Inc. (2019) 141–148.

[42] S. Chawla, S. Devi, P. Calvachi, W.B. Gormley, R. Rueda-Esteban, Evaluation of simulation models in neurosurgical training according to face, content, and construct validity: a systematic review, Acta Neurochir. 164 (2022) 947–966.

[43] D. Mehrotra, A.F. Markus, Emerging simulation technologies in global craniofacial surgical training, J. Oral Biol. Craniofacial Res. 11 (2021) 486–499.

[44] M. Wasif Abdul Basit Shah Vardag Ainulakbar Mughal Syed Akbar Abbas Shayan Khalid, M. Wasif, A. Basit Shah Vardag, A. Mughal, S. Akbar Abbas, S. Khalid, H. Ahmed Pasha, Training in temporal bone surgery: A review of current practices Training in temporal bone surgery: A review of current practices. J Pak Med Assoc. 71(2021):S99-S102.

[45] A. Frithioff, M. Frendø, D.B. Pedersen, M.S. Sørensen, S.A. Wuyts Andersen, 3D-Printed Models for Temporal Bone Surgical Training: A Systematic Review, Otolaryngol. - Head Neck Surg. 165 (2021)

617–625.

[46] V.N. Vakharia, N.N. Vakharia, C.S. Hill, Review of 3-Dimensional Printing on Cranial Neurosurgery Simulation Training, World Neurosurg. 88 (2016) 188–198.

[47] R. Ratinam, M. Quayle, J. Crock, M. Lazarus, Q. Fogg, P. McMenamin, Challenges in creating dissectible anatomical 3D prints for surgical teaching, J. Anat. 234 (2019) 419–437.

[48] Z. Jin, Y. Li, K. Yu, L. Liu, J. Fu, X. Yao, A. Zhang, Y. He, 3D Printing of Physical Organ Models: Recent Developments and Challenges, Adv. Sci. 8 (2021).

[49] M. Haffner, A. Quinn, T.Y. Hsieh, E.B. Strong, T. Steele, Optimization of 3D Print Material for the Recreation of Patient-Specific Temporal Bone Models, Ann. Otol. Rhinol. Laryngol. 127 (2018) 338–343.

[50] K. Qiu, G. Haghiashtiani, M.C. Mcalpine, Annual Review of Analytical Chemistry 3D Printed Organ Models for Surgical Applications. Annu Rev Anal Chem. 11 (2018) 287-306.

[51] G. Kalaivani, V.R. Balaji, D. Manikandan, G. Rohini, Expectation and reality of guided implant surgery protocol using computer-assisted static and dynamic navigation system at present scenario: Evidence-based literature review, J. Indian Soc. Periodontol. 24 (2020) 398–408.

[52] M.S. Block, R.W. Emery, Static or Dynamic Navigation for Implant Placement - Choosing the Method of Guidance, J. Oral Maxillofac. Surg. 74 (2016) 269–277.

[53] J. Gargallo-Albiol, S. Barootchi, O. Salomó-Coll, H. lay Wang, Advantages and disadvantages of implant navigation surgery. A systematic review, Ann. Anat. 225 (2019) 1–10.

[54] G. Gasparini, R. Boniello, A. Laforì, P. De Angelis, V. Del Deo, A. Moro, G. Saponaro, S. Pelo, Navigation system approach in zygomatic implant technique, J. Craniofac. Surg. 28 (2017) 250–251.

[55] G. Pellegrino, A. Ferri, M. Del Fabbro, C. Prati, M.G. Gandolfi, C. Marchetti, Dynamic Navigation in Implant Dentistry: A Systematic Review and Meta-analysis. Int. J. Oral Maxillofac. Implants. 36 (2021) e121–e140.

[56] M. Vercruyssen, T. Fortin, G. Widmann, R. Jacobs, M. Quirynen, Different techniques of static/dynamic guided implant surgery: Modalities and indications, Periodontol. 2000. 66 (2014) 214–227.

[57] S. Schnutenhaus, C. Edelmann, A. Knipper, R.G. Luthardt, Accuracy of dynamic computer-assisted implant placement: A systematic review and meta-analysis of clinical and in vitro studies, J. Clin. Med. 10 (2021) 1–20.

[58] A. Tahmaseb, V. Wu, D. Wismeijer, W. Coucke, C. Evans, The accuracy of static computer-aided implant surgery: A systematic review and meta-analysis, Clin. Oral Implants Res. 29 (2018) 416–435.

[59] R. D'haese, T. Vrombaut, G. Hommez, H. De Bruyn, S. Vandeweghe, Accuracy of guided implant surgery in the edentulous jaw using desktop 3D-printed mucosal supported guides, J. Clin. Med. 10 (2021) 1–10.

[60] K. El Kholy, S.F.M. Janner, M. Schimmel, D. Buser, The influence of guided sleeve height, drilling distance, and drilling key length on the accuracy of static Computer-Assisted Implant Surgery, Clin. Implant Dent. Relat. Res. 21 (2019) 101–107.

[61] O. Schubert, J. Schweiger, M. Stimmelmayr, E. Nold, J.F. Güth, Digital implant planning and guided

implant surgery – workflow and reliability, Br. Dent. J. 226 (2019) 101–108.

[62] D. Wu, L. Zhou, J. Yang, B. Zhang, Y. Lin, J. Chen, W. Huang, Y. Chen, Accuracy of dynamic navigation compared to static surgical guide for dental implant placement, Int. J. Implant Dent. 6 (2020) 78.

[63] G. Pellegrino, P. Bellini, P.F. Cavallini, A. Ferri, A. Zacchino, V. Taraschi, C. Marchetti, U. Consolo, Dynamic navigation in dental implantology: The influence of surgical experience on implant placement accuracy and operating time. An in vitro study, Int. J. Environ. Res. Public Health. 17 (2020).

[64] C. ILHAN, M. DIKMEN, E. YÜZBASIOGLU, Accuracy and efficiency of digital implant planning and guided implant surgery: An update and review, J. Exp. Clin. Med. 38 (2021) 148–156.

[65] A. Jorba-García, R. Figueiredo, A. González-Barnadas, O. Camps-Font, E. Valmaseda-Castellón, Accuracy and the role of experience in dynamic computer guided dental implant surgery: An in-vitro study, Med. Oral Patol. Oral y Cir. Bucal. 24 (2019) e76–e83.

[66] G. Pellegrino, P. Bellini, P.F. Cavallini, A. Ferri, A. Zacchino, V. Taraschi, C. Marchetti, U. Consolo, Dynamic navigation in dental implantology: The influence of surgical experience on implant placement accuracy and operating time. An in vitro study, Int. J. Environ. Res. Public Health. 17 (2020).

[67] J.C. Gore, Artificial intelligence in medical imaging, Magn. Reson. Imaging. 68 (2020) A1–A4.

[68] A. Barragán-Montero, U. Javaid, G. Valdés, D. Nguyen, P. Desbordes, B. Macq, S. Willems, L. Vandewinckele, M. Holmström, F. Löfman, S. Michiels, K. Souris, E. Sterpin, J.A. Lee, Artificial intelligence and machine learning for medical imaging: A technology review, Phys. Medica. 83 (2021) 242–256.

[69] S. Wang, G. Cao, Y. Wang, S. Liao, Q. Wang, J. Shi, C. Li, D. Shen, Review and Prospect: Artificial Intelligence in Advanced Medical Imaging, Front. Radiol. 1 (2021).

[70] S.N. Saw, K.H. Ng, Current challenges of implementing artificial intelligence in medical imaging, Phys. Medica. 100 (2022) 12–17.

[71] A. Becker, Artificial intelligence in medicine: What is it doing for us today?, Heal. Policy Technol. 8 (2019) 198–205.

[72] J. Olveres, G. González, F. Torres, J.C. Moreno-Tagle, E. Carbajal-Degante, A. Valencia-Rodríguez, N. Méndez-Sánchez, B. Escalante- Ramírez, What is new in computer vision and artificial intelligence in medical image analysis applications, Quant. Imaging Med. Surg. 11 (2021) 3830–3853.

[73] S. Shujaat, M. Riaz, R. Jacobs, Synergy between artificial intelligence and precision medicine for computer - assisted oral and maxillofacial surgical planning, Clin. Oral Investig. (2022).

[74] V. Kaul, S. Enslin, S.A. Gross, History of artificial intelligence in medicine, Gastrointest. Endosc. 92 (2020) 807–812.

[75] M. Mahmud, M.S. Kaiser, T.M. McGinnity, A. Hussain, Deep Learning in Mining Biological Data, Cognit Comput . 13 (2021) 1-33.

[76] O. Ronneberger, P. Fischer, T. Brox, U-net: Convolutional networks for biomedical image segmentation, Lect. Notes Comput. Sci. 9351 (2015) 234–241.

[77] Y. Li, S. Wang, J. Wang, G. Zeng, W. Liu, Q. Zhang, Q. Jin, Y. Wang, GT U-Net: A U-Net Like Group Transformer Network for Tooth Root Segmentation, Lect. Notes Comput. Sci. 12966 LNCS (2021) 386–

395.

[78] W. Duan, Y. Chen, Q. Zhang, X. Lin, X. Yang, Refined tooth and pulp segmentation using U-Net in CBCT image, Dentomaxillofacial Radiol. 50 (2021) 20200251.

[79] W. Shang, Z. Li, Y. Li, Identification of Common Oral Disease Lesions Based on U-Net, 2021 IEEE 3rd Int. Conf. Front. Technol. Inf. Comput. ICFTIC 2021. (2021) 194–200.

[80] M.A.A. Hegazy, M.H. Cho, M.H. Cho, S.Y. Lee, U-net based metal segmentation on projection domain for metal artifact reduction in dental CT, Biomed. Eng. Lett. 9 (2019) 375–385.

[81] H.A. Khan, M.A. Haider, H.A. Ansari, H. Ishaq, A. Kiyani, K. Sohail, M. Muhammad, S.A. Khurram, Automated feature detection in dental periapical radiographs by using deep learning, Oral Surg. Oral Med. Oral Pathol. Oral Radiol. 131 (2021) 711–720.

[82] Z. Zheng, H. Yan, F.C. Setzer, K.J. Shi, M. Mupparapu, J. Li, Anatomically Constrained Deep Learning for Automating Dental CBCT Segmentation and Lesion Detection, IEEE Trans. Autom. Sci. Eng. 18 (2021) 603–614.

[83] J. Zhang, W. Xia, J. Dong, Z. Tang, Q. Zhao, Root Canal Segmentation in CBCT Images by 3D U-Net with Global and Local Combination Loss, Proc. Annu. Int. Conf. IEEE Eng. Med. Biol. Soc. EMBS. (2021) 3097–3100.

[84] Z. Chen, C. Wang, J. Li, N. Xie, Y. Han, J. Du, Reconstruction bias U-Net for road extraction from optical remote sensing images, IEEE J. Sel. Top. Appl. Earth Obs. Remote Sens. 14 (2021) 2284–2294.

[85] J. Guo, Y. Wu, L. Chen, S. Long, D. Chen, H. Ouyang, C. Zhang, Y. Tang, W. Wang, A perspective on the diagnosis of cracked tooth: imaging modalities evolve to AI-based analysis, Biomed. Eng. OnLine 2022 211. 21 (2022) 1–22.

[86] S.E. Gerard, T.J. Patton, G.E. Christensen, J.E. Bayouth, J.M. Reinhardt, FissureNet: A deep learning approach for pulmonary fissure detection in CT images, IEEE Trans. Med. Imaging. 38 (2019) 156–166.

[87] W. Chen, B. Liu, S. Peng, J. Sun, X. Qiao, S3D-UNET: Separable 3D U-Net for brain tumor segmentation, Lect. Notes Comput. Sci. (Including Subser. Lect. Notes Artif. Intell. Lect. Notes Bioinformatics). 11384 LNCS (2019) 358–368.

[88] D. Lin, Y. Li, T.L. Nwe, S. Dong, Z.M. Oo, RefineU-Net: Improved U-Net with progressive global feedbacks and residual attention guided local refinement for medical image segmentation, Pattern Recognit. Lett. 138 (2020) 267–275.

[89] S. Lian, L. Li, G. Lian, X. Xiao, Z. Luo, S. Li, A Global and Local Enhanced Residual U-Net for Accurate Retinal Vessel Segmentation, IEEE/ACM Trans. Comput. Biol. Bioinforma. 18 (2021) 852–862.

[90] D. Li, D.A. Dharmawan, B.P. Ng, S. Rahardja, Residual U-Net for Retinal Vessel Segmentation, Proc. - Int. Conf. Image Process. ICIP. 2019-September (2019) 1425–1429.

[91] C. Guo, M. Szemenyei, Y. Yi, W. Wang, B. Chen, C. Fan, SA-UNET: Spatial attention U-net for retinal vessel segmentation, Proc. - Int. Conf. Pattern Recognit. (2020) 1236–1242.

[92] F. Preda, N. Morgan, A. Van Gerven, F. Nogueira-reis, A. Smolders, X. Wang, S. Nomidis, E. Shaheen,

H. Willems, Deep convolutional neural network-based automated segmentation of the maxillofacial complex from cone-beam computed tomography : A validation study, J. Dent. 124 (2022) 104238.

[93] S. Shujaat, O. Jazil, H. Willems, A. Van Gerven, E. Shaheen, Automatic segmentation of the pharyngeal airway space with convolutional neural network, J. Dent. 111 (2021) 103705.

[94] P. Lahoud, S. Diels, L. Niclaes, S. Van Aelst, H. Willems, A. Van Gerven, M. Quirynen, R. Jacobs, Development and validation of a novel artificial intelligence driven tool for accurate mandibular canal segmentation on CBCT, J. Dent. 116 (2022) 103891.

[95] C. Pinto, A. Van Gerven, H. Willems, R. Jacobs, Influence of dental fillings and tooth type on the performance of a novel artificial intelligence-driven tool for automatic tooth segmentation on CBCT images – A validation study, 119 (2022).

[96] P.J. Verhelst, A. Smolders, T. Beznik, J. Meewis, A. Vandemeulebroucke, E. Shaheen, A. Van Gerven, H. Willems, C. Politis, R. Jacobs, Layered deep learning for automatic mandibular segmentation in cone-beam computed tomography, J. Dent. (2021).

[97] E. Shaheen, A. Leite, K.A. Alqahtani, A. Smolders, A. Van Gerven, H. Willems, R. Jacobs, A novel deep learning system for multi-class tooth segmentation and classification on cone beam computed tomography. A validation study: Deep learning for teeth segmentation and classification, J. Dent. 115 (2021).

[98] N. Gerhardt, R. Cavalcante, F. Leite, P. Lahoud, A. Van Gerven, H. Willems, A. Smolders, T. Beznik, R. Jacobs, Automated detection and labelling of teeth and small edentulous regions on cone-beam computed tomography using convolutional neural networks, J Dent. 122 (2022).

[99] N. Morgan, A. Van Gerven, A. Smolders, K.D.F. Vasconcelos, Convolutional neural network for automatic maxillary sinus segmentation on cone - beam computed tomographic images, Sci. Rep. (2022) 1–9.

[100] S. Kulkarni, N. Seneviratne, M.S. Baig, A.H.A. Khan, Artificial Intelligence in Medicine: Where Are We Now?, Acad. Radiol. 27 (2020) 62–70.

Part I

3D MODELING

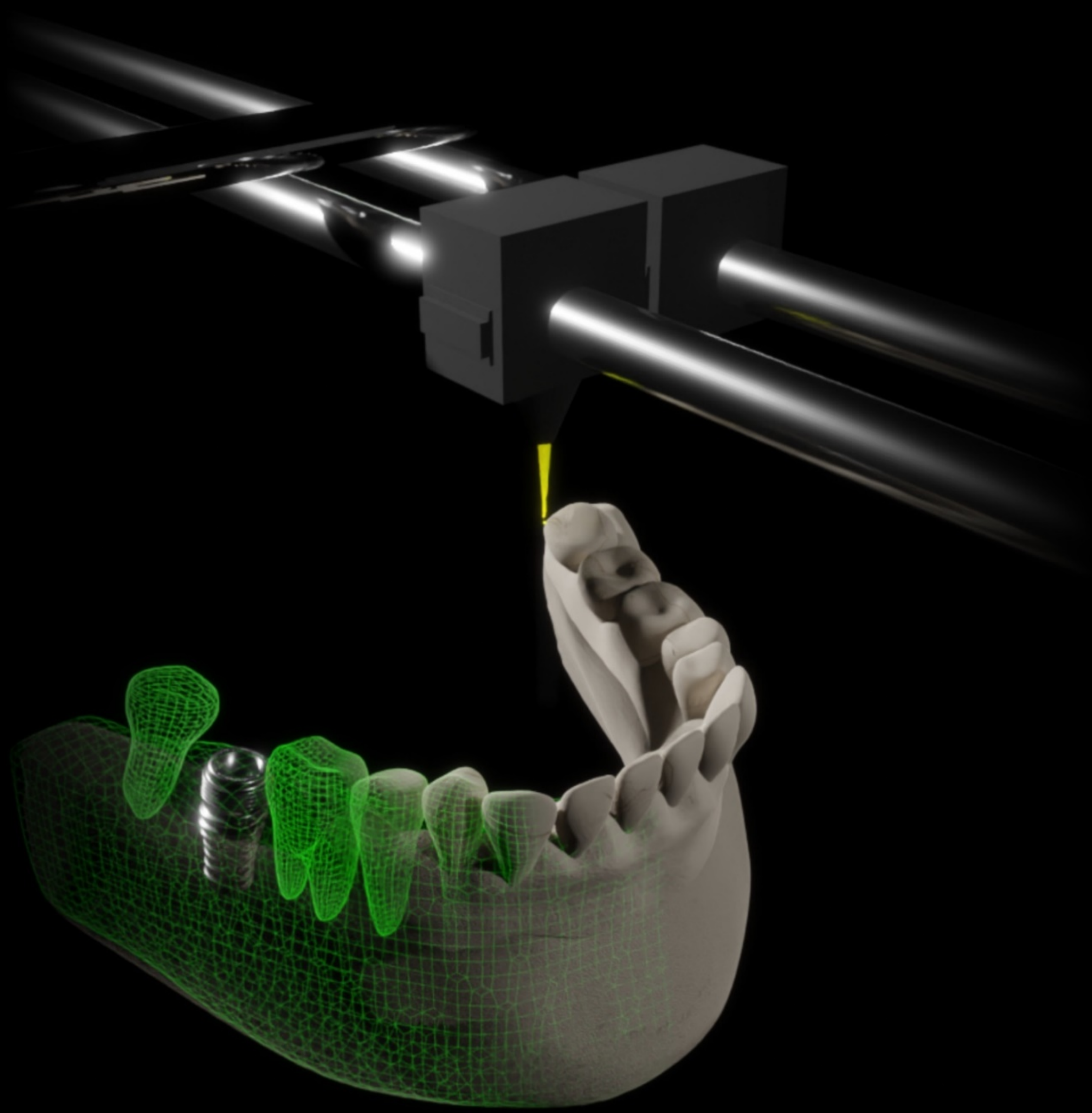

ARTICLE 1

Accuracy of desktop versus professional 3D printers for maxillofacial model production. A systematic review and meta-analysis

Wang X. [1]

Shujaat S. [1]

Shaheen E. [1]

Jacobs R. [1,2]

[1] OMFS IMPATH research group, Department of Imaging & Pathology, Faculty of Medicine, KU Leuven & Department of Oral and Maxillofacial Surgery, University Hospitals Leuven, Leuven, Belgium.

[2] Department of Dental Medicine, Karolinska Institutet, Huddinge, Sweden.

Published in *Journal of Dentistry* 2021 Sep;112:103741.

Abstract

Objectives: The present review systematically analyzed the accuracy of three-dimensional (3D) maxillofacial skeletal models generated from desktop and professional 3D printers.

***Data/sources*:** Electronic literature search was conducted in the following databases: PubMed, Embase, Web of Science and Cochrane Library up to September 2020. Two reviewers independently performed the study selection, data extraction and quality assessment of the included studies. Risk of bias was assessed using the Joanna Briggs Critical Appraisal Checklist for Diagnostic Test Accuracy.

Study selection/results: The search strategy retrieved 5680 articles. Following removal of duplicates, title and abstract screening and full-text reading, 20 publications were eligible to be included in the review which focused towards the accuracy of skeletal models generated from either desktop or professional printer. Both types of printers were defined based on their cost, size and layer thickness, where desktop printers cost between \$1500–\$7000, have a build size of 10×10×10 inches or less and a minimum layer thickness of 100 μm. Whereas, the professional printers' cost was between \$20,000- \$200,000 with a build size of 12×12×12 inches or more and a layer thickness of as less as 3 μm. The risk of bias was found to be low to moderate. Meta-analysis results indicated no significant mean absolute error (MAE) ($p = 0.9487$) between desktop (0.12 mm, 95% CI: 0.00–0.27 mm) and professional printers (0.10 mm, 95% CI: 0.04–0.16 mm). Amongst the printing technology, material jetting (0.09 mm, 95% CI: 0.00–0.17 mm) and selective laser sintering (0.09 mm, 95% CI: 0.00–0.26 mm) offered the lowest MAE and the highest difference was observed with the fused deposition modeling (0.22 mm, 95% CI: 0.00–0.53 mm).

***Conclusions*:** The maxillofacial skeletal models generated from desktop printers offered comparable accuracy to that acquired with professional printers.

***Clinical significance*:** The desktop 3D printers may be a viable option to print maxillofacial skeletal models for surgical planning, simulation, guide manufacturing and education purposes.

Keywords: Printing, three-dimensional; Computer-aided design; Dimensional measurement accuracy; Tomography

1. Introduction

Since the introduction of three-dimensional (3D) printing also known as additive manufacturing (AM) or rapid prototyping (RP), various 3D printing techniques have been developed [1]. The major RP technologies used in the maxillofacial field include stereolithography (SLA), selective laser sintering (SLS), fused deposition modeling (FDM), binder jetting (BJ), material jetting (MJ) or termed polyjet, digital light processing (DLP), and selective deposition lamination (SDL) [2]. These printing technologies have been largely applied for the production of patient-specific skeletal models for pre-operative planning, clinical education and research [3].

The 3D models are commonly utilized for the production of surgical guides and contouring of the osteosynthesis or reconstruction plates at the treatment planning phase of various oral and maxillofacial surgical procedures [4]. The pre-bending of plates on a 3D model has also been known to offer higher precision compared to the conventional intraoperative approach [5]. Furthermore, the physical manipulation of the anatomical structures on a model during planning of the complex surgical procedures allows more control and better comprehension of the different surgical approaches, thereby allowing surgeons to be familiarized with intraoperative situation beforehand and lead to predictable intra-operative results [6].

The most essential characteristic of a skeletal model is its accuracy [7]. An accurate and realistic 3D printed maxillofacial skeletal model has been known to decrease the operation time, bleeding time and patient's postoperative morbidities [8]. If a model does not offer optimal dimensional accuracy then it might lead to an inaccurate pre-operative evaluation and measurements, ill-fitting guides or plates intra-operatively and an unpredictable treatment outcome [9]. From a clinical teaching perspective, anatomically accurate models with a haptic feedback to that of a real bone are a necessity for improving the psychomotor, cognitive and affective skills of the residents, and for the reconciliation of the prior knowledge gained from the traditional teaching methods [10]. The combination of anatomical teaching and surgery simulation on the 3D models allows the residents to be better oriented in the operating room [11]. A model which fails to accurately depict the actual anatomical or pathological scenario might cause the trainees to sub-optimally translate their skills during a real surgical procedure [12].

The production of the skeletal models can be achieved with either a desktop/consumer-grade or a professional printer [13]. The difference between these two types of printers is dependent on three main factors which include, printer cost, build size and layer thickness [14, 15]. The desktop 3D printer usually costs between \$1500 and \$7000 [16] with a build size of 10×10×10 inches or less and offers a layer thickness of approximately 100 μm. In contrast, professional printers mostly cost between \$20,000 and \$200,000 with a build size of 12×12×12 inches or more and a layer thickness of as low as 3 μm [17]. The issue of high cost, availability of trained operators and expensive printing material associated with professional printers is of major concern which limits its widespread implementation in hospitals [18]. Although 3D printing of skeletal models was previously restricted to high-end professional printers, nevertheless, recent technological advancements have led to the development of more affordable desktop printers offering an improved accuracy [13]. The accuracy of a 3D printed skeletal model is greatly dependent on the image acquisition and manipulation, model fabrication and finishing process, as well as the precision evaluation approach [7]. A dimensional error within the range of 2% variation has been proposed to offer clinically acceptable accuracy for 3D printed skeletal models [19]. Since the past few years, the desktop 3D printers have undergone innovative changes allowing the production of cheap and accurate models [17]. The technologies such as FDM, SLA, DLP and SLS have been incorporated into the desktop printers with a wider range of materials, taking its performance equal to that of the professional applications [15]. Many studies have reported that cost-effective desktop printers are clinically acceptable for producing patient-specific skeletal models [20-22]. However, there is lack of evidence related to the accuracy comparison of desktop and professional printers for the production of maxillofacial skeletal models. Therefore, the aim of the systematic review was to compare the accuracy of the maxillofacial skeletal models generated from desktop 3D printers compared with professional 3D printers.

2. Methods and materials

The systematic review followed the Preferred Reporting Items for Systematic Reviews and Meta-Analyses (PRISMA) guidelines [23]. In addition, the study protocol was registered in the PROSPERO database under the number CRD42020168236.

2.1 Review question

The focused question was structured according to the PICO (Population, Intervention, Comparison, and Outcome) principle: "Do the 3D printed maxillofacial skeletal models (P) generated by desktop or professional printers (I) offer the same two-dimensional (2D) or three-dimensional (3D) dimensional accuracy (O) in comparison to the reference model (C) ?"

2.2 Eligibility criteria

All study designs including in-vivo or in-vitro experiments which evaluated the accuracy of 3D printed human maxillofacial skeletal models of any sample size utilizing desktop or professional 3D printers were selected for this review. Case report, case series, pilot studies and comparative studies were also included in the review. Exclusion criteria were non-English articles, animal studies, review articles or editorial comments.

2.3 Search strategy and data collection

An electronic search was performed in PubMed, Embase, Web of Science and Cochrane Library up to the period of September 2020. Search strategy was prepared with the help of a librarian and is presented in Supplementary Table 1. The mesh search term used were "Printing, Three-Dimensional", "Jaw", "Mandible", "Maxilla" and "Skull".

Following removal of duplicate studies, two reviewers independently screened the relevant articles based on the titles and abstracts, and then read the full text of the included studies. The categorization of the printed as desktop or professional was performed by either searching for the pertaining information from within the published articles or manufacturers website. Two reviewers extracted the data and any disagreement was resolved through consensus. Grey literature and references within the selected studies were also screened. The Kappa statistic was reported to assess the agreement between the reviewers for the selection process.

The data extracted from the selected articles included title, author, year of publication, skeletal structure assessed, sample size, imaging modality, printer type as desktop or professional printer, printing technique, printing material, printing settings, layer resolution, assessment methodology and accuracy. The corresponding author of included articles were contacted for the provision of missing data.

2.4 Critical appraisal

Risk of bias was assessed according to the Joanna Briggs Institute (JBI) through the Critical Appraisal Checklist for Diagnostic Test Accuracy [24]. The tool was modified to allow for better interpretation of the methodological quality. We focused on the questions to observe for the potential problems in the way the index test was conducted and interpreted. In the present review, the following question was modified “If a threshold was used, was it pre-specified?” and split into three questions: 1. Were the imaging modality and parameters described; 2. Was the measuring protocol described; 3. Was the layer resolution described? Two reviewers judged each question as yes, no or unclear.

2.5 Statistical analysis

A meta-analysis was conducted with R software (version 3.5.2) to compare the accuracy of desktop and professional 3D printers based on the mean and absolute mean difference and standard deviation. The heterogeneity was investigated using Q-value and I^2 statistics. Kendall's tau was applied to assess the publication bias and data were pooled using a fixed-effects model to generate a forest plot. A p-value of less than 0.05 was regarded as statistically significant.

3. Results

3.1 Study selection

After eliminating duplicates, 3429 articles were retrieved; 3405 were excluded based on the title and abstract (**Fig. 1**). The remaining 23 studies were analyzed in full and 3 articles [19, 25, 26] were excluded which did not match the inclusion criteria, resulting in 20 articles being eligible for the systematic review. The Kappa value for the agreement between the reviewers was 0.856, which was categorized as an almost perfect agreement according to Landis and Koch [27].

Five studies evaluated the model accuracy utilizing 3D measurements [13, 18, 28-30], whereas 15 articles performed 2D measurements [9, 20-22, 31-41]. The quantitative synthesis only included 5 articles which offered a similar three-dimensional methodology of evaluation and provision of the accuracy as the mean or absolute mean difference between the reference and the printed model.

The 3D evaluation in the studies was performed by an objective color-coded part comparison analysis, which allowed calculation of the mean or mean absolute error between the superimposed original and printed skeletal structure in a Standard Triangle Language (STL) format. The mean difference refers to the difference with the direction of error, while the mean absolute error quantifies the overall magnitude of the error. The studies assessing accuracy based on the 2D linear and/or angular measurements were excluded from the meta-analysis due to the heterogeneity of landmark selection and assessment methodology.

3.2 Study characteristics

The sample size ranged between 1 and 50 printed anatomical models generated from dry human bone [18, 20, 22, 29, 31, 32, 34-38, 41], fresh cadaver [9] or patient data [13, 21, 28, 30, 33, 39, 40]. The included studies focused primarily on printed skeletal models of the mandible (n = 11, 55%) and craniomaxillary complex (n = 9, 45%). The skeletal structures printed in the craniomaxillary region involved craniofacial region, maxilla, midface, orbital region, skull base and whole skull. A summary of the methodologies utilized for preparing the skeletal models and the method of analyzing their accuracy is shown in Supplementary Table 2. The included studies reported that the computed tomography (CT)/ cone-beam CT (CBCT) threshold value for reconstructing the model were determined empirically or (semi-)automatically ranging from 500 to 4000 HU for mandible [21, 33, 37] and 400 to 4000 HU for craniomaxillary complex [33, 35, 37]. The reference models included: dry skull (n = 10), fresh skull (n =

1), patient's CT image (n = 3), STL generated from patient's CT (n = 3) or STL generated from dry skull (n = 2). In addition, one study utilized the model printed with professional printer as a reference [21].

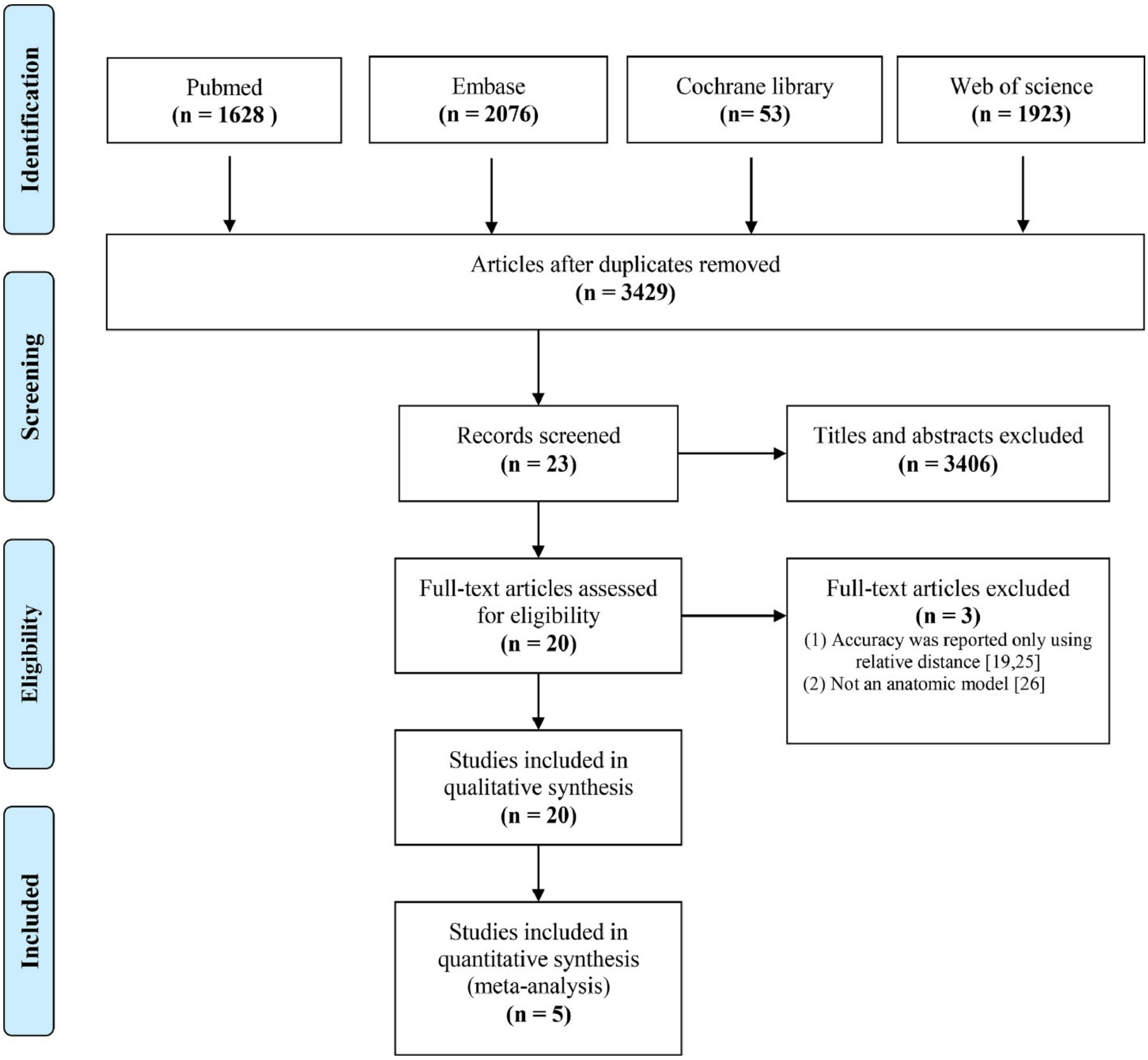

Figure 1. Preferred Reporting Items for Systematic Reviews and Meta-Analyses flowchart of included studies.

3.3 Risk of bias

The risk of bias was found to be low to moderate and the domains which introduced bias were patient selection, index test and reference standard (Supplementary Table 3). The main methodological limitations were related to the index test because some studies did not explicitly provide the fabrication procedure and parameters regarding the printer classification, material, layer resolution, printer settings and post-processing. The imaging modality and parameters were unclear related to the CT/CBCT's field of view, voxel size and slice thickness. The “consecutive or random sample of patients enrolled” and “reference standard results interpreted without knowledge of the results of the index tests” were unclear in all selected studies.

3.4 Qualitative synthesis

The selected studies evaluated the accuracy of 43 printing systems utilizing seven different 3D printing technologies. FDM technology was employed in 11 systems (25.6%), SLA in 8 (18.6%), SLS in 7 (16.3%), MJ in 6 (13.95%), BJ in 6 (13.95%), DLP in 4 (9.3%), and SDL in 1 (2.3%).

Supplementary Table 4 describes the 2D accuracy of the models. The accuracy of mandibular printed models with desktop printers varied between 0.145 mm-0.65 mm [20-22, 31]. For professional printed models, accuracy ranged between 0.079 mm-1.44 mm [31-34, 36-38]. The accuracy of professional printers for printing a craniomaxillary model, ranged between 0.108 mm-1.98 mm [9, 31, 33, 35-37, 40, 41], whereas, only one article reported on the accuracy of printing with a desktop printer (0.28 mm) [31]. One article [39] reported on an overall accuracy of a full cranio-facial skeletal model (craniomaxillary complex + mandible) and found a mean difference of 0.7±0.9 mm between the real anatomical structure and printed model. Based on the layer resolution, 500 µm FDM models had approximately double the error compared to the 100 µm or 250 µm resolutions, both of which showed similar accuracy [31].

Supplementary Table 5 describes the 3D accuracy of the models. Three selected studies assessed the accuracy as absolute value [18, 28, 30] and two studies provide mean value [13, 29]. Based on the absolute value, the accuracy of desktop printed mandibular models varied from 0.08±0.08 mm to 0.60±0.72 mm [18, 28]. For professional printed models, results ranged from 0.07±0.05 mm to 0.15±0.17 mm [28, 30]. Whereas, based on mean values, the mean differences of desktop printed mandibular models was within the range of –0.01±0.16 mm and 0.23±0.39 mm, whereas the professional showed a discrepancy from –0.07±0.08 mm to 0.17±0.13 mm [13, 29].

3.5 Quantitative synthesis

The 3D accuracy of models was compared based on the type of printers (desktop printer and professional printer), printing technology and layer resolution. The included studies analyzed the data based on either mean or absolute mean, which was the basis of the meta-analysis [42]. The p-value of the heterogeneity was not significant, thereby, a fixed effects model was used.

In relation to the printer type, the accuracy of desktop was considered comparable to that of professional printers with low heterogeneity in both subgroups. The professional printer was found to be more accurate. However, no statistically significant difference was observed between both types of printers (**Fig. 2** and **3**). Based on absolute mean values, MJ and SLS technology showed the highest accuracy, followed by

BJ, SLA and DLP, while the FDM technology showed the least accuracy (**Fig. 4**). Nevertheless, when considering the mean values (**Fig. 5**), FDM showed the highest accuracy, followed by SLS, BJ, MJ and SLA, however, a high heterogeneity was detected (I^2: 83.4%). Overall, no significant difference was observed within the technologies. In relation to the layer resolution, differences were compared within two value limits of 0.15 mm and 0.2 mm. The accuracy of models printed with a layer resolution of ≤ 0.15 mm was found to be more accurate compared to a resolution of ≥0.2 mm (**Fig. 6** and **7**). However, no significant difference existed, and the heterogeneity was also found to be low (I^2: 0%).

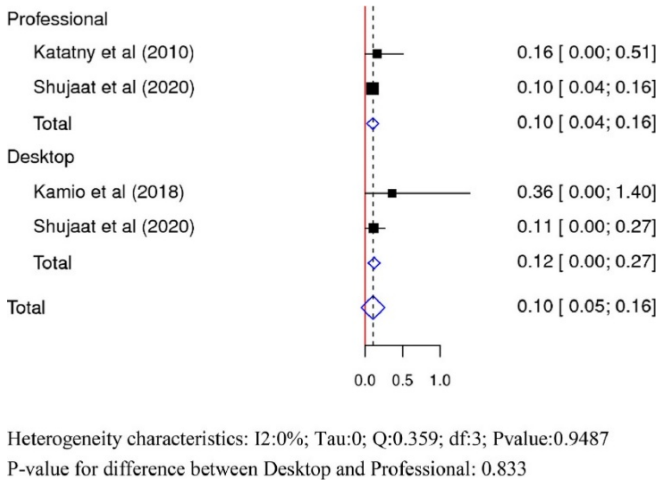

Figure 2. Meta-analysis for deviations expressed as absolute values considering Printer type.

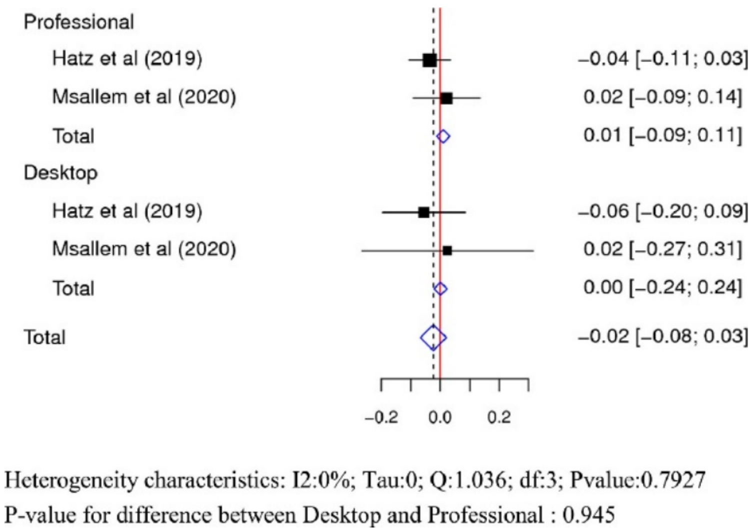

Figure 3. Meta-analysis for deviations expressed as mean values considering Printer type.

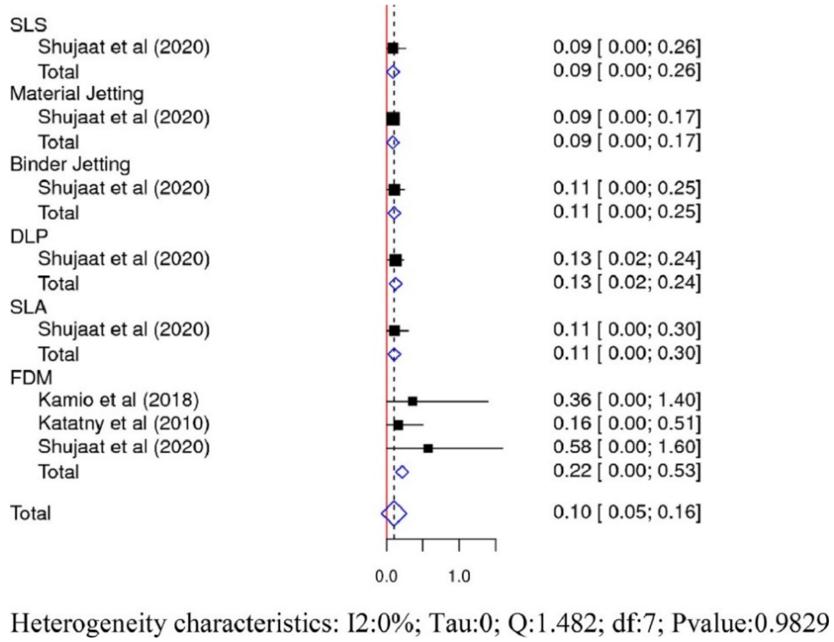

Figure 4. Meta-analysis for deviations expressed as absolute values considering Printing technology.

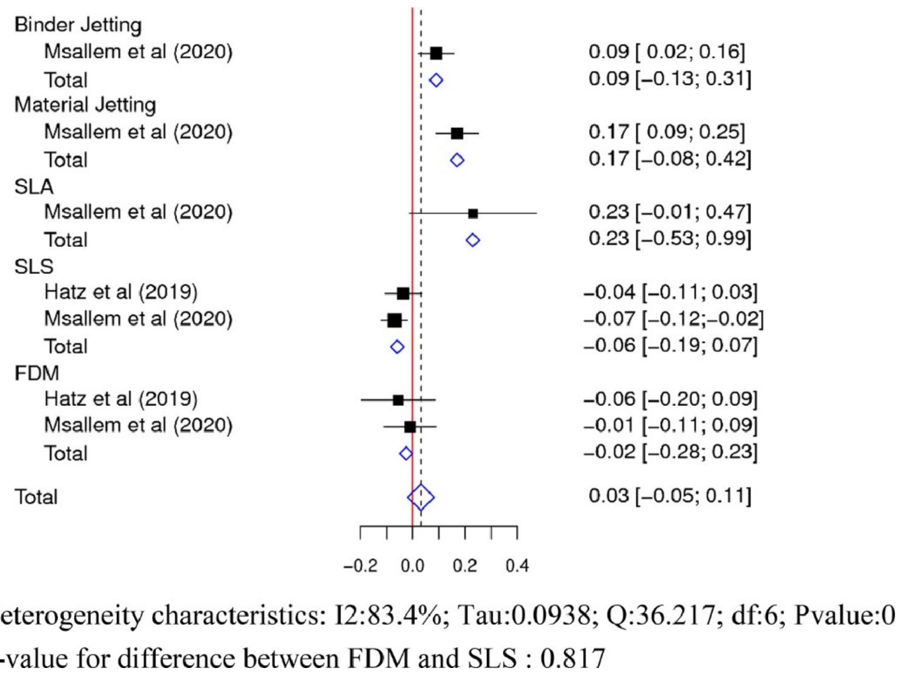

Figure 5. Meta-analysis for deviations expressed as mean values considering Printing technology.

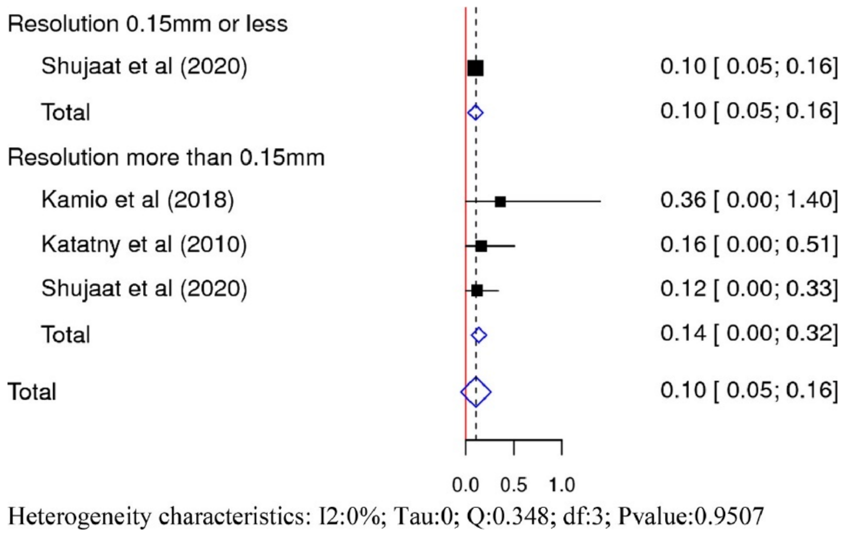

Figure 6. Meta-analysis for deviations expressed as absolute values considering Resolution larger than 0.15 or not.

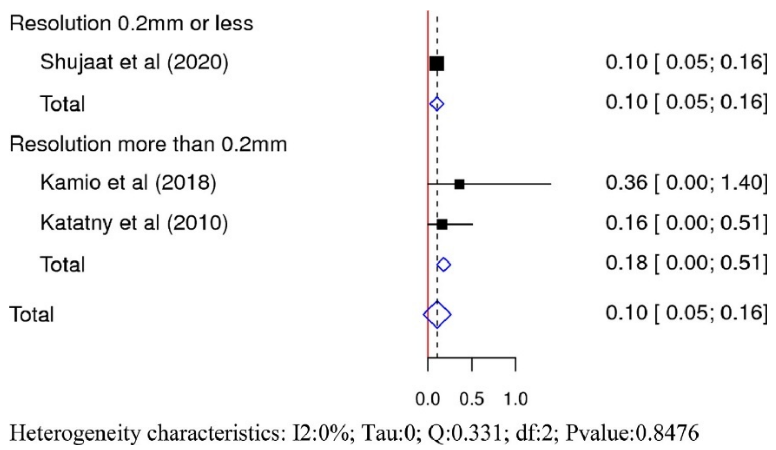

Figure 7. Meta-analysis for deviations expressed as absolute values considering Resolution larger than 0.2 or not.

4. Discussion

The following systematic review aimed to compare the accuracy of desktop and professional 3D printers for printing maxillofacial skeletal models. Based on our findings, the desktop printers offered a clinically acceptable accuracy in comparison to the professional ones, where both type of printers showed a dimensional error within an acceptable range of 2% variability [19]. In relation to the technology, both MJ and SLS revealed a higher accuracy followed by BJ, SLA, DLP and FDM based models.

The desktop printers could be regarded as an excellent alternative for printing skeletal models. However, one might argue that the acceptable range of accuracy of a model should depend on its area of application [43]. For instance, shaping of plates on models might require higher accuracy compared to the model for anatomy teaching, surgery simulation or as a medium for communicating with a patient [10]. In this review, the majority of printers, whether desktop or professional, offered a clinically acceptable dimensional precision which could be utilized for the purpose of preoperative training, surgical guide manufacturing and pre-bending osteosynthesis or reconstruction plates. However, for better understanding the influence of the accuracy of printed model depending on the area of application, it is important to first standardize the methodology of evaluation, as currently no acceptable 2D or 3D methodology exists for defining the clinical acceptable range of the accuracy [28].

With regards to the printing technology, the MJ-based printers are composed of hundreds of micro jetting heads [34] which offered a higher accuracy compared to the FDM technology, where the details of thin bone could not be adequately replicated by a large nozzle diameter of 0.5 mm [31]. Additionally, the FDM-based printers involved in this review were mostly desktop-grade which have a relative longer printing time, low resolution, require post-processing for the removal of support structures and the model has a tendency to shrink and warp during the cooling process [13, 18, 20, 31], thus harming the surface quality. Similarly, the SLA printers require cleaning residual resin and post-curing with ultraviolet light which might partially explain the slightly greater error compared with other technologies [29]. In contrast, the SLS and BJ- based models were printed without support structures and the finishing process only involved sandblasting which might have led to a higher accuracy. Nevertheless, the meta-analysis showed that all technologies showed a similar range of error for printing maxillofacial skeletal models irrespective of the printer type or technology.

Another key aspect of the printing process is the layer resolution, which not only influences the printing time but also the accuracy [18]. Our results demonstrated that the accuracy offered by a desktop printer with a layer resolution of less than 0.2 mm was comparable to that of the professional ones. Additionally, a resolution of ≤0.15 mm showed a higher accuracy compared to a resolution larger than 0.15 mm. Overall, the geometric accuracy of the printed model is highly dependent on the AM technology, the material and layer resolution. At the same instance, further studies need to be performed to investigate the magnitude of error arising at the production and post-processing stage.

Furthermore, the accuracy of models has also been reported to be affected by certain factors during the modeling procedure which include data acquisition, computer data processing [44] and model fabrication [45]. Although it is difficult to quantify the exact error contributed at each step. However, overall most of the included studies showed a dimensional error within a 2% variation, which could be considered as clinically acceptable for the production of maxillofacial skeletal models [19]. Additionally, different imaging modalities and characteristics of anatomy used for creating models inevitably caused standardization issues. Most of the models in this review were generated from a dry skull, which were directly scanned and segmented without soft tissue, whereas the models obtained from patients can generate greater errors due to the obstruction from soft tissue and patient movement [31]. The variability due to slice thickness, voxel size, pitch, tube current and voltage and artifacts have been considered as the main cause of error when printing patient-specific models [46].The majority of included studies relied on computed tomography (CT) scans with a slice thickness less than 1.5 mm to decrease the error for capturing regions of thin bone in the orbital floor or walls of the maxillary sinus [9]. Additionally, a higher resolution was required to obtain detailed information which is prone to a higher risk of patient radiation exposure [9]. A possible alternative to overcome the associated risk of the increased dose is to utilize the state-of-art CBCT devices offering low-dose high-resolution images with artefact reduction algorithms [29].

Another factor which might have influenced the accuracy of models was the application of semiautomatic thresholding for segmenting the structures. The proficiency of an observer for using computer-aided design software can affect the output results [21]. The most optimal method to overcome this error is to apply manual thresholding, however this method is also prone to observer variability and is considered to be labor-intensive [28]. Thereby, requiring further research to optimize the segmentation process by introducing artificial intelligence-based segmentation algorithms [47, 48]. Future studies should concentrate on building a patient-specific model to replicate a realistic scenario, keeping in mind the limitations associated with the segmentation process.

This review had certain limitations. Firstly, the included studies utilized different imaging devices and scanning parameters for the purpose of virtual modeling without considering the error induced at the imaging chain, which could have led to variability within the findings. Secondly, most of the studies assessed accuracy through different non-standardized 2D landmark-based methodologies, thereby further causing bias within the results. Thirdly, the meta-analysis was based on a limited number of studies based on 3D comparison, therefore the results should be interpreted with caution. Fourthly, the models were fabricated with a variety of 3D printers working under different principles, printing parameters, materials and post-processing protocols which also might have resulted in data heterogeneity. The layer resolution of the x, y and z axes was different in the included studies, where the z-axis layer resolution of the included studies was mostly determined by the manufacturer settings and x-y resolution was fixed or manually changed by the operator depending on the printing technique. Other factors such as laser diameter of the SLA and SLS- technology based printers, nozzle diameter of FDM and droplet dimensions of MJ and BJ-based printers were also variable. The dimensional accuracy could also have been influenced by the build orientation i.e. vertical or horizontal and presence of support structure which the studies failed to clarify. Additionally, the curing and post-processing varied amongst different studies, depending on the printing process which might have influenced the mean error. Keep these limitations in mind, all the aforementioned parameters should be standardized if a definite conclusion needs to be drawn. Further research should be conducted to objectively evaluate the amount of error introduced at each step of the printing process and which printer parameters should be standardized to optimize the skeletal models printing in a clinical setting.

5. Conclusions

In the present systematic review, the maxillofacial skeletal models generated from desktop printers offered comparable accuracy to those acquired with professional printers. At the same instance, the geometric accuracy of the model was found to be highly dependent on the printing technology, material and layer resolution, irrespective of the printer classification. However, these findings should be interpreted with caution as the outcomes were based on a limited number of studies utilizing different imaging and printing devices with variable settings. Future studies should be conducted to optimize the imaging and printing parameters to assess the amount of error induced at each step of the printing process before a printer can be qualified for medical–surgical applications.

References

[1] T.D. Ngo, A. Kashani, G. Imbalzano, K.T.Q. Nguyen, D. Hui, Additive manufacturing (3D printing): A review of materials, methods, applications and challenges, Compos. Part B Eng. 143 (2018) 172–196.

[2] A Kessler, R Hickel, M Reymus, 3D printing in dentistry-State of the art, Oper Dent. 45 (2020) 30-40.

[3] A. Louvrier, P. Marty, A. Barrabé, E. Euvrard, B. Chatelain, E. Weber, C. Meyer, How useful is 3D printing in maxillofacial surgery?, J. Stomatol. Oral Maxillofac. Surg. 118 (2017) 206–212.

[4] O.M. Jacobo, V.E. Giachero, D.K. Hartwig, G.A. Mantrana, Three-dimensional printing modeling: application in maxillofacial and hand fractures and resident training, Eur. J. Plast. Surg. 41 (2018) 137–146.

[5] M. Azuma, T. Yanagawa, N. Ishibashi-Kanno, F. Uchida, T. Ito, K. Yamagata, S. Hasegawa, K. Sasaki, K. Adachi, K. Tabuchi, M. Sekido, H. Bukawa, Mandibular reconstruction using plates prebent to fit rapid prototyping 3-dimensional printing models ameliorates contour deformity, Head Face Med. 10 (2014) 45.

[6] D. Hoang, D. Perrault, M. Stevanovic, A. Ghiassi, Today surgical applications of three-dimensional printing: A review of the current literature & how to get started, Ann. Transl. Med. 4 (2016).

[7] E. George, P. Liacouras, F.J. Rybicki, D. Mitsouras, Measuring and establishing the accuracy and reproducibility of 3D printed medical models, Radiographics. 37 (2017) 1424–1450.

[8] N. Martelli, C. Serrano, H. Van Den Brink, J. Pineau, P. Prognon, I. Borget, S. El Batti, Advantages and disadvantages of 3-dimensional printing in surgery: A systematic review, Surg. (United States). 159 (2016) 1485–1500.

[9] P.S. Chang, T.H. Parker, C.W. Patrick Jr, M.J. Miller, The accuracy of stereolithography in planning craniofacial bone replacement., J. Craniofac. Surg. 14 (2003) 164-70.

[10] M. Meglioli, A. Naveau, G.M. Macaluso, S. Catros, Correction to: 3D printed bone models in oral and craniomaxillofacial surgery: a systematic review, 3D Print. Med. 6 (2020) 1–19.

[11] G. Oberoi, S. Nitsch, M. Edelmayer, K. Janjic, A.S. Müller, H. Agis, 3D printing-Encompassing the facets of dentistry, Front. Bioeng. Biotechnol. 6 (2018) 1–13.

[12] S. Ford, T. Minshall, Invited review article: Where and how 3D printing is used in teaching and education, Addit. Manuf. 25 (2019) 131–150.

[13] C.R. Hatz, B. Msallem, S. Aghlmandi, P. Brantner, F.M. Thieringer, Can an entry-level 3D printer create high-quality anatomical models? Accuracy assessment of mandibular models printed by a desktop 3D printer and a professional device, Int. J. Oral Maxillofac. Surg. 49 (2020) 143–148.

[14] G.W. Melenka, J.S. Schofield, M.R. Dawson, J.P. Carey, Evaluation of dimensional accuracy and material properties of the MakerBot 3D desktop printer, Rapid Prototyp. J. 21 (2015) 618–627.

[15] R.H. Awad, S.A. Habash, C.J. Hansen, 3D printing methods, Elsevier Inc., 2018.

[16] S.E. Mowry, H. Jammal, Ã. Clementino, A. Solares, P. Weinberger, A novel temporal bone simulation model using 3D printing techniques, Otol Neurotol. 36 (2015) 1562-5.

[17] Meghan Coakley, Darrell E. Hurt, 3D printing in the laboratory: Maximize time and funds with

customized and Open-Source labware, J Lab Autom. 21 (2016) 489–495.

[18] T. Kamio, K. Hayashi, T. Onda, T. Takaki, T. Shibahara, T. Yakushiji, T. Shibui, H. Kato, Utilizing a low-cost desktop 3D printer to develop a “one-stop 3D printing lab” for oral and maxillofacial surgery and dentistry fields, 3D Print. Med. 4 (2018) 1–2.

[19] J. Asaumi, N. Kawai, Y. Honda, H. Shigehara, T. Wakasa, K. Kishi, Comparison of three-dimensional computed tomography with rapid prototype models in the management of coronoid hyperplasia, Dentomaxillofacial Radiol. 30 (2001) 330–335.

[20] F. Maschio, M. Pandya, R. Olszewski, Experimental validation of plastic mandible models produced by a “low-cost” 3-dimensional fused deposition modeling printer, Med. Sci. Monit. 22 (2016) 943–957.

[21] A.T. Legocki, A. Duffy-Peter, A.R. Scott, Benefits and limitations of entry-level 3-dimensional printing of maxillofacial skeletal models, JAMA Otolaryngol. - Head Neck Surg. 143 (2017) 389–394.

[22] M.A. Rendón-Medina, L. Andrade-Delgado, J.E. Telich-Tarriba, A. Fuente-Del-Campo, C.A. Altamirano-Arcos, Dimensional error in rapid prototyping with open source software and low-cost 3D-printer, Plast. Reconstr. Surg. - Glob. Open. 6 (2018) 1–4.

[23] A. Liberati, D.G. Altman, J. Tetzlaff, C. Mulrow, P.C. Gøtzsche, J.P.A. Ioannidis, M. Clarke, P.J. Devereaux, J. Kleijnen, D. Moher, The PRISMA statement for reporting systematic reviews and meta-analyses of studies that evaluate health care interventions: explanation and elaboration, 2009.

[24] G. Moreno G, T. Pantoja C, Systematic reviews of studies of diagnostic test accuracy, Rev. Med. Chil. 137 (2009) 303–307.

[25] D.J. Thomas, M.A.B.M. Azmi, Z. Tehrani, 3D additive manufacture of oral and maxillofacial surgical models for preoperative planning, Int. J. Adv. Manuf. Technol. 71 (2014) 1643–1651.

[26] G. Sander, H. Kärcher, A. Gaggl, R. Kern, Stereolithography versus milled Three-Dimensional models: Comparison of production method, indication, and accuracy, Comput. Aided Surg. 3 (1998) 248–256.

[27] J. Kottner, L. Audige, S. Brorson, A. Donner, B.J. Gajewski, A. Hróbjartsson, C. Roberts, M. Shoukri, D.L. Streiner, Guidelines for Reporting Reliability and Agreement Studies (GRRAS) were proposed, Int. J. Nurs. Stud. 48 (2011) 661–671.

[28] S. Shujaat, E. Shaheen, F. Novillo, C. Politis, R. Jacobs, Accuracy of cone beam computed tomography–derived casts: A comparative study, J. Prosthet. Dent. (2020) 1–8.

[29] B. Msallem, N. Sharma, S. Cao, F.S. Halbeisen, H.-F. Zeilhofer, F.M. Thieringer, Evaluation of the dimensional accuracy of 3D-printed anatomical mandibular models using FFF, SLA, SLS, MJ, and BJ printing technology, J. Clin. Med. 9 (2020) 817.

[30] I. E-Katatny, S.H. Masood, Y.S. Morsi, Evaluation and validation of the shape accuracy of FDM fabricated medical models, Adv. Mater. Res. 83–86 (2010) 275–280.

[31] C. Petropolis, D. Kozan, L. Sigurdson, Accuracy of medical models made by consumer-grade fused deposition modelling printers, Can. J. Plast. Surg. 23 (2015) 91–94.

[32] R. Olszewski, P. Szymor, M. Kozakiewicz, Accuracy of three-dimensional, paper-based models generated using a low-cost, three-dimensional printer, J. Cranio-Maxillofacial Surg. 42 (2014) 1847–1852.

[33] I. El-Katatny, S.H. Masood, Y.S. Morsi, Error analysis of FDM fabricated medical replicas, Rapid Prototyp. J. 16 (2010) 36–43.

[34] D. Ibrahim, T.L. Broilo, C. Heitz, M.G. de Oliveira, H.W. de Oliveira, S.M.W. Nobre, J.H.G. dos Santos Filho, D.N. Silva, Dimensional error of selective laser sintering, three-dimensional printing and PolyJet™ models in the reproduction of mandibular anatomy, J. Cranio-Maxillofacial Surg. 37 (2009) 167–173.

[35] D.N. Silva, M. Gerhardt de Oliveira, E. Meurer, M.I. Meurer, J.V. Lopes da Silva, A. Santa-Bárbara, Dimensional error in selective laser sintering and 3D-printing of models for craniomaxillary anatomy reconstruction, J. Cranio-Maxillofacial Surg. 36 (2008) 443–449.

[36] A. Nizam, R.N. Gopal, L. Naing, A. B. Hakim, A. R. Samsudin, Dimensional accuracy of the skull models produced by Rapid Prototyping technology using Stereolithography apparatus, Arch. Orofac. Sci. 1 (2006) 60–66.

[37] J.Y. Choi, J.H. Choi, N.K. Kim, Y. Kim, J.K. Lee, M.K. Kim, J.H. Lee, M.J. Kim, Analysis of errors in medical rapid prototyping models, Int. J. Oral Maxillofac. Surg. 31 (2002) 23–32.

[38] J.F. Bouyssié, S. Bouyssié, P. Sharrock, D. Duran, Stereolithographic models derived from X-ray computed tomography Reproduction accuracy, Surg. Radiol. Anat. 19 (1997) 193–199.

[39] E. Berry, J.M. Brown, M. Connell, C.M. Craven, N.D. Efford, A. Radjenovic, M.A. Smith, Preliminary experience with medical applications of rapid prototyping by selective laser sintering, Med. Eng. Phys. 19 (1997) 90–96.

[40] J. Kragskov, S. Sindet-Pedersen, C. Gyldensted, K.L. Jensen, A comparison of three-dimensional computed tomography scans and stereolithographic models for evaluation of craniofacial anomalies, J. Oral Maxillofac. Surg. 54 (1996) 402–411.

[41] T.M. Barker, W.J.S. Earwaker, D.A. Lisle, Accuracy of stereolithographic models of human anatomy, Australas. Radiol. 38 (1994) 106–111.

[42] P. Galanis, Systematic review and meta-analysis, Arch. Hell. Med. 26 (2009) 826–841.

[43] R. Olszewski, Three-dimensional rapid prototyping models in cranio-maxillofacial surgery: systematic review and new clinical applications, 2013.

[44] E. Huotilainen, R. Jaanimets, J. Valášek, P. Marcián, M. Salmi, J. Tuomi, A. Mäkitie, J. Wolff, Inaccuracies in additive manufactured medical skull models caused by the DICOM to STL conversion process, J. Cranio-Maxillofacial Surg. 42 (2014) 259–265.

[45] J.M. Pinto, C. Arrieta, M.E. Andia, S. Uribe, J. Ramos-Grez, A. Vargas, P. Irarrazaval, C. Tejos, Sensitivity analysis of geometric errors in additive manufacturing medical models, Med. Eng. Phys. 37 (2015) 328–334.

[46] J. Winder, R. Bibb, Medical rapid prototyping technologies: State of the art and current limitations for application in oral and maxillofacial surgery, J. Oral Maxillofac. Surg. 63 (2005) 1006–1015.

[47] Z. Kong, T. Li, J. Luo, S. Xu, Automatic tissue image segmentation based on image processing

and Deep Learning, J. Healthc. Eng. (2019).

[48] J. Minnema, M. van Eijnatten, W. Kouw, F. Diblen, A. Mendrik, J. Wolff, CT image segmentation of bone for medical additive manufacturing using a convolutional neural network, Comput. Biol. Med. 103 (2018) 130–139.

ARTICLE 2

Trueness of cone-beam computed tomography-derived skull models fabricated by different technology-based three-dimensional printers

Wang X. [1,2]
Shujaat S. [1,3]
Shaheen E. [1]
Ferraris E. [4]
Jacobs R. [1,5]

[1] OMFS-IMPATH Research Group, Department of Imaging & Pathology, Faculty of Medicine, KU Leuven & Oral and Maxillofacial Surgery, University Hospitals Leuven, Leuven, Belgium.

[2] Department of Oral and Maxillofacial Surgery, The First Affiliated Hospital of Harbin Medical University, Harbin, China.

[3] Department of Maxillofacial Surgery and Diagnostic Sciences, College of Dentistry, King Saud Bin Abdulaziz University for Health Sciences, Saudi Arabia.

[4] Department of Mechanical Engineering, KU Leuven Campus De Nayer, Sint-Katelijne-Waver, Belgium.

[5] Department of Dental Medicine, Karolinska Institutet, Huddinge, Sweden.

Accepted in *BMC Oral Health*.

Abstract

Background: Three-dimensional (3D) printing is a novel innovation in the field of craniomaxillofacial surgery, however, a lack of evidence exists related to the comparison of the trueness of skull models fabricated using different technology-based printers belonging to different cost segments.

Methods: A study was performed to investigate the trueness of cone-beam computed tomography-derived skull models fabricated using different technology based on low-, medium-, and high-cost 3D printers. Following the segmentation of a patient's skull, the model was printed by: i) a low-cost fused filament fabrication printer; ii) a medium-cost stereolithography printer; and iii) a high-cost material jetting printer. The fabricated models were later scanned by industrial computed tomography and superimposed onto the original reference virtual model by applying surface-based registration. A part comparison color-coded analysis was conducted for assessing the difference between the reference and scanned models. A one-way analysis of variance (ANOVA) with Bonferroni correction was applied for statistical analysis.

Results: The model printed with the low-cost fused filament fabrication printer showed the highest mean absolute error (1.33±0.24 mm), whereas both medium-cost stereolithography-based and the high-cost material jetting models had an overall similar dimensional error of 0.07±0.03 mm and 0.07±0.01 mm, respectively. Overall, the models printed with medium- and high-cost printers showed a significantly ($p<0.01$) lower error compared to the low-cost printer.

Conclusions: Both stereolithography and material jetting based printers, belonging to the medium- and high-cost market segment, were able to replicate the skeletal anatomy with optimal trueness, which might be suitable for patient-specific treatment planning tasks in craniomaxillofacial surgery. In contrast, the low-cost fused filament fabrication printer could serve as a cost-effective alternative for anatomical education, and/or patient communication.

Keywords: Printing, three-dimensional; Computer-aided design; Dimensional measurement accuracy; Tomography; Skull

1. Introduction

Recent advancements in additive manufacturing (AM), also known as three-dimensional (3D) printing and rapid prototyping (RP), have led to an ever-increasing impact on the field of craniomaxillofacial surgery [1]. The manufacturing of anatomically true skull models from cone-beam computed tomography (CBCT) and computed tomography (CT) data have been successfully used for improving diagnostic accuracy, treatment planning and simulation of complex surgical procedures, training, and anatomical education [2]. By offering further spatial details on a patient's anatomy and pathology, these models act as a surgical aid, increasing the accuracy of the procedure and leading to more predictable post-operative results with reduced risk of complications [3]. The main clinical applications of patient-specific 3D printed skull models include pre-bending reconstruction plates, prosthesis engineering, and fabrication of personalized surgical guides and titanium-based implants for craniomaxillofacial defects [4]. Additionally, 3D printed models also serve as a supplementary tool to improve the informed consent process and offer an effective way of communication with the patients. From an educational perspective, compared to the intangible virtual models and ethically challenged cadaveric skull models, 3D printed skull models are a key for laying a solid foundation for novices to learn the maxillofacial surgical procedures and anatomical learning [5, 6].

Currently, a wide variety of 3D printers exist in the market for printing maxillofacial skeletal models. These printers can be further classified as low-cost desktop/consumer grade and high-cost professional 3D printers [7]. Fused filament fabrication machines are among the most widely adopted low-cost/consumer grade desktop 3D printers [8]. They are mostly priced between $\$1500$–$\$7000$, having a build size of less than $10 \times 10 \times 10$ inches, layer thickness between 100-$300\ \mu\mathrm{m}$, 0.5% dimensional tolerance normally based on calibration cube as a benchmark, slow printing process and utilize thermoplastic filaments as the main printing material, such as polylactic acid (PLA) and acrylonitrile butadiene styrene (ABS). In contrast, the majority of higher cost professional 3D printers are either selective laser sintering (SLS), selective laser melting (SLM), or UV (ultraviolet) jet-based technologies (e.g. multi jetting) for printing metals and high-performance polymers in addition to the aforementioned materials. They are priced between \$20,000-\$200,000 with a build size bigger than $12 \times 12 \times 12$ inches, layer thickness down to a few tens of microns, dimensional tolerance of 0.15% based on calibration cube, and the ability of fast and batch printing [9, 10, 11].

For preoperative planning and clinical training, craniomaxillofacial 3D models are typically manufactured via in-house or by commercial external printing service centers utilizing high-cost professional-grade 3D printers. The expertise of operators, cost and delivery time of the models might influence the patient's treatment process, consequently, limiting their general applicability [12, 13]. In order to propel the application of 3D printers and increase their generalizability, it is essential to assess whether desktop printers can produce skull models with comparable trueness to high-cost printers. Previous studies have demonstrated that low-cost printers offer comparable trueness to that of professional ones when printing specific anatomical structures, such as the mandible and orbital region [7, 14, 15]. However, there is insufficient evidence to assess the trueness or precision of a 3D printed complete skull model consisting of craniomaxillary complex and mandible. In addition, only a few studies have utilized a 3D assessment method [7, 16]. Most studies have been dependent on landmark-based methodologies that are prone to human error and variability [17, 18]. There is a lack of evidence comparing the trueness of skull models fabricated using printers from different cost segments. Therefore, the aim of this study was to investigate the trueness of CBCT-derived skull models fabricated using different technology based on low-, medium-, and high-cost 3D printers.

2. Methods and materials

This study followed the World Medical Association Declaration of Helsinki on medical research. The study's retrospective collection and use of patient imaging data was approved by the Ethical Review Board of the University Hospitals Leuven in Leuven, Belgium (reference number: S64493).

2.1 Data acquisition

A 32-year-old female patient's CBCT image consisting of a normal complete skull (craniomaxillary complex and mandible) without any pathological condition or artefacts was retrospectively obtained from the Dentomaxillofacial Radiology Center (University Hospitals of Leuven, Leuven, Belgium). The scanning was performed using NewTom VGI evo (Verona, Italy) at 110 kV tube voltage, 0.3 mm slice thickness and 24×19 cm field of view. The image was stored in a Digital Imaging and Communications in Medicine (DICOM) format.

2.2 Model design

The DICOM images were imported into Mimics 22.0 (Materialise, Leuven, Belgium), where thresholding-based semi-automatic segmentation of the skeletal structures was performed (**Fig. 1a, 1b, 1c**). Manual delineation of the bony contours was carried out to improve either the quality of overall segmentation or in situations where thresholding was not enough to sufficiently segment the regions with thin structures, such as sinuses, nasal region and margins of foramina. It involved manual addition or removal of the bone mask using eclipse and the livewire function of the software. The operator scrolled through all the slices in coronal, axial, and sagittal planes to confirm that the region of interest was completely masked without any over- or under-estimation of the margins. The segmented skull was converted to standard tessellation language (STL) format and imported into 3-Matic 14.0 (Materialise, Leuven, Belgium), where the craniomaxillary part of the skull was split at the mid-sagittal plane into two halves (**Fig. 1d**). The splitting was performed to allow for surface inspection of the interior parts of the skull at a later step. Additionally, snap hooks and grooves were designed to attach and detach the two segments. The final STL data for the purpose of printing consisted of left skull, right skull and mandible (**Fig. 1e**).

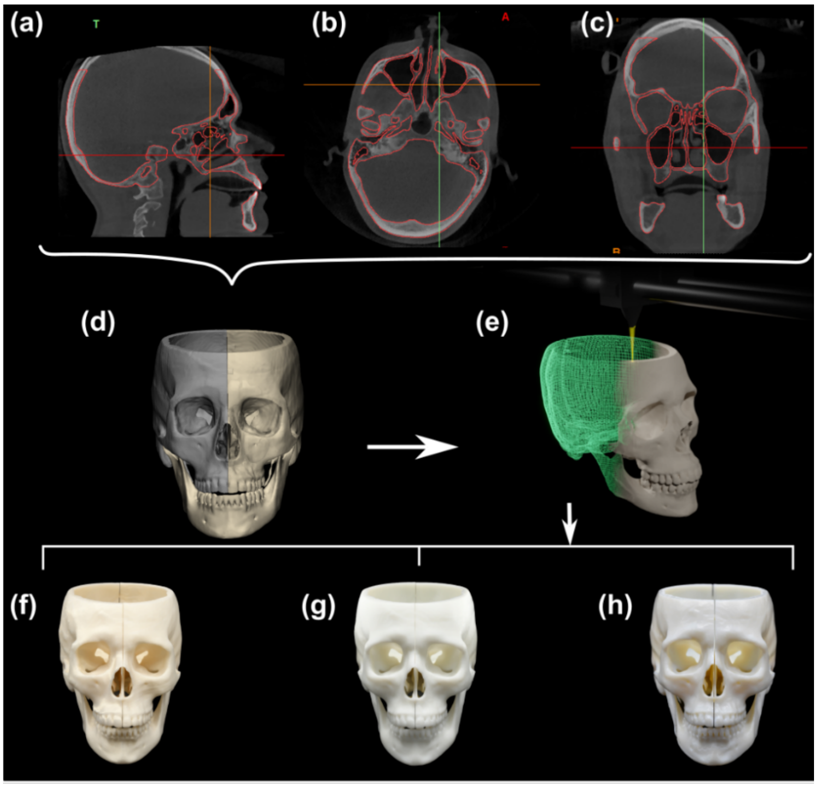

Figure 1. Workflow of 3D printing. (a) Segmentation of the CBCT-derived skull in sagittal view. (b) Segmentation of the CBCT-derived skull in axial view. (c) Segmentation of the CBCT-derived skull in coronal view. (d) STL of designed 3 anatomical parts: a mandible and 2 hemimaxillofacial complexes. (e) Model fabrication. (f) A photo of 3D printed low-cost FFF model by Prusa i3 MK3S. (g) A photo of 3D printed medium-cost SLA model by ShapeSolid A600. (h) A photo of 3D printed high-cost MJ model by Objet 350.

2.3 3D printing

Three different printing technologies and printers were utilized for the fabrication of the model: a low-cost Prusa i3 MK3S printer (Prusa research, Prague, Czech Republic; Fused Filament Fabrication, FFF technology) (**Fig. 1f**), a medium-cost ShapeSolid A600 printer (Lexcent, Shenzhen, China;

Stereolithography, SLA technology) (**Fig. 1g**), and a high-cost Objet 350 printer (Stratasys, Eden Prairie, MN, USA; Material Jetting, MJ technology) (**Fig. 1h**). **Table 1** describes the specifications of the printers and materials. The selection of material and settings were based on each company's recommendations for printing anatomical skeletal models.

Table 1. Model specifications of the high, medium and low-cost printers.

Printer type	Printer name, manufacturer	Printing technique	Material	Post-processing
High-cost printer	Objet Connex 350 (Stratasys, Eden Prairie, MN, USA)	MJ	VeroWhite	Pressured waterjet
Medium-cost printer	ShapeSolid A600 (Lexcent, Shenzhen,China)	SLA	DSM123 resin	Support removal, sanding, rinsing, sand-blasted
Low-cost printer	Prusa i3 MK3S (Prusa research, Prague, Czech Republic)	FFF	Prusament PLA Vanilla White	Support removal

Figure 2 shows the printing parameters and cost of the low, medium and high-cost printers. Each printer was used to fabricate one model (n=3). Since the model printing had been outsourced, the model printing and post-processing procedures were conducted by experienced 3D printing technicians.

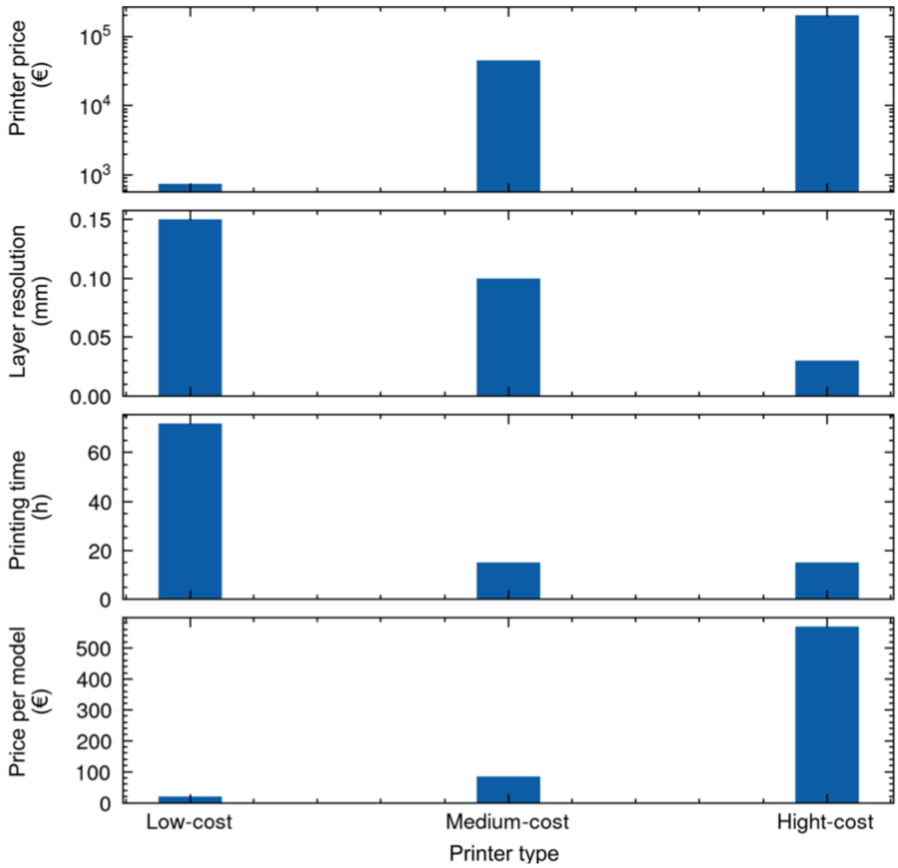

Figure 2. Printing parameters and cost of the low, medium and high-cost printers.

2.4 3D scanning and model comparison

The fabricated models were scanned with an industrial CT (Zeiss Metrotom 6 Scout system, Zeiss, US) at $140\,\mathrm{kV}$, $50\,\mathrm{W}$, $350\,\mathrm{ms}$ exposure time per picture, 3008 pictures in $360°$ and $80\,\mu\mathrm{m}$ original voxel size. STL files were calculated in GOM Volume Inspect (GOM Inspect, Braunschweig, Germany). Later, both the original (reference) and scanned STLs were imported into 3-Matic 14.0 (Materialise). The scanned STLs of the printed models were superimposed onto the original STL by applying surface-based registration. The registration was semi-automated in nature where the operator first added corresponding reference points onto the reference and scanned models for achieving a close alignment of the matched data in a similar 3D space. Following point-based registration, a global co-registration function with enough iterations was applied which automatically fine-tuned the registration with maximal conformance till best fit of both models was achieved without the presence of any visible spatial changes. A part comparison color-coded distance analysis was conducted for assessing the overall 3D differences or discrepancies between the surfaces of reference and scanned STLs of the printed models.

2.5 Statistical analysis

Mean error, mean absolute error (MAE) and root mean square (RMS) values were calculated, where the mean error refers to the positive or negative deviation error, while the MAE refers to the overall magnitude of the error as shown in the Equation (1).

$$MAE = \frac{1}{n}\sum_{i=1}^{n}|x_i - x| \tag{1}$$

The volumetric error between reference and printed models was calculated using relative volumetric difference (RVD) as shown in the Equation (2). It allows to compare the magnitude of volumetric difference regardless of the absolute values.

$$\mathrm{RVD} = \frac{|\mathrm{Volume}_1 - \mathrm{Volume}_2|}{(\mathrm{Volume}_1 + \mathrm{Volume}_2) \div 2} \times 100\% \tag{2}$$

Data were analyzed using IBM SPSS Statistics for Windows, version 21.0 (IBM Corp., Armonk, NY, USA). The Shapiro-Wilk test was used to investigate assumptions of normality. A one-way analysis of variance (ANOVA) with Bonferroni correction was applied for multiple comparisons between different printers and *p* value of < 0.05 was considered statistically significant.

3. Results

The printing process of all printers went smoothly without any issues. However, qualitative observation of the models following post-processing stage revealed that the low-cost FFF model exhibited noticeable rough patches at the right temporal region and left skull base. Apart from that, no other flaws were detected with the other models.

Taking into account the RMS values, the high-cost MJ, medium-cost SLA and low-cost FFF models observed an average discrepancy of $0.13 \pm 0.04\,\mathrm{mm}$, $0.10 \pm 0.04\,\mathrm{mm}$, and $1.69 \pm 0.31\,\mathrm{mm}$, respectively (**Table 2**), where low-cost FFF model showed significantly higher discrepancy compared to both high-cost MJ- and medium-cost SLA-based models (p=<0.001). Considering the overall mean absolute error, the low-cost FFF model showed the highest discrepancy ($1.33 \pm 0.24\,\mathrm{mm}$), whereas both the high-cost MJ- and medium-cost SLA-based models had an overall similar dimensional error of $0.07 \pm 0.01\,\mathrm{mm}$ and $0.07 \pm 0.03\,\mathrm{mm}$, respectively (**Fig. 3a, 3b, 3c**).

Table 2. Summary of mean absolute error (mm) for each printed model; mean ± standard deviation values.

3D printed model	Anatomy	MAE	RMS
High-cost MJ model	Left skull	0.08 ± 0.14	0.16
	Right skull	0.07 ± 0.12	0.14
	Mandible	0.07 ± 0.06	0.09
	Overall	0.07 ± 0.01	0.13 ± 0.04
Medium-cost SLA model	Left skull	0.08 ± 0.08	0.11
	Right skull	0.09 ± 0.09	0.13
	Mandible	0.04 ± 0.04	0.06
	Overall	0.07 ± 0.03	0.10 ± 0.04
Low-cost FFF model	Left skull	1.17 ± 0.95	1.51
	Right skull	1.22 ± 0.91	1.52
	Mandible	1.60 ± 1.29	2.06
	Overall	1.33 ± 0.24	1.69 ± 0.31

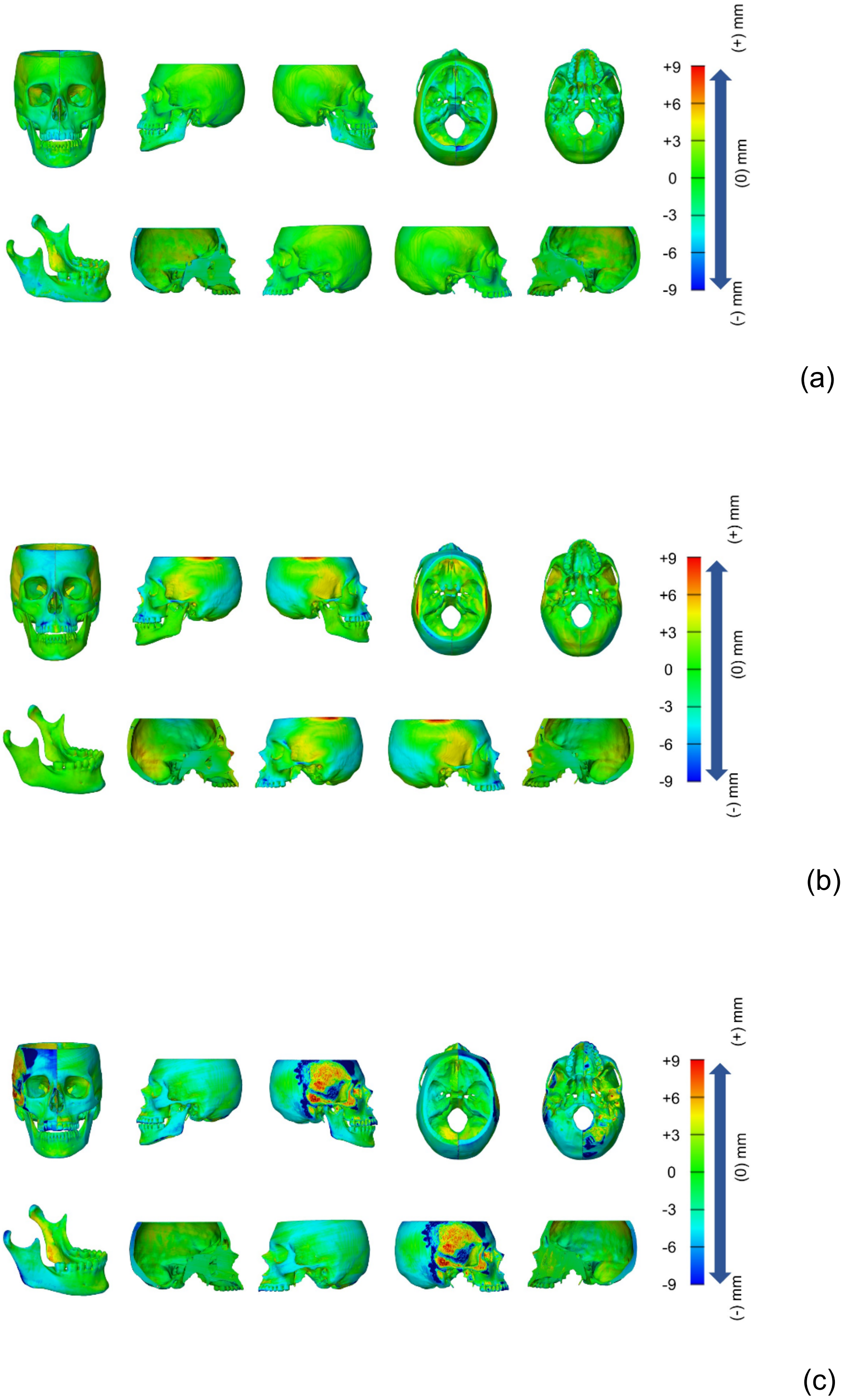

Figure 3. Part comparison analysis of color mapping between the reference and scanned STLs of the models printed with high-, medium-, and low-cost 3D printers. (a) High-cost MJ model by Objet 350. (b) Medium-cost SLA model by ShapeSolid A600. (c) Low-cost FFF model by Prusa i3 MK3S. From left to right: front view of skull; left view of skull; right view of skull; upper view of craniomaxillary complex; bottom

view of craniomaxillary complex; side view of mandible; internal side of left skull; external side of left skull; external side of right skull; internal side of right skull.

Based on the mean error, the FFF model had the highest overall surface error of $-1.23 \pm 0.32\,\mathrm{mm}$ (**Table 3**). The medium-cost SLA model provided a more precise replica ($0.03 \pm 0.01\,\mathrm{mm}$), however, slight expansion was observed at the superior margin of the skull. The high-cost MJ model demonstrated the lowest mean error ($-0.00 \pm 0.03\,\mathrm{mm}$). Overall, the models printed with medium- and high-cost printers showed a significantly ($p < 0.01$) lower error compared to the low-cost printer, while there were no additional significant geometrical differences found. According to the RVD of printed anatomical structures (Table 4), the high-cost MJ and medium-cost SLA models had relatively low RVD values, ranging from 0.88% to 9.51%. In contrast, the low-cost FFF printer had significantly higher RVD values, ranging from 49.86% to 77.45% across all three anatomical structures. Overall, both MJ and SLA model showed significantly lower RVD compared to low-cost FFF models (p<0.001). In relation to anatomical structures, both MJ and SLA models exhibited a lower RVD for mandible compared to the craniomaxillary complex.

On the other hand, as from **Figure 2**, the FFF model costed a fraction of the others (about 5% and 25% as compared to the MJ and SLA 3D printed models, respectively), but required approximately 5 times longer to print.

Table 3. Summary of mean error (mm) for each printer; mean ± standard deviation values.

3D printed model	Anatomy	Mean	RMS
High-cost MJ model	Left skull	0.01 ± 0.16	0.16
	Right skull	0.01 ± 0.14	0.14
	Mandible	-0.03 ± 0.08	0.09
	Overall	-0.00 ± 0.03	0.13 ± 0.04
Medium-cost SLA model	Left skull	0.02 ± 0.11	0.11
	Right skull	0.03 ± 0.12	0.13
	Mandible	0.03 ± 0.05	0.06
	Overall	0.02 ± 0.01	0.10 ± 0.04
Low-cost FFF model	Left skull	-1.10 ± 1.00	1.50
	Right skull	-1.00 ± 1.10	1.50
	Mandible	-1.60 ± 1.30	2.10
	Overall	-1.23 ± 0.32	1.70 ± 0.31

Table 4. Summary of relative volume difference (%) for each printer.

3D printed model	Anatomy	RVD
High-cost MJ model	Left skull	6.19%
	Right skull	9.04%
	Mandible	0.93%
Medium-cost SLA model	Left skull	6.32%
	Right skull	9.51%
	Mandible	0.88%
Low-cost FFF model	Left skull	61.73%
	Right skull	49.86%
	Mandible	77.45%

4. Discussion

In the era of personalized precision medicine, patient-specific 3D printed skeletal models derived from medical imaging datasets have become a standard tool [19]. An anatomically true skull is a fundamental requirement in the treatment planning workflow for complex craniomaxillofacial surgical cases and modern medical education [5]. Recent advances in the 3D printing industry have drastically lowered the price tag of the printers, however, few studies have been performed to assess whether consumer grade 3D printing technologies, such as FFF can offer a precise and true alternative to the higher-cost and professional solutions. As a result, 3D printers can be integrated into the workflows of majority of the hospitals with financial constraints. In this work, the trueness of printed skull models using a low-, a medium-, and a high-cost 3D printer was evaluated.

Due to the multi-dimensionality and complex nature of a human skull, its accurate anatomical representation is vital in all areas of craniomaxillofacial surgery [14]. The trueness of a 3D printed model is greatly dependent on the image acquisition and assessment technique [20, 21]. Since the trueness of 3D printing may be affected by the variety of imaging modalities and parameters related to slice thickness and voxel size [10], the current work employed CBCT data with a slice thickness of 0.3 mm. It would be intriguing to investigate the result of acquiring data from a pathological skull generated by a conventional CT with various scanning parameters. Traditional evaluation methods include landmark-based linear and/or angular measurements using calipers or virtual models of the printed models scanned with CT/CBCT acquisition devices [10]. In the present study, an industrial CT scanner was used to generate the surface of the printed skulls and after surface registration, part comparison analysis was employed to compare the printed skulls to the reference model. The industrial CT scanners have been known to offer higher accuracy for inspection of complex and internal features produced by additive manufacturing compared to CT/CBCT devices [22]. Furthermore, compared to traditional landmark-based methods, which are prone to human error and variability depending on the observer, the semi-automatic trueness assessment methodology applied in the present work is more reliable [23].

A previous study showed that a dimensional linear error within the range of 2% variability could be considered as clinically acceptable for the production of maxillofacial skeletal models [24]. Similarly, no studies were found assessing the clinically acceptable range of error based on 3D methodologies. It should be kept in mind that the trueness of a model is dependent on the task at hand, where higher trueness is mandatory in cases where pre-bending of reconstructive plates, surgical guide manufacturing and implant fabrication are required. Evidence suggests that trueness value of a model is also a prerequisite for reducing the time of operation, the duration of bleeding, and the postoperative morbidities of the patient [20]. In contrast, a slight room for compromise exists if a 3D model is printed for educational purposes where trueness is not a crucial requirement as that for surgical simulation or clinical scenario replication [14].

According to the findings of the current study, SLA and MJ offer a medium- and high-cost solution with a comparable mean absolute error of less than 0.1 mm, respectively, which could be considered as clinically acceptable for tasks involving treatment planning in craniomaxillofacial surgery. The low-cost FFF model showed an overall discrepancy of greater than 1 mm that might affect how pre-bent plates, surgical guides and implants fit. Furthermore, the longer printing time, up to 5 times longer than the medium- and high-cost printer, could further influence its efficiency in a 3D workflow, thereby, confirming its inapplicability for clinical applications. Nonetheless, it provides a practical and cost-effective solution for simulating procedures and anatomical education, as the printer was able to replicate the skeletal anatomy. It is also noteworthy that complexity of anatomical structures being printed should also be taken into consideration, as the craniomaxillary complex showed more deviation than mandible.

The low-cost FFF printer utilized in the present study showed a higher amount of discrepancy compared to other studies, whereas both consumer-grade and professional printers showed comparable trueness for printing skeletal models [7, 8, 16, 25]. The trueness of an FFF based model has been known to be mostly affected by the layer thickness and nozzle diameter. In this study, a nozzle size of 0.4 mm was used with a layer thickness of 0.15 mm. The printing strategy, infill density and print orientation, along with the manufacturing parameters (extrusion temperature and bed temperature) might also play a role towards the model's trueness [26]. The infill density applied in the present study was 15%, which was similar to the range of 10% to 50% reported in the previous studies [7, 12, 15, 16]. The manufacturing settings of 0.15 mm layer resolution, 200°C extruder temperature and bed heat of 60°C, were in accordance with the settings proposed by Rendón-Medina et al [17]. Even with the optimized settings, an increased error was observed specifically at the temporal region and skull base of the right and left skull respectively, which could have been due to the build orientation. Another source of error could have been induced by the removal of support structures at the post-processing step. In this context, it is also relevant to know that the use of high-end/professional FFF industrial 3D printers, featuring high throughput nozzle, temperature controlled closed chamber and/or higher axes resolution, could have facilitated the productions of more true models, albeit at higher cost with a longer print time [20]. Moreover, the impact of build orientation on the trueness of the models was not investigated, which should be considered in future studies.

The trueness of the SLA model was in accordance with other studies, where SLA was found to be optimal for fabricating skeletal structures with intricate details, given its superior resolution, ultimately related to the laser positional accuracy [27]. Likewise, MJ was able to optimally print the complex anatomical structures with a finest layer resolution and provided a better surface quality, which was also consistent with previous studies [27].

The study had certain limitations. Firstly, the study was limited to a small sample of three printers with different technologies and materials which cannot be generalized to all the printers. Secondly, the selection of material could have also influenced the trueness, which also needs to be investigated in further studies. Hence, it is important to investigate the impact of different materials and additive components on material conversion and properties [26]. Thirdly, since just one normal skull was examined in this work, further research is required to determine how it relates to the pathological skull. Fourthly, owing to the small sample size and only trueness being evaluated, the findings of the study should be interpreted with caution. Future studies are recommended to assess the model's accuracy with a larger sample size. Fifthly, the cost-effectiveness in this study was only based on the printer and the model price, thereby, further studies are also recommended to perform a detailed cost-analysis to include the costs related to electricity, maintenance, labor and license acquisition/renewal. Lastly, haptic feedback of the models for simulating surgical procedures was not assessed. In this respect, although the FFF and SLA material pallet is continuously enlarging, MJ technology is still the most viable option offering the largest range of materials for simulating soft and hard tissue.

5. Conclusions

Both stereolithography and multi-jetting were able to replicate the skeletal anatomy on a medium- and high-cost printer, respectively, with the least amount of error, thereby confirming their applicability for clinical application, such as pre-bending plates and fabricating implants. Desktop/consumer grade FFF printer offered the highest discrepancy which might not be optimal for clinical applications, however, it could serve as a cost-effective alternative for surgical simulation, anatomical education, and/or patient communication.

References

[1] Chadha U, Abrol A, Vora NP, Tiwari A, Shanker SK, Selvaraj SK. Performance evaluation of 3D printing technologies: a review, recent advances, current challenges, and future directions. Progress in Additive Manufacturing. (2022) 853–886.

[2] Ostaș D, Almășan O, Ileșan RR, Andrei V, Thieringer FM, Hedeșiu M, et al. Point-of-care virtual surgical planning and 3D printing in oral and cranio-maxillofacial surgery: a narrative review. J Clin Med. 11(2022).

[3] S. Pillai, A. Upadhyay, P. Khayambashi, I. Farooq, H. Sabri, M. Tarar, K.T. Lee, I. Harb, S. Zhou, Y. Wang, S.D. Dental 3d-printing: Transferring art from the laboratories to the clinics, Polymers (Basel). 13 (2021) 1–25.

[4] Zoabi A, Redenski I, Oren D, Kasem A, Zigron A, Daoud S, et al. 3D Printing and virtual surgical planning in oral and maxillofacial surgery. J Clin Med. 11 (2022).

[5] M. Meglioli, A. Naveau, G.M. Macaluso, S. Catros, Correction to: 3D printed bone models in oral and craniomaxillofacial surgery: a systematic review, 3D Print. Med. 6 (2020) 1–19.

[6] M. G Noureldin, N. Y Dessoky, 3D Printing: Towards the Future of Oral and Maxillofacial Surgery, Acta Sci. Dent. Scienecs. 4 (2020) 107–112.

[7] C.R. Hatz, B. Msallem, S. Aghlmandi, P. Brantner, F.M. Thieringer, Can an entry-level 3D printer create high-quality anatomical models? Accuracy assessment of mandibular models printed by a desktop 3D printer and a professional device, Int. J. Oral Maxillofac. Surg. 49 (2020) 143–148.

[8] Kamio T, Onda T. Fused deposition modeling 3D printing in oral and maxillofacial surgery: problems and solutions. Cureus. 14(2022).

[9] Melenka GW, Schofield JS, Dawson MR, Carey JP. Evaluation of dimensional accuracy and material properties of the MakerBot 3D desktop printer. Rapid Prototyp J. (2015) 21(5):618–27.

[10] X. Wang, S. Shujaat, E. Shaheen, R. Jacobs, Accuracy of desktop versus professional 3D printers for maxillofacial model production. A systematic review and meta-analysis, J. Dent. (2021) 103741.

[11] C. Meghan, E.H. Darrell. 3D printing in the laboratory: maximize time and funds with customized and open-source labware, J Lab Autom. 21 (2016) 489–95.

[12] Czyżewski W, Jachimczyk J, Hoffman Z, Szymoniuk M, Litak J, Maciejewski M, et al. Low-cost cranioplasty—a systematic review of 3D printing in medicine. Materials (Basel). 15(2022).

[13] R.H. Khonsari, J. Adam, M. Benassarou, H. Bertin, B. Billotet, J. Bouaoud, P. Bouletreau, R. Garmi, T. Gellée, P. Haen, S. Ketoff, G. Lescaille, A. Louvrier, J.C. Lutz, M. Makaremi, R. Nicot, N. Pham-Dang, M. Praud, F. Saint-Pierre, T. Schouman, L. Sicard, F. Simon, T. Wojcik, C. Meyer, In-house 3D printing: Why, when, and how? Overview of the national French good practice guidelines for

in-house 3D-printing in maxillo-facial surgery, stomatology, and oral surgery, J. Stomatol. Oral Maxillofac. Surg. 122 (2021) 458–461.

[14] M. Narita, T. Takaki, T. Shibahara, M. Iwamoto, T. Yakushiji, T. Kamio, Utilization of desktop 3D printer-fabricated “Cost-Effective” 3D models in orthognathic surgery, Maxillofac. Plast. Reconstr. Surg. 42 (2020).

[15] Ravi P, Chepelev LL, Stichweh G V., Jones BS, Rybicki FJ. Medical 3D printing dimensional accuracy for multi-pathological anatomical models 3d printed using material extrusion. J Digit Imaging. 35(2022):613–22.

[16] B. Msallem, N. Sharma, S. Cao, F.S. Halbeisen, H.-F. Zeilhofer, F.M. Thieringer, Evaluation of the Dimensional Accuracy of 3D-Printed Anatomical Mandibular Models Using FFF, SLA, SLS, MJ, and BJ Printing Technology, J. Clin. Med. 9 (2020) 817.

[17] Aristotle S, Patil S, Jayakumar S. Dimensional accuracy of medical models of the skull produced by three-dimensional printing technology by advanced morphometric analysis. J Anat Soc India.71(2022):186–90.

[18] Pakvasa M, Prescher H, Hendren-Santiago B, Da Lomba T, McKenzie N, Orsbon C, et al. An easy-to-use protocol for segmenting and 3-d printing craniofacial ct-images using open-source software. Face. 3(2022):66–73.

[19] M.E. Prendergast, J.A. Burdick, Recent Advances in Enabling Technologies in 3D Printing for Precision Medicine, Adv. Mater. 32 (2020) 1–14.

[20] E. George, P. Liacouras, F.J. Rybicki, D. Mitsouras, Measuring and establishing the accuracy and reproducibility of 3D printed medical models, Radiographics. 37 (2017) 1424–1450.

[21] Jin Z, Li Y, Yu K, Liu L, Fu J, Yao X, et al. 3D printing of physical organ models: recent developments and challenges. Adv Sci (Weinh). 8(2021):e2101394.

[22] S. Carmignato, A. Pierobon, P. Rampazzo, M. Parisatto, E. Savio, CT for Industrial Metrology – Accuracy and Structural Resolution of CT Dimensional Measurements, Conf. Ind. Comput. Tomogr. (2012) 161–172.

[23] S. Shujaat, E. Shaheen, F. Novillo, C. Politis, R. Jacobs, Accuracy of cone beam computed tomography–derived casts: A comparative study, J. Prosthet. Dent. (2020) 1–8.

[24] J. Asaumi, N. Kawai, Y. Honda, H. Shigehara, T. Wakasa, K. Kishi, Comparison of three-dimensional computed tomography with rapid prototype models in the management of coronoid hyperplasia, Dentomaxillofacial Radiol. 30 (2001) 330–335.

[25] Kamio T, Hayashi K, Onda T, Takaki T, Shibahara T, Yakushiji T, et al. Utilizing a low-cost desktop 3D printer to develop a “one-stop 3D printing lab” for oral and maxillofacial surgery and dentistry

fields. 3D Print Med. 4(2018):1–2.

[26] Tian Y, Chen CX, Xu X, Wang J, Hou X, Li K, et al. A Review of 3D printing in dentistry: technologies, affecting factors, and applications. Scanning. 2021(2021):9950131.

[27] D. Khorsandi, A. Fahimipour, P. Abasian, S.S. Saber, M. Seyedi, S. Ghanavati, A. Ahmad, A.A. De Stephanis, F. Taghavinezhaddilami, A. Leonova, R. Mohammadinejad, M. Shabani, B. Mazzolai, V. Mattoli, F.R. Tay, P. Makvandi, 3D and 4D printing in dentistry and maxillofacial surgery: Printing techniques, materials, and applications, Acta Biomater. 122 (2021) 26–49.

ARTICLE 3

Quality and haptic feedback of three-dimensionally printed models for simulating dental implant surgery

Wang X. [1,2]

Shujaat S. [1]

Shaheen E. [1]

Jacobs R. [1,3]

[1] OMFS-IMPATH Research Group, Department of Imaging & Pathology, Faculty of Medicine, KU Leuven & Oral and Maxillofacial Surgery, University Hospitals Leuven, Leuven, Belgium.

[2] Department of Oral and Maxillofacial Surgery, The First Affiliated Hospital of Harbin Medical University, Harbin, China.

[3] Department of Dental Medicine, Karolinska Institutet, Huddinge, Sweden.

Published in *Journal of Prosthetic Dentistry* 2022 May 2;S0022-3913(22)00201-3.

Abstract

Statement of problem: A model offering anatomic replication and haptic feedback similar to that of real bone is essential for hands-on surgical dental implant training. Patient-specific skeletal models can be produced with 3-dimensional (3D) printing, but whether these models can offer optimal haptic feedback for simulating implant surgery is unknown.

***Purpose*:** The purpose of this trial was to compare the haptic feedback of different 3D-printed models for simulating dental implant surgery.

Material and methods: A cone beam computed tomography image of a 60-year-old man with a partially edentulous mandible was manipulated to segment the mandible and isolated from the rest of the scan. Three-dimensional models were printed with 6 different printers and materials: material jetting-based printer (MJ, acrylic-based resin); digital light processing-based printer (DLP, acrylic-based resin); fused filament fabrication-based printer (FFF1, polycarbonate filament; FFF2, polylactic acid filament); stereolithography-based printer (SLA, acrylic-based resin); and selective laser sintering-based printer (SLS, polyamide filament). Five experienced maxillofacial surgeons performed a simulated implant surgery on the models. A 5-point Likert scale questionnaire was established to assess the haptic feedback. The Friedman test and cumulative logit models were applied to evaluate differences among the models (α=.05).

***Results*:** The median score for drilling perception and implant insertion was highest for the MJ-based model and lowest for the SLS-based model. In relation to the drill chips, a median score of ≥3 was observed for all models. The score for corticotrabecular transition was highest for the MJ-based model and lowest for the FFF2-based model. Overall, the MJ-based model offered the highest score compared with the other models.

***Conclusions*:** The 3D-printed model with MJ technology and acrylic-based resin provided the best haptic feedback for performing implant surgery. However, none of the models were able to completely replicate the haptic perception of real bone.

***Clinical Implications*:** Three-dimensional printed models could serve as an effective clinical training tool for simulating dental implant surgery. Improvements to obtaining haptic feedback from these models are still required to accurately match surgery in real bone.

Keywords: Printing, three-dimensional; Computer-aided design; Dimensional measurement accuracy; Tomography

1. Introduction

Hands-on dental implant surgery training programs have been incorporated into predoctoral and postdoctoral curricula to provide students with anatomic and haptic understanding before encountering actual patients [1]. In addition, the demand for surgical training among general dentists has increased with the growing popularity of implant-supported prostheses and technological advancements, where previously implant surgery was only provided by specialists [1]. Preclinical implant surgery training increases the trainee's confidence and competency, increasing the survival rate and lowering the complication rate of implant placements [2].

For optimal training, the model used should offer both anatomic replication and haptic feedback similar to those of real bone. Current training models for implant placement include cadaveric or animal bone, polymeric models, and virtual reality-based haptic simulators [3, 4], each with limitations. Cadaveric bone has been considered the prime choice for enhancing preclinical dental implant surgical skills, but its use is limited because of reasons ranging from ethical issues to its limited availability because of high cost and demand. Furthermore, the use of cadaveric bone has been a subject of controversy for training novice practitioners [5]. Bovine or porcine bone models offer haptic feedback comparable with that of real bone, but the human anatomy is not represented [2, 6]. Various polymeric models made of polyurethane or synthetic foams have been incorporated into implant training programs, but they do not replicate patient-specific anatomy and the haptic feedback does not match that of real bone [6, 7]. Currently available virtual reality haptic simulators are inadequate for reproducing a realistic dental drilling force and are not sufficiently robust to be widely applied for implant training [4, 8, 9].

Three-dimensional (3D) printing has allowed the production of visuo-haptic patient-specific models to be used for both medical education and craniomaxillofacial surgical training [10, 11, 12, 13, 14]. The application of 3D-printed patient-specific models for rehearsing complex maxillofacial procedures has been reported to reduce operation and bleeding time and to improve clinical outcomes [15, 16]. In addition, 3D-printed models can enhance a clinician's comprehension of anatomic structures, thereby improving treatment delivery and patient care [17]. Various fields of craniomaxillofacial surgery have successfully used 3D models that offer visuohaptic feedback similar to that of real bone for clinical training. However, evidence as to whether these models can offer optimal haptic feedback for dental implant surgery is lacking. Furthermore, printing technologies and materials have been reported to affect the mechanical properties of a 3D-printed model [18, 19, 20, 21, 22]. Therefore, this study compared the haptic feedback of different technology- and material-based 3D-printed models to assess whether these models can offer realistic haptic feedback for dental implant placement. The null hypothesis was that the haptic feedback of different models would be similar.

2. Methods and materials

This research was performed in compliance with the World Medical Association Declaration of Helsinki on medical research and the principles of Good Clinical Practice. The study was approved by the Ethics Committee Research UZ/KU Leuven (reference number: S64493; registration number: B3222020000240). This study complied with the Standards for Reporting Qualitative Research (SRQR) guidelines. A cone beam computed tomography (CBCT) scan of a 60-year-old male patient was recruited from the database of the Dentomaxillofacial Radiology Center (University Hospitals Leuven, Leuven, Belgium). The scan was acquired with a CBCT device (Newtom VGi-evo; QR Srl), and the scanning parameters were 110 kV, 10×10-cm field of view, and voxel size of 0.2 mm. Inclusion criteria involved a partially edentulous mandible with at least 5 missing teeth in the posterior region, minimum bone height of 10 mm, presence of adequate bone width at the planned implant placement sites, good-quality image with normal cortical bone, and dense trabecular architecture. Exclusion criteria were the presence of any pathological condition, unhealed extraction sockets, and motion or metal artifacts in the mandibular region. The CBCT data were saved in the digital imaging and communications in medicine (DICOM) format and then imported into a 3D software program (Mimics 22.0; Materialise) for threshold-based segmentation [23]. The mandibular trabecular bone was segmented by generating a mask by using a threshold value of 350 Hounsfield units (HU), followed by manual delineation for the correction of the mask boundaries in the coronal, axial, and sagittal planes. The teeth and cortical bone masks were manually delineated in all planes. Thereafter, all the masks were combined by using Boolean operations and converted to a single segmented 3D object consisting of bone and teeth in the standard tessellation language (STL) format. Following the 3D model calculation, 3 smoothing iterations with a factor of 1 were applied to obtain a smooth 3D model without any overestimation or underestimation of the segmented structures (**Fig. 1A**). Subsequently, the STL file was imported into a 3D modeling software program (3-matic 14.0; Materialise) to design a base with a cavity in the middle (**Fig. 1B**). The designed mandibular model was printed with 6 different printers (**Fig. 2**). The specifications of the printers and materials are described in **Table 1**. The printing technologies included SLA, FFF, MJ, SLS, and DLP. The selection of materials was based on manufacturer recommendations, and they were those most commonly used for printing skeletal models. Following the printing process, all models were stored at room temperature.

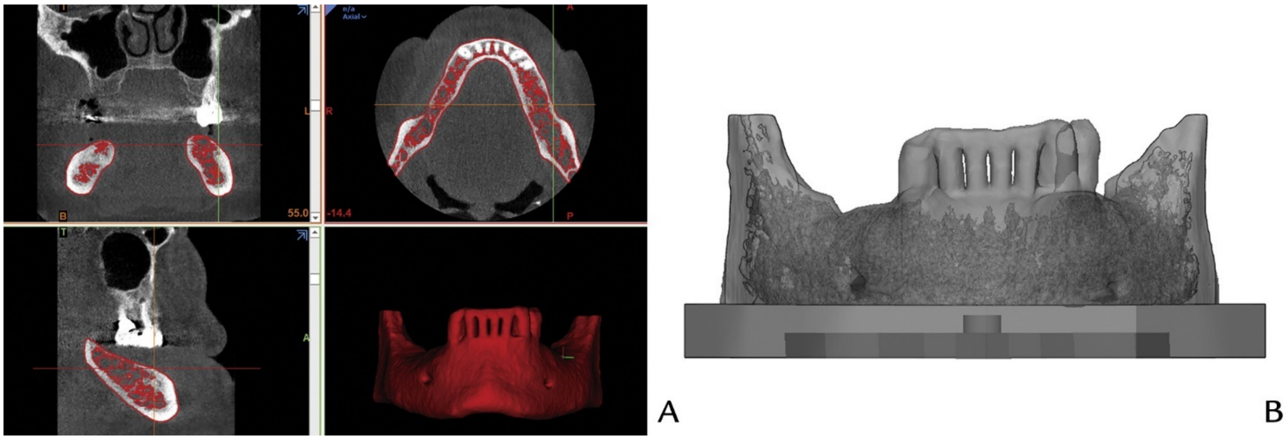

Figure 1. Workflow for 3D model processing. A, Manual segmentation of mandibular bone including cortical bone, trabecular bone, and teeth from patient's CBCT. B, Base design and model processing. 3D, Three-dimensional; CBCT, cone beam computed tomography.

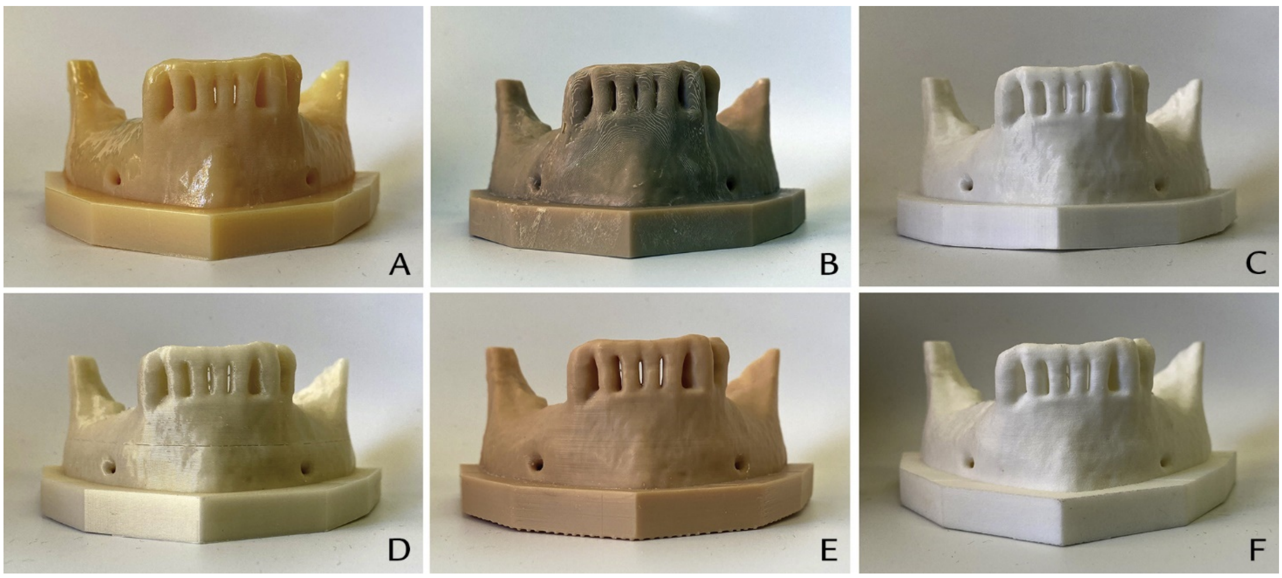

Figure 2. Frontal view of 6 printed models. A, Material jetting (MJ, Objet Connex 350 with acrylic-based resin). B, Digital light processing (DLP, Nextdent 5100 with acrylic-based resin). C, Fused filament fabrication 1 (FFF1, Raise3D E2 with polycarbonate filament). D, FFF2 (Prusa i3 MK3S with polylactic acid filament). E, Stereolithography (SLA, Form 2 with acrylic-based resin). F, Selective laser sintering (SLS, TPM3D P550DL with polyamide filament).

Table 1. Model specifications

Printer name	Manufacturer of printer	Technology	Material commercial name	Manufacturer of material	Material composition	Tensile Strength (MPa)	Young's Modulus (MPa)	Layer resolution (μm)	Post-processing	Printing time (h)	Model weight (g)	Printer price (€)	Model price (€)
Objet Connex 350	Stratasys	MJ	VeroDent MED670	Stratasys	Acrylic-based resin: Proprietary	50-60	2000-3000	30	Pressured water jet	3.5	99	200000	44
Nextdent 5100	3D systems	DLP	NextDent Model 2.0	3D systems	Acrylic-based resin: Ethoxylated bisphenol A dimethacrylate	NR	NR	50	Post-polymerization	0.5	100	12000	25
Raise3D E2	Raise3D	FFF	PolyMax PC	Polymaker	Polycarbonate	59.7 ±1.8	2048±66	200	Supports removed, airborne-particle abraded	15.3	46	2540	6.24
Prusa i3 MK3S	Prusa research	FFF	Prusament PLA Vanilla White	Prusa research	Polylactic acid filament	57.4 ±0.4	2200-2400	100	Supports removed	14	67	750	1.84
Form 2	Formlabs Inc.	SLA	Model resin	Formlabs Inc.	Acrylic-based resin: Urethane Dimethacrylate (UDMA)	33-61	1600-2700	100	Isopropyl alcohol bath, postpolymerized, supports removed	10.25	89	2914	23.6
TPM3D P550DL	TPM3D	SLS	Precimid 1172 Pro	TPM3D	Polyamide	50	2000	120	Airborne-particle abraded	3	75	208156	18

Five oral and maxillofacial surgeons with a minimum clinical experience of 4 years in implant dentistry performed implant surgery on the printed models. All participants had been trained and calibrated beforehand. Additionally, they were blinded to the printer's information, and the models were assigned a random number from 1 to 6 generated in a spreadsheet (Excel; Microsoft Corp). The models were fixed to a dental phantom head by embedding an M6 hexagonal nut into the cavity prepared at the model's base with cyanoacrylate resin to be attached to the bolt of the phantom head (**Fig. 3A**) [24].

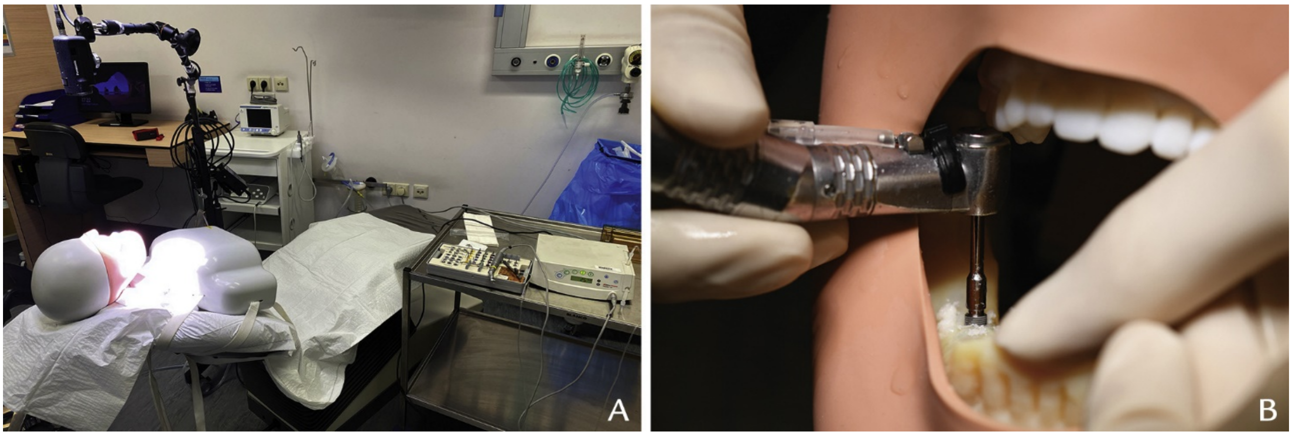

Figure 3. Three-dimensional model surgery. A, Clinical arrangement. B, Dental implant surgery.

The surgical procedure consisted of drilling freehand, followed by implant and cover screw placement (**Fig. 3B**). The drilling was performed with an implant motor (OsseoSet 100; Nobel Biocare) and a contra-angle handpiece with irrigation. The motor was set to 800 rpm with a torque control of 45 Ncm. The dental implant was a customized experimental device derived from a commercially available dental implant (In-Hex, 3.8×9 mm; Wego). The drilling order was as follows: 2.2-mm-round drill followed by 1.8-mm pilot, 2.2-mm pilot, 3.3-mm form drill, and 3.8-mm final drill. The depth of the drilling (9 mm) was guided by the markings on the drills. An insertion torque of 45 Ncm, maximum, was applied, and if necessary, a manual torque wrench was used (Wego). A total of 30 implants were placed in the posterior mandibular region (left and right first molar, left and right second molar, right second premolar) by the 5 surgeons, with each surgeon placing 1 implant in all the models (6 models×5 insertions=30 implants).

The surgeons were asked to report the similarity between the model and implant placement in an actual patient based on their clinical experience by using a 5-point Likert scale questionnaire (ranging from 1=strongly disagree to 5=strongly agree). The questionnaire consisted of 4 questions adapted from previous studies, and its face validity was approved by 2 independent experts (S.S., R.J.) [11,25, 26, 27]. The questions evaluated the 3D model quality based on bone chips and the haptic feedback of drilling, corticocancellous transition, and implant insertion (**Table 2**). The questionnaire was answered after each implant placement and before the drilling of the next model. One surgeon repeated the experiment after 2 weeks.

Table 2. Questionnaire for evaluating haptic feedback using 5-point Likert scale

Question no.	Questionnaire	Strongly disagree 1	Disagree 2	Neutral 3	Agree 4	Strongly Agree 5
1	Were chips of this model similar to real bone chips					
2	Was tactile perception and resistance while drilling equal to that of real bone					
3	Was transition from cortical bone layer to trabecular bone observed during drilling					
4	Was tactile perception and resistance of implant placement equal to that of real bone					

The data were analyzed by using statistical software programs (IBM SPSS Statistics for Windows, v21.0; IBM Corp, and S-Plus 8.0 for Linux). Median and interquartile range were calculated, and the Friedman test with the surgeon as a blocking factor was used for rank sum test of each question. A cumulative logit model was built with the surgeon as a random factor to assess differences in the proportion of observations below specific threshold values. Thresholds were the percentage of evaluations lower than or equal to 1, 2, 3, and 4, respectively. Test-retest reliability was computed, and the Cronbach alpha was applied to measure the reliability of the groups of questions (α=.05).

3. Results

All the implants were covered with a screw and achieved primary stability without any failure, irrespective of the surgeon or model. The test-retest reliability and Cronbach alpha showed a high correlation (r=0.759) and an acceptable reliability (α=.791), respectively [28]. The raw scoring of the questionnaire for each model is provided in Supplemental Table 1 (available online).

Fig. 4 describes the median and interquartile range of the scoring achieved with each printed model. The median score for drilling perception and implant insertion was highest for the MJ-based model and lowest for the SLS-based model. In relation to the drill chips, a median score of ≥3 was observed for all models. The score for corticotrabecular transition was highest for the MJ-based model and lowest for the FFF2-

based model. The haptic feedback for implant insertion was highest for the MJ-, followed by the DLP-, FFF1-, and FFF2-based models, all of which had a median score of ≥3. However, the SLA- and SLS-based models achieved a score of 2 and were considered not sufficiently realistic for implant insertion. When comparing the differences among 3D-printed models based on each question individually, no significant differences were observed (P>.05). Overall, the MJ-based model offered the highest score compared with other models, whereas the SLS-based model scored the lowest.

When all questions were combined for each model, the percentage of scores for a certain level was as summarized in **Fig. 5**. The results were expressed as odds ratio (OR). In terms of probability that a score would be smaller than or equal to 3 (**Table 3**), a significant difference was observed for DLP-MJ (OR=9.044, P=.045), MJ-FFF2 (OR=0.075, P=.016), and MJ-SLS (OR=0.046, P=.007).

Table 3. Comparison between 3D printed models with cumulative logit models with probability that score smaller than or equal to 3

Model	Odds ratio	*P*
Form 2 (SLA)-Nextdent 5100 (DLP)	0.411	.901
Form 2 (SLA)-Object Connex 350 (MJ)	3.714	.546
Form 2 (SLA)-Prusa i3 MK3S (FFF2)	0.280	.716
Form 2 (SLA)-Raise3D E2 (FFF1)	1.297	.100
Form 2 (SLA)-TPM3D P550DL (SLS)	0.170	.409
Nextdent 5100 (DLP)-Object Connex 350 (MJ)	9.044	**.045**
Nextdent 5100 (DLP)-Prusa i3 MK3S (FFF2)	0.681	.999
Nextdent 5100 (DLP)-Raise3D E2 (FFF1)	3.159	.747
Nextdent 5100 (DLP)-TPM3D P550DL (SLS)	0.414	.960
Object Connex 350 (MJ)-Prusa i3 MK3S (FFF2)	0.075	**.016**
Object Connex 350 (MJ)-Raise3D E2 (FFF1)	0.349	.775
Object Connex 350 (MJ)-TPM3D P550DL (SLS)	0.046	**.007**
Prusa i3 MK3S (FFF2)-Raise3D E2 (FFF1)	4.642	.464
Prusa i3 MK3S (FFF2)-TPM3D P550DL (SLS)	0.608	.998
Raise3D E2 (FFF1)-TPM3D P550DL (SLS)	0.131	.210

Significant difference values in bold.

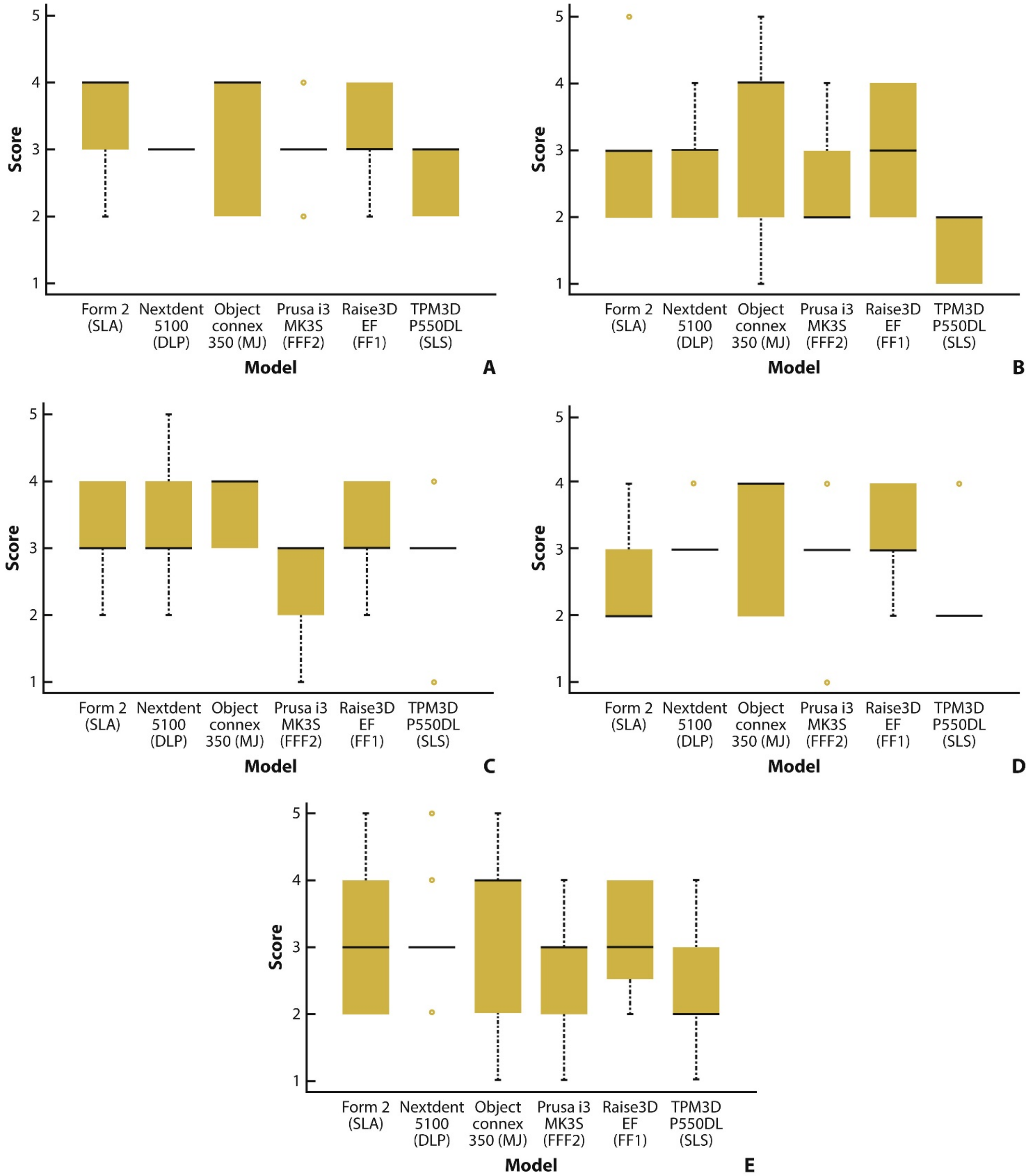

Figure 4. Median and interquartile range of scoring achieved with each printed model. A, Bone chips. B, Drilling perception. C, Corticotrabecular transition feedback. D, Implant insertion perception. E, Overall haptic feedback considering all questions. Boxes comprise 25th and 75th quartiles and median values, upper and lower whisker measure out 1.5 times box length, and circles represent values outside of given percentiles. DLP, digital light processing; FFF, fused filament fabrication; MJ, material jetting; SLA, stereolithography; SLS, selective laser sintering.

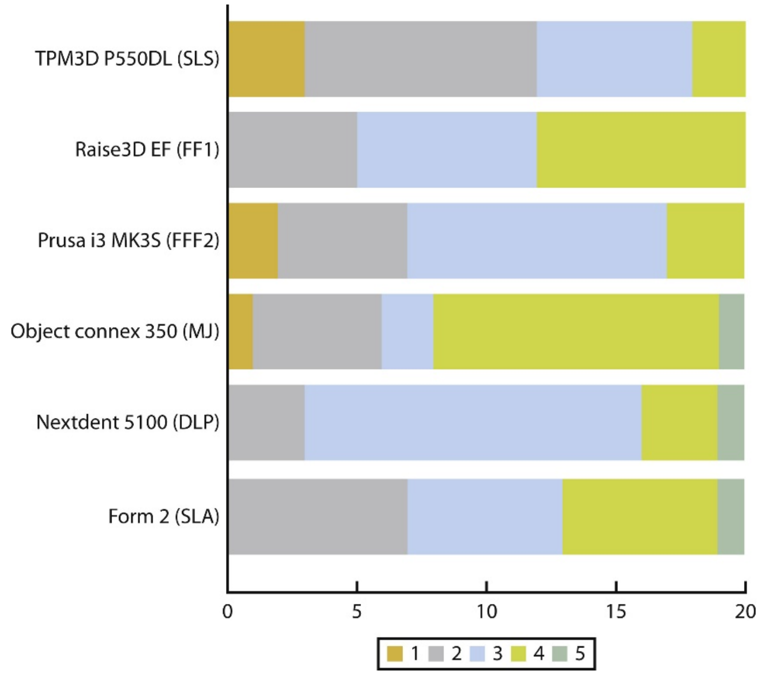

Figure 5. Scoring percentage for all questions based on each model. Scores from 1 (strongly disagree) to 5 (strongly agree) represented by different color. Horizontal axis stands for total score value of 20 based on all questions.

4. Discussion

The results of the present study showed differences among the haptic feedback of different models. Therefore, the null hypothesis was rejected. A CBCT scan of the patient was used as a clinical standard to print both cortical and trabecular bone instead of relying on high-resolution scans or bone blocks to determine whether patient-specific modeling of the hard-tissue structures could offer realistic conditions for performing dental implant surgery. Based on the findings, the median score for corticotrabecular transition was highest for the MJ-based model and lowest for the FFF2-based model. The low score could be because the FFF2 printer was unable to optimally replicate the trabecular architecture, FFF printers generate output with low mechanical properties, and the printed model was highly dependent on the material, structural parameters, and printer settings [18]. On the contrary, MJ-based printers are generally able to replicate the model more precisely with finer layer resolution [10].

In relation to drilling perception, the MJ-based model with acrylic-based resin achieved the highest score, but none of the models were able to offer resistance comparable with that of real bone. Additionally, SLA was identified as being better for drilling than the DLP-based model, possibly because of the polymerization process. SLA polymerizes the resin point by point, while DLP polymerizes a layer at a time at a faster rate [18]. Therefore, the SLA polymerization process leads to a better quality model and was rated higher than the DLP printer [18]. Consequently, the postprocessing might also have negatively influenced the drilling feedback for all models. The internal structures were dense because the support material of trabecular bone could not be removed efficiently as the structures in the SLA-, DLP-, MJ-, and FFF-based models are fragile. Although no support was required for printing with the SLS-based printer, powder was retained within the internal architecture and could not be removed properly without fracturing the thin trabecular architecture, thereby further adding to the thickness of the structures.

Apart from technology, an adequate tactile sensation also depends on the mechanical properties of the material, including the Young modulus and hardness, which impact the drilling force [10, 19]. All models included in this study had a Young modulus below the 3000-MPa value of mandibular bone [29]. The MJ-based model with acrylic resin showed the closest modulus to that of real bone, which might have further enhanced its capability for achieving a higher haptic feedback than the other models. The SLS-based model with polyamide was found to be too hard for drilling cortical bone. The present findings were consistent with those of Favier et al [20], who reported that polyamide displayed higher mechanical properties than those in real patients. Additionally, Haffner et al [21] and Shujaat et al [26] also reported that polyamide offered limited actual bone resistance when performing temporal bone surgery and mandibular orthognathic surgery, respectively. Furthermore, the FFF2-based model printed with polylactic acid filament was unable to replicate the trabecular architecture optimally, consistent with a previous study [26].

As for the bone chips, all models achieved a median score of 3. The FFF2-based model with polylactic acid tended to melt during drilling even with irrigation because the thermal properties of the material generated increased heat. Furthermore, the SLA-based model with urethane dimethacrylate (UDMA) resin scored better than other materials [30]. Despite the different mechanical properties of the selected materials, the size and shape of chips during drilling for all models were similar to those of fine powder apart from polylactic acid. Additionally, because of the susceptibility of photopolymers to heat, all the models were stored at room temperature [22].

When inserting the dental implants, all models were able to achieve primary stability but with a tactile perception lower than that of real bone. The perception of inserting an implant in the SLA-based model with acrylic resin was considered soft, as the implant was inserted with the least effort, while the SLS-based model with PA required higher pressure with manual tightening because of the material's hardness.

An essential requirement for a training model is that it has to be of low cost [5]. Based on the present findings, 3D-printed models could act as a cost-effective method for teaching clinical anatomy and simulating dental implantology procedure. Overall, the MJ-based model with acrylic-based resin best replicated the haptic feedback of real bone. However, depending on the availability of printer and material, FFF1-, DLP-, and SLA-based models could also act as an alternative for implant surgery simulation.

Limitations of the study included that haptic feedback was assessed subjectively and only 5 surgeons were included. Future work should focus on quantitatively analyzing the mechanical properties of the printing material and the printer's capability to print real bone-like structures. Second, as only 6 medical printers with different parameters were used for comparison, the findings of this study should be interpreted with caution and cannot be generalized to other printers, which might offer a better outcome. Third, the study lacked a comparison of haptic feedback with real bone; instead, this was assessed based on the surgeon's experience, which could have led to bias. The investigation of haptic feedback for implant surgery assessed in this study with different technologies and materials could motivate further studies to improve the perception of these models. Future studies should also assess the performance of 3D printers for printing and evaluating the surgical haptic feedback of bone structures with different densities.

5. Conclusions

Based on the findings of this trial, the following conclusions were drawn:

1. The 3D-printed model with MJ technology and acrylic-based resin provided the best haptic feedback and could act as a standard for simulating dental implant surgery.
2. None of the models were able to completely replicate the haptic perception of real bone.

References

[1] S. Prasad, N. Bansal, Predoctoral dental students' perceptions of dental implant training: Effect of. preclinical simulation and clinical experience, J. Dent. Educ. 81 (2017) 395–403.

[2] S. Vandeweghe, S. Koole, F. Younes, P. De Coster, H. De Bruyn, Dental implants placed by undergraduate students: Clinical outcomes and patients'/students' perceptions, Eur. J. Dent. Educ. 18 (2014) 60–69.

[3] Ferro, Nicholson, Koka, Innovative Trends in Implant Dentistry Training and Education: A Narrative Review, J. Clin. Med. 8 (2019) 1618.

[4] X. Chen, P. Sun, D. Liao, A patient-specific haptic drilling simulator based on virtual reality for dental implant surgery, Int. J. Comput. Assist. Radiol. Surg. 13 (2018) 1861–1870.

[5] L.B. Seifert, B. Schnurr, C. Herrera-Vizcaino, A. Begic, F. Thieringer, F. Schwarz, R. Sader, 3D-printed patient individualised models vs cadaveric models in an undergraduate oral and maxillofacial surgery curriculum: Comparison of student's perceptions, Eur. J. Dent. Educ. 24 (2020) 799–806.

[6] M.A. Alkhodary, A.E.E. Abdelraheim, A.E.H. Elsantawy, The development of a composite bone model for training on placement of dental implants, Int. J. Health Sci. (Qassim). 9 (2015) 151–158.

[7] R. Tobias, M. Neto, D.A. Hiramatsu, V. Suedam, P. César, R. Conti, J.H. Rubo, Validation of an experimental polyurethane model for biomechanical studies on implant-supported prosthesis-compression tests, J Appl Oral Sci. 19 (2011) 47-51.

[8] H. Kinoshita, M. Nagahata, N. Takano, S. Takemoto, S. Matsunaga, S. Abe, M. Yoshinari, E. Kawada, Development of a Drilling Simulator for Dental Implant Surgery, J. Dent. Educ. 80 (2016) 83–90.

[9] F. Zheng, W.F. Lu, Y.S. Wong, K.W.C. Foong, Graphic processing units (GPUs)-based haptic simulator for dental implant surgery, J. Comput. Inf. Sci. Eng. 13 (2013) 041005.

[10] M. Meglioli, A. Naveau, G.M. Macaluso, S. Catros, Correction to: 3D printed bone models in oral and craniomaxillofacial surgery: a systematic review, 3D Print. Med. 6 (2020) 1–19.

[11] S.M. Werz, S.J. Zeichner, B.I. Berg, H.F. Zeilhofer, F. Thieringer, 3D Printed Surgical Simulation Models as educational tool by maxillofacial surgeons, Eur. J. Dent. Educ. 22 (2018) e500–e505.

[12] S.E. Mowry, H. Jammal, Ã. Clementino, A. Solares, P. Weinberger, A novel temporal bone simulation. model using 3D printing techniques, Otol Neurotol. 36 (2015) 1562-5.

[13] A.P. George, R. De, Review of temporal bone dissection teaching: How it was, is and will be, J. Laryngol. Otol. 124 (2010) 119–125.

[14] R. Probst, R. Stump, M. Mokosch, C. Röösli, Evaluation of an Infant Temporal-Bone Model as

Training Tool, Otol. Neurotol. 39 (2018) e448–e452.

[15] N. Martelli, C. Serrano, H. Van Den Brink, J. Pineau, P. Prognon, I. Borget, S. El Batti, Advantages and disadvantages of 3-dimensional printing in surgery: A systematic review, Surg. 159 (2016) 1485–1500.

[16] S.H. Somji, A. Valladares, S. Ho Kim, Y. Cheng Paul Yu, S.J. Froum, The use of 3D models to improve sinus augmentation outcomes - A case report, Singapore Dent. J. 38 (2017) 63–70.

[17] A. Louvrier, P. Marty, A. Barrabé, E. Euvrard, B. Chatelain, E. Weber, C. Meyer, How useful is 3D printing in maxillofacial surgery?, J. Stomatol. Oral Maxillofac. Surg. 118 (2017) 206–212.

[18] D. Khorsandi, A. Fahimipour, P. Abasian, S.S. Saber, M. Seyedi, S. Ghanavati, A. Ahmad, A.A. De Stephanis, F. Taghavinezhaddilami, A. Leonova, R. Mohammadinejad, M. Shabani, B. Mazzolai, V. Mattoli, F.R. Tay, P. Makvandi, 3D and 4D printing in dentistry and maxillofacial surgery: Printing techniques, materials, and applications, Acta Biomater. 122 (2021) 26–49.

[19] J.B. Hochman, J. Kraut, K. Kazmerik, B.J. Unger, Generation of a 3D printed temporal bone model with internal fidelity and validation of the mechanical construct, Otolaryngol. - Head Neck Surg. 150 (2014) 448–454.

[20] V. Favier, N. Zemiti, O.C. Mora, G. Subsol, G. Captier, R. Lebrun, L. Crampette, M. Mondain, B. Gilles, Geometric and mechanical evaluation of 3D-printing materials for skull base anatomical education and endoscopic surgery simulation – A first step to create reliable customized simulators, PLoS One. 12 (2017) 1–16.

[21] M. Haffner, A. Quinn, T.Y. Hsieh, E.B. Strong, T. Steele, Optimization of 3D Print Material for the Recreation of Patient-Specific Temporal Bone Models, Ann. Otol. Rhinol. Laryngol. 127 (2018) 338–343.

[22] A. Kessler, R. Hickel, M. Reymus. 3D printing in dentistry-State of the art, Oper Dent. 45 (2020) 30-40.

[23] S. Shujaat, O. da Costa Senior, E. Shaheen, C. Politis, R. Jacobs, Visual and haptic perceptibility of 3D printed skeletal models in orthognathic surgery, J. Dent. (2021) 103660.

[24] A. Torres, G. Boelen, P. Lambrechts, M.S. Pedano, R. Jacobs, Dynamic navigation: a laboratory study on the accuracy and potential use of guided root canal treatment, Int. Endod. J. (2021) 0–2.

[25] A.S. Rose, J.S. Kimbell, C.E. Webster, O.L.A. Harrysson, E.J. Formeister, C.A. Buchman, Multi-material 3D models for temporal bone surgical simulation, Ann. Otol. Rhinol. Laryngol. 124 (2015) 528–536.

[26] S. Shujaat, O. da Costa Senior, E. Shaheen, C. Politis, R. Jacobs. Visual and haptic perceptibility. of 3D printed skeletal models in orthognathic surgery, J Dent. 109 (2021) 103660.

[27] A. McMillan, A. Kocharyan, S.E. Dekker, E.G. Kikano, A. Garg, V.W. Huang, N. Moon, M. Cooke, S.E. Mowry, Comparison of. materials used for 3D-printing temporal bone models to simulate surgical dissection, Ann. Otol. Rhinol. Laryngol. 129 (2020) 1168-73.

[28] G.J. Matheson. We need to talk about reliability: Making better use of test-retest studies for study design and interpretation, PeerJ. 7 (2019) e6918.

[29] G. Odin, C. Savoldelli, P. Bouchard, Y. Tillier, G. Odin, C. Savoldelli, P. Bouchard, Y.T. Determination of Young' s modulus of mandibular, Med Eng Phys. 32 (2010) 630-7.

[30] A. Bagheri, J. Jin, Photopolymerization in 3D Printing, ACS Appl. Polym. Mater. 1 (2019) 593–611.

Part II

COMPUTER ASSISTED SURGERY ON 3D-PRINTED MODELS

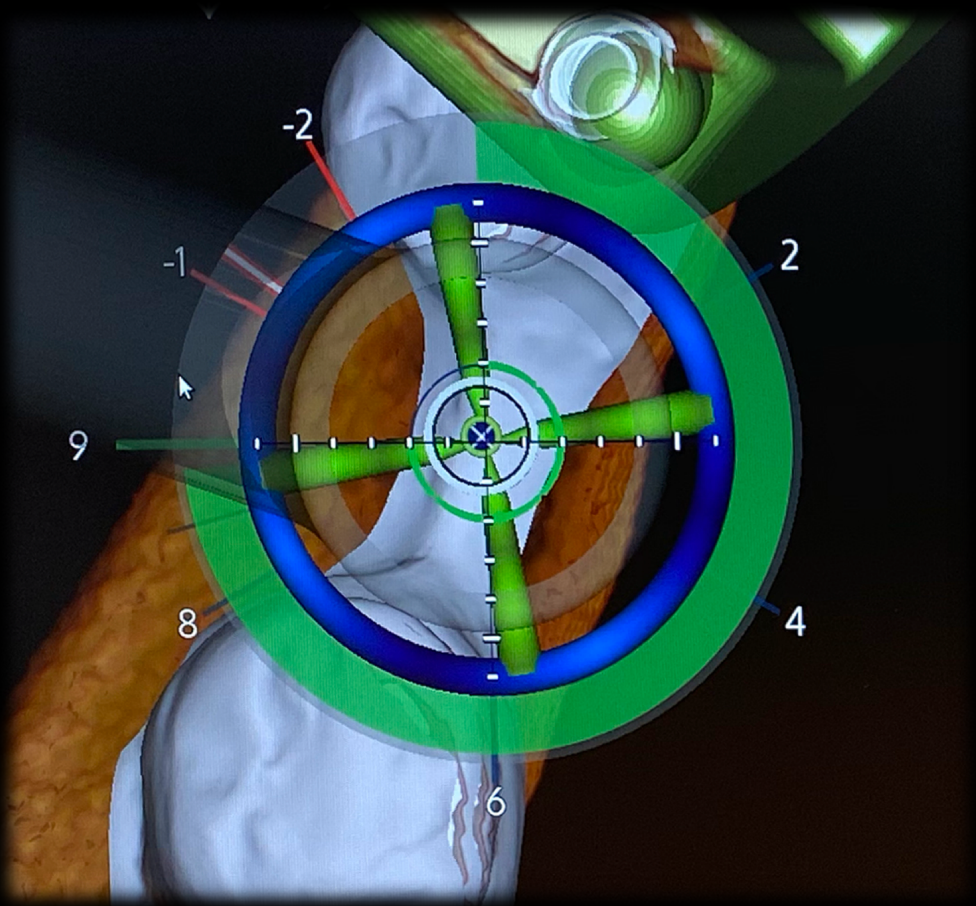

Implant placement using a static surgical guide can be categorized as fully or partially guided, where partial guidance involves pilot-guided or half-guided surgical guide [1]. A fully-guided approach offers less deviation from the planned implant position compared to a partially guided approach [2]. However, pilot-drill partial guidance is the most commonly used technique in dental practice due to its ease of use, reduced irrigation problems, and ability to make minor adjustments to implant position if necessary [3]. In order to train novice surgeons, it may be beneficial to evaluate the effectiveness of pilot-guided surgical guides. With this method, the surgeon has more control over the implant placement as they manually inspect each step after the pilot drilling. Fully-guided surgical guides rely heavily on the guide itself and do not require strict monitoring [4]. Half-guided surgical guides involve drilling dictated by the guide, followed by freehand implant placement [5]. Therefore, a pilot study was conducted to compare the accuracy of implant placement between novice and experienced surgeons using pilot-guided and half-guided surgical guides.

Four CBCT-based simulation models of bilateral missing first molars (Fédération Dentaire Internationale [FDI]: 36 for lower left 1st molar, 46 for lower right 1st molar) were created using a 3D printer, following the same protocol outlined in Article 3. The experienced surgeon had more than five years of experience in implant surgery, while the novice surgeon had no prior experience in surgical implantology. The experienced surgeon was responsible for the implant planning. Afterwards, the 3D printer (Objet Connex 350 printer, Stratasys) was used to design and fabricate both pilot-guided and half-guided surgical guides and attached surgical sleeves to the guides with glue.

The surgical procedure for the pilot-guided group followed the manufacturer’s kit protocol (Wego, China). The drill order was: 2-mm pilot drill using the surgical guide, followed by freehand drilling with a 3.3-mm form drill, and 3.8-mm final drill. For the half-guided group, the drilling procedure involved using the Nobel Parallel CC Kit (Nobel Biocare). This involved inserting drill keys into the sleeve inside the surgical guide to guide the consecutive drills with different diameters in the planned positions and angulation. A variety of keys with increasing diameters (2 mm, 2.8 mm, 3.2 mm, and 3.6 mm) were used to guide each individual drill, and markers on all the drills were used to control the drilling depth. After drilling, the surgical guide was removed to finalize the implant placement by freehand. All implants (customized experimental In-Hex implants, 3.8mm x 9mm, Wego, China) were inserted using a motor unit (OsseoSet, Nobel Biocare AB, Goteborg, Sweden) at a speed of 15 rpm and a maximum torque of 50 N.cm.

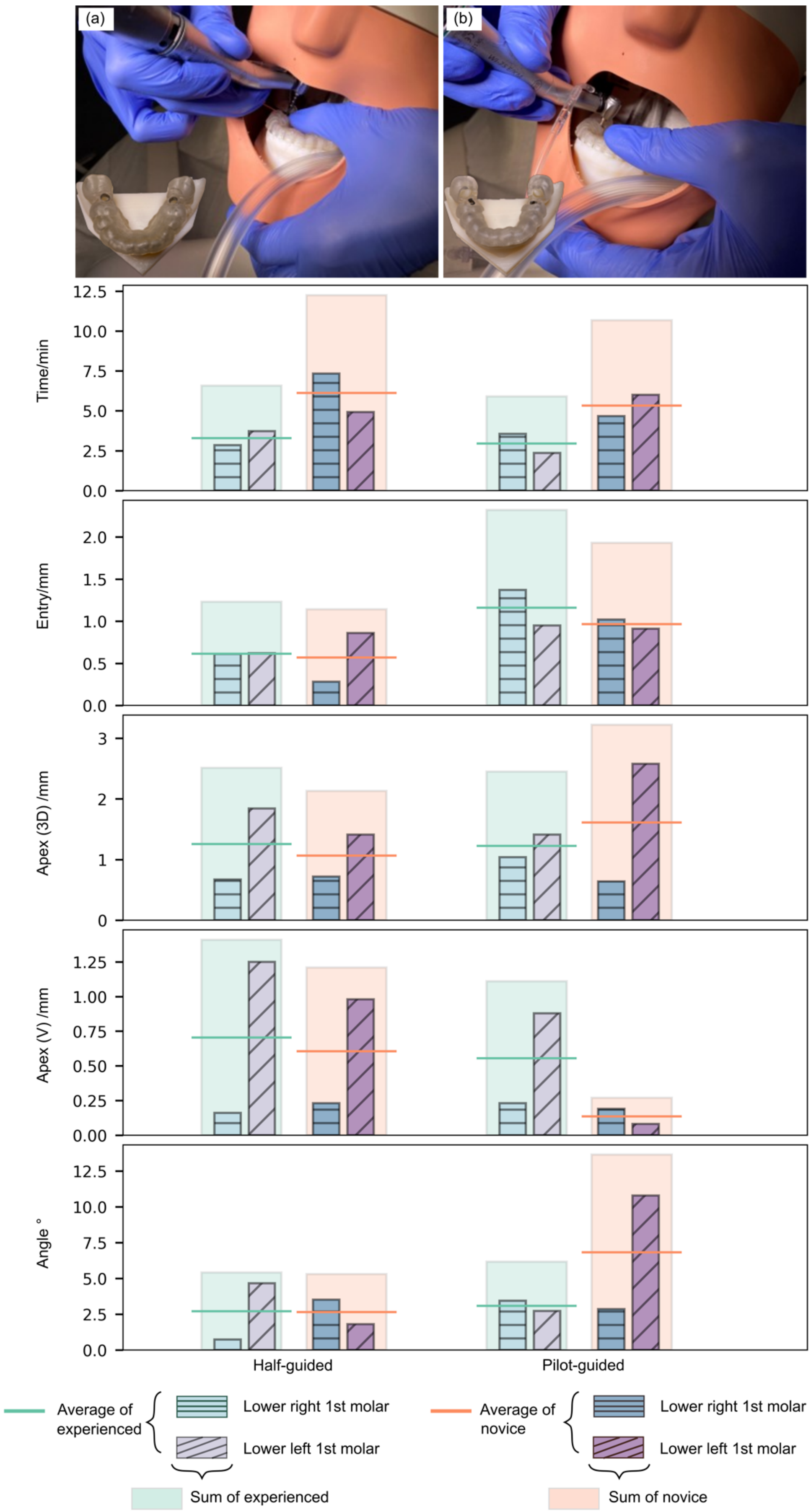

Figure 1. Values of time, deviation of entry, apex 3D, apex (V), and angle categorized by surgical approach (a: half-guided, b: pilot-guided), experience (experienced and novice) and implant site (lower

right 1st molar, lower left 1st molar)

All models were subsequently scanned using a CBCT device and the pre-operative CBCT scan with virtual implant position and the post-operative CBCT scan with actual position were superimposed using EvaluNav software (ClaroNav Technology Inc., Toronto, Canada). Following that, the program automatically compared the planned and actual implant sites by measuring the following parameters: entry 2D deviation (horizontal coronal deviation), apex 3D deviation (3D apical deviation), apex (V) deviation (vertical depth deviation), and angular deviation. Time required for the surgical procedure was also recorded.

The result (**Table 1**, **Fig. 1**) showed that the experienced surgeon performed less surgical time than novice surgeon. According to the accuracy results, implant accuracy between experienced and novice surgeons is comparable when using a half-guided approach. However, with a pilot-guided approach, a novice surgeon using right-handed drilling showed less accuracy on the left implant surgical site compared to the right site. Overall, both pilot-guided and half-guided approaches are suitable for surgeons of all skill levels to use in daily practice.

Table 1. Descriptive values categorized by surgical approach (half-guided and pilot-guided) and experience (experienced and novice)

		Half-guided		**Pilot-guided**	
Experience	Site / Value	46	36	46	36
Experienced	Time/min	2.85	3.717	3.55	2.35
	Entry/mm	0.61	0.62	1.37	0.95
	Apex (3D)/mm	0.67	1.84	1.04	1.41
	Apex (V)/mm	0.16	1.25	0.23	0.88
	Angle/°	0.74	4.67	3.44	2.72
Novice	Time/min	7.333	4.917	4.667	6.00
	Entry/mm	0.28	0.86	1.02	0.91
	Apex (3D)/mm	0.72	1.41	0.64	2.58
	Apex (V)/mm	0.23	0.98	0.19	0.08
	Angle/°	3.51	1.8	2.86	10.79

In conclusion, the results suggest that both pilot-guided and half-guided approaches are effective options for implant placement, but that novice surgeons may need additional training to achieve optimal results and less surgical time. Additionally, it was noted that novice surgeons may find it challenging to place the implant in the opposite location of their drilling hand using pilot-guided surgical guide.

References

[1] J. Gargallo-Albiol, S. Barootchi, O. Salomó-Coll, H. lay Wang, Advantages and disadvantages of implant navigation surgery. A systematic review, Ann. Anat. 225 (2019) 1–10.

[2] M.C. Schulz, F. Hofmann, U. Range, G. Lauer, D. Haim, Pilot-drill guided vs. full-guided implant insertion in artificial mandibles—a prospective laboratory study in fifth-year dental students, Int. J. Implant Dent. 5 (2019).

[3] J. Abduo, D. Lau, Duration, deviation and operator's perception of static computer assisted implant placements by inexperienced clinicians, Eur J Dent Educ. 00 (2021) 1–11.

[4] F. Younes, A. Eghbali, T. De Bruyckere, R. Cleymaet, J. Cosyn, A randomized controlled trial on the efficiency of free-handed, pilot-drill guided and fully guided implant surgery in partially edentulous patients, Clin. Oral Implants Res. 30 (2019) 131–138.

[5] J. Abduo, D. Lau, Accuracy of static computer-assisted implant placement in anterior and posterior sites by clinicians new to implant dentistry: in vitro comparison of fully guided, pilot-guided, and freehand protocols, Int. J. Implant Dent. 6 (2020).

ARTICLE 4

Influence of experience on dental implant placement. An in vitro comparison of freehand, static guided and dynamic navigation approaches

Wang X. [1,2]

Shaheen E. [1]

Shujaat S. [1]

Meeus J. [3]

Legrand P. [1]

Lahoud P. [1]

Gerhardt M. [1,4]

Politis C. [1]

Jacobs R. [1,5]

[1] OMFS-IMPATH Research Group, Department of Imaging & Pathology, Faculty of Medicine, KU Leuven & Oral and Maxillofacial Surgery, University Hospitals Leuven, Leuven, Belgium.

[2] Department of Oral and Maxillofacial Surgery, The First Affiliated Hospital of Harbin Medical University, Harbin, China.

[3] Department of Oral and Maxillofacial Surgery, University Hospitals Leuven, Leuven, Belgium.

[4] School of Health Sciences, Faculty of Dentistry, Pontifical Catholic University of Rio Grande do Sul, Porto Alegre, Brazil.

[5] Department of Dental Medicine, Karolinska Institutet, Huddinge, Sweden.

Published in Int. J. Implant Dent. 2022 Oct 10;8(1):42.

Abstract

Purpose: This study aimed to investigate the performance of novice versus experienced practitioners for placing dental implant using freehand, static guided and dynamic navigation approaches.

Methods: A total of 72 implants were placed in 36 simulation models. Three experienced and three novice practitioners were recruited for performing the osteotomy and implant insertion with freehand, surgical guide (pilot-drill guidance) and navigation (X-Guide, X-Nav technologies) approaches. Each practitioner inserted 4 implants per approach randomly with a 1-week gap to avoid memory bias (4 insertion sites × 3 approaches × 6 practitioners = 72 implants). The performance of practitioners was assessed by comparing actual implant deviation to the planned position, time required for implant placement and questionnaire-based self-confidence evaluation of practitioners on a scale of 1–30.

Results**:** The navigation approach significantly improved angular deviation compared with freehand ($P < 0.001$) and surgical guide ($P < 0.001$) irrespective of the experience. Surgical time with navigation was significantly longer compared to the freehand approach ($P < 0.001$), where experienced practitioners performed significantly faster compared to novice practitioners ($P < 0.001$). Overall, self-confidence was higher in favor of novice practitioners with both guided approaches. In addition, the confidence of novice practitioners (median score = 26) was comparable to that of experienced practitioners (median score = 27) for placing implants with the navigation approach.

Conclusions**:** Dynamic navigation system could act as a viable tool for dental implant placement. Unlike freehand and pilot-drill static-guided approaches, novice practitioners showed comparable accuracy and self-confidence to that of experienced practitioners with the navigation approach.

Keywords: Dental implant, Surgical guide, Dynamic navigation, Dental education

Graphical Abstract

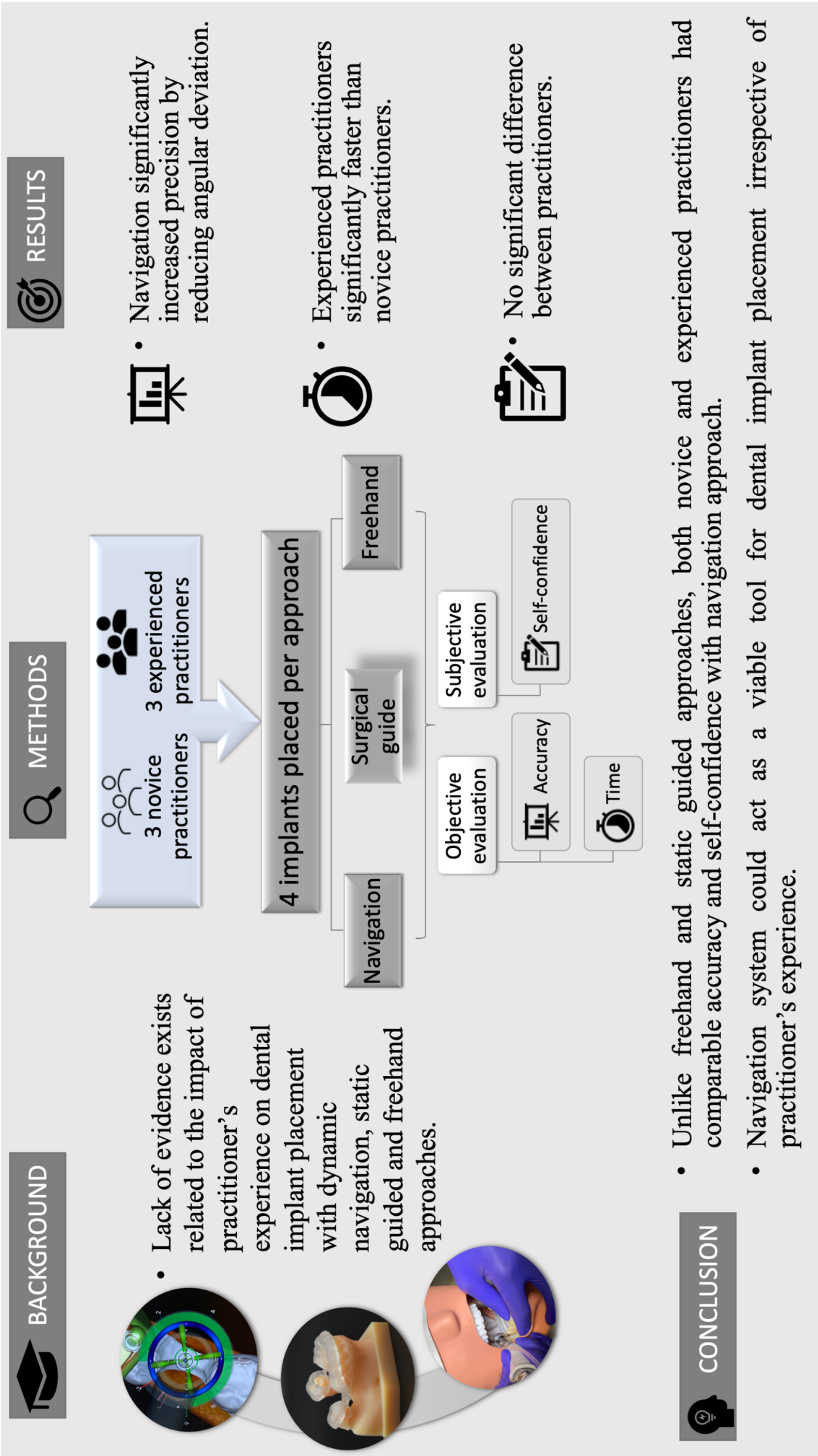

1. Introduction

Dental implant surgery has become a common practice for novice dental practitioners, which was once considered only under the domain of implant specialists and consultants. With its growing popularity for oral rehabilitation, the demand for clinical training has also increased [1]. A practitioner must be well-acquainted with the procedure and should have sufficient training for delivering a successful surgical and restorative outcome. However, most practitioners have limited surgical training which could increase the risk of inaccurate implant placement and complication rate [2]. In addition, one of the main challenges observed by novice practitioners is the optimal controlling of surgical osteotomy and implant positioning. A non-ideal implant placement makes the restoration far more difficult with the possibility of increased cost and time [3].

Recently, the application of cone-beam computed tomographic (CBCT) imaging and virtual planning software programs have facilitated accurate implant placement with a relative reduction in intraoperative complications [4–6]. Furthermore, the development of computer-guided surgical techniques, including static and dynamic approaches have improved the performance of novice practitioners and made it possible to transfer the planned implant position to the surgical site with a higher precision and less observer variability compared to conventional freehand technique [7, 8].

The commonly applied static guided techniques for implant placement involve either a pilot drill guided approach (only guided pilot osteotomy followed by freehand osteotomy and implant placement) or a fully guided approach (fully guided osteotomy and implant placement) [9]. In general, a static fully guided approach offers less deviation compared to a pilot-drill guidance; however, both approaches are considered clinically acceptable [10]. Nevertheless, pilot-drill guidance is a more simplified and commonly applied technique in a clinical setting with added advantages of controlled irrigation, easy access in patients with limited mouth opening and ability to manually adjust implant position or angulation [10]. In contrast to static approaches, the dynamic navigation systems have further improved the precision of the implant placement procedure which offer a real-time tracking of the drills and implant in accordance with the virtual planning [4, 7, 11].

Previous studies have reported that novice practitioners offer an improved level of accuracy for implant placement with lesser deviation with both static and dynamic guided approaches [5, 10, 12, 13]. However, lack of evidence exists related to the assessment of the accuracy and efficacy of novice compared to experienced practitioners for dental implant placement with freehand and guided approaches. Therefore, the primary aim of this in-vitro study was to evaluate the influence of practitioner's experience on the accuracy of dental implant placement using freehand, static guided and dynamic navigation approaches. The secondary aims were to assess the surgical timing and self-confidence of practitioners. The null hypothesis was that no significant differences would exist between novice and experienced practitioners for implant placement with freehand, static guided and dynamic navigation approaches in relation to accuracy, surgical timing and self-confidence.

2. Methods and materials

2.1 Study sample

This research was performed in compliance with the World Medical Association Declaration of Helsinki on medical research. The study was approved by the Ethical Review Board of the University Hospitals Leuven, Belgium (reference number: S64493).

Dental implants were placed using three surgical approaches, i.e., freehand, surgical guide (pilot-drill guidance) and navigation system (Dynamic Navigation system, X-Guide, X-Nav technologies, LLC, Lansdale, PA). Sample size was calculated in G*Power v.3.1 (Heinrich-Heine Universität, Düsseldorf, Germany) with the following parameters: angular deviation data extracted from a study as the primary outcome variable [14] with alpha level of 0.05, statistical power of 80%, and effect size of 0.08 [15]. The calculation resulted in a total sample size of 36 implants required for the comparison of three approaches (n = 12 per approach).

A mandibular CBCT image having missing bilateral first molars (Fédération Dentaire Internationale [FDI], lower left 1st molar: 36, lower right 1st molar: 46) was retrospectively recruited from a radiological database. The scanning parameters were 110 kV, 8 × 10-cm field of view (FOV), and voxel size of 0.25 mm. Volumetric reconstruction of the mandibular bone was performed in Mimics software (version 21.0, Materialise, Leuven, Belgium). Thereafter, 36 identical simulation models were fabricated using Objet Connex 350 printer (Stratasys, Eden Prairie, MN, USA) with an acrylic-based resin (VeroDent MED670, Stratasys, Eden Prairie, MN, USA) [16].

Three experienced and three novice practitioners were recruited. Experienced practitioners consisted of oral surgeons with a clinical experience of over 5 years in implant dentistry and novice practitioners were general dentists with no clinical experience in implant dentistry. Prior to research, all practitioners received standard hands-on training for virtual planning with implant treatment planning software (DTX Studio™ Implant 3.4.3.3, Nobel Biocare AG) and surgical procedure simulation with the navigation system to achieve minimal proficiency. In addition, novice practitioners were also trained by an experienced clinician for performing implant placement with surgical guide and freehand approaches.

2.2 Treatment planning

The planning for static-guide-based implant placement was performed using an open-source implant planning software (Blue Sky Plan 4, Blue Sky Bio LLC, Grayslake, IL, USA), where CBCT and intraoral scanned (IOS) images of the teeth were imported and registered. As the teeth derived from CBCT data set fail to display teeth accurately, the integration of intraoral scanned image through the registration step allowed to achieve precise occlusal surface details for the construction of a properly fitting surgical guide. Following virtual implant placement, a surgical guide was designed and exported in standard tessellation language (STL) format. The guide was printed using Objet Connex 350 printer with a polyjet material (MED610, Stratasys, Eden Prairie, MN, USA) and surgical sleeves were fixed onto the guide with an adhesive.

For navigation-based planning, a tracking device (X-Clip, X-Nav Technologies) with 3 radiopaque fiducials was fixed to the mandibular anterior and premolar teeth with a thermoplastic impression material. The acquired impression surface was printed with a soft transparent material (Tango+, Stratasys, Eden Prairie, MN, USA) which was then used to fix the X-clip with the teeth. This allowed replication of the registration with exact seating of the device onto the teeth of each model. A CBCT scan (Accuitomo, J. Morita, Kyoto, Japan) of the model with the adapted clip was acquired with the following acquisition parameters: 90 kV, 5 mA, full-scan mode (360°) with Hi-Fi, 0.125 mm voxel size and 8 × 8 cm FOV.

The CBCT images of both patient and model were imported to Mimics Innovation Suite (Materialise, Leuven, Belgium) in Digital Imaging and Communications in Medicine (DICOM) format for aligning and combining the two images. This combined DICOM data set and IOS image of the teeth were uploaded and registered in DTX Studio implant software. The implants were virtually positioned at 36 and 46 sites similar to the static guide-based planning. Thereafter, all the images and virtual planning were transferred to the navigation system. **Fig. 1** represents the workflow for the surgery.

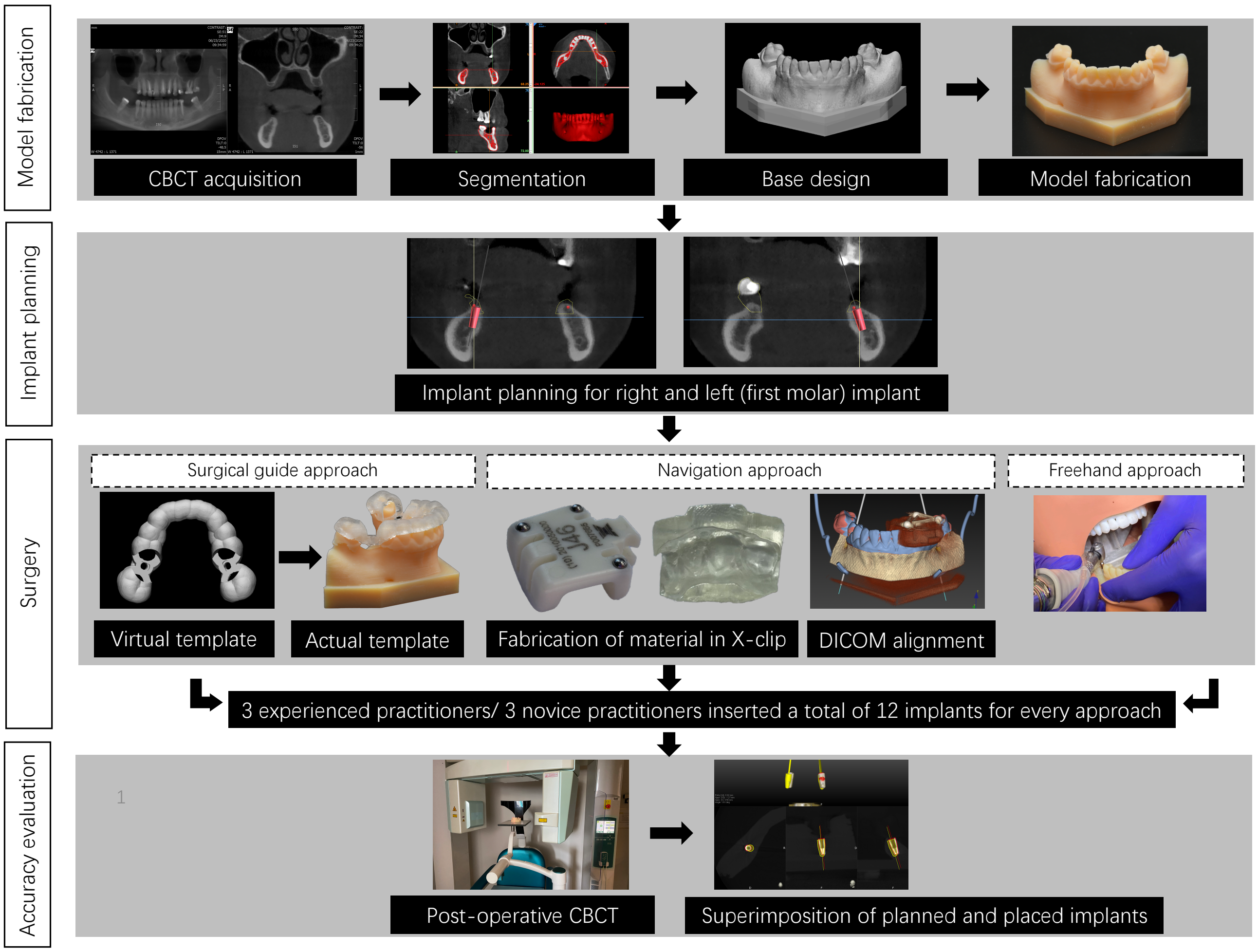

Figure 1. Workflow for surgery

2.3 Research procedure

All the practitioners were assigned with the task of inserting implants by each approach. The approach order was randomized for each practitioner using the random function of Microsoft Excel (version 16.38, Microsoft Corp, Redmond, US) and a 1-week gap was applied in-between approaches to avoid memory bias. The surgical procedure was standardized beforehand and the drilling sequence was prepared with irrigation based on a protocol recommended by the manufacturer (Wego, China). Following osteotomy, implants (customized experimental In-Hex implant, 3.8 mm × 9 mm, Wego, China) were placed using a surgical motor (EXPERTsurg™ LUX, KaVo, Germany) at 15 rpm and with a maximum torque of 50 N.cm. Each model was fixed onto a dental phantom head (Frasaco GmbH, Tettnang, Germany) for mimicking a clinical scenario (**Fig. 2a**). For the freehand approach, the practitioners used the planned implant position displayed on the Blue Sky Plan software as a reference. The static guide-based approach involved pilot drill guided osteotomy followed by freehand osteotomy and implant insertion.

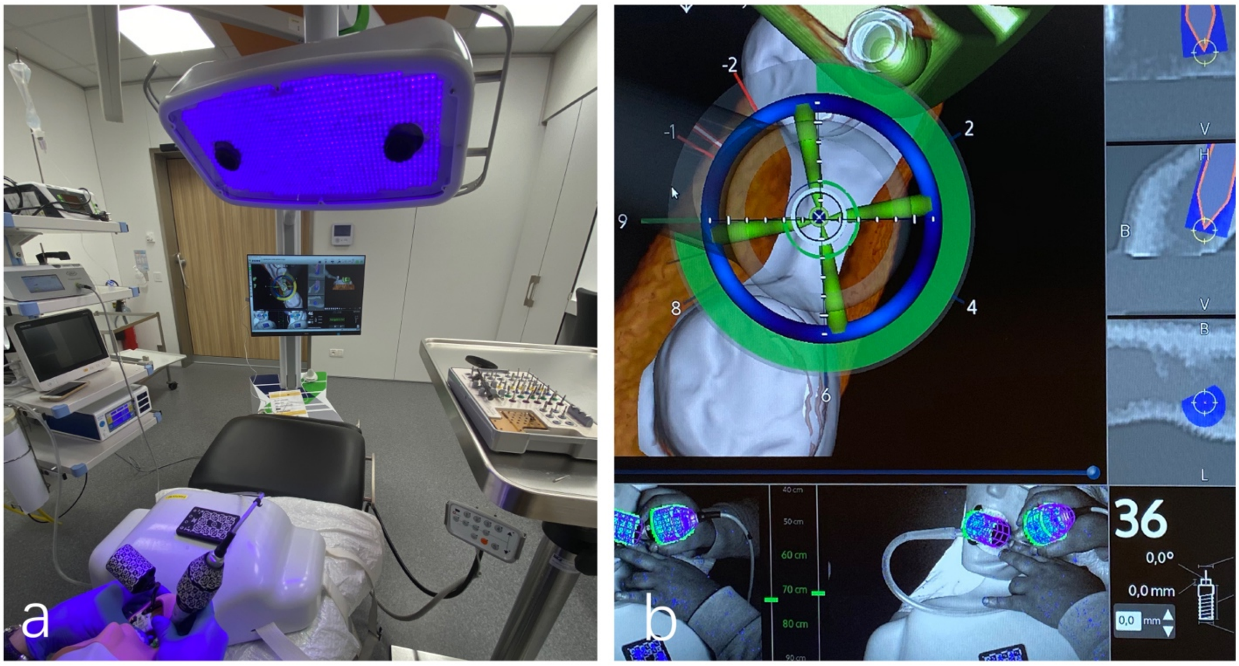

Figure 2. Navigation surgery. a Navigation system overview. b Screen displays implant site preparation

The navigation-based approach involved rigid fixation of the X-clip onto the teeth with the printed impression surface of teeth. A rigid fixation allowed to keep the clip stable, as any clip movement and its instability during the procedure could induce error in the registration and calibration process of the navigation system. Hence, directly impact the accuracy of implant placement. The calibration of tracking arrays and handpiece were performed with a calibrating plate for verifying any deviation prior to the surgery. Both the drills and implant were tracked live by the system during insertion and the practitioners followed the planned path as displayed on the screen (**Fig. 2b**).

A post-operative CBCT scan of the drilled models was acquired using prior acquisition parameters. Thereafter, both pre-operative and post-operative CBCT images were superimposed to assess the deviation between planned and actual implant placement automatically with EvaluNav software (ClaroNav Technology Inc., Toronto, Canada). The parameters for assessing deviation included:

i) entry two-dimensional (2D) deviation (horizontal drilling point deviation),

ii) apex three-dimensional (3D) deviation (3D deviation at implant's apex location),

iii) apex (V) deviation (vertical depth deviation)

iv) angular deviation.

The surgical time was recorded. In addition, a validated self-confidence questionnaire was conducted for evaluating the self-efficacy of practitioners on a scale of 1–30 for each approach (Additional file 1: Table S1) [17].

2.4 Statistical analysis

Data were analyzed using IBM SPSS Statistics for Windows, version 21.0 (IBM Corp., Armonk, NY, USA). Descriptive statistics for all the parameters were recorded (entry 2D, apex 3D, apex V, angulation and surgical time). The Shapiro–Wilk test was used to test the normality of data distribution and data transformation was applied if required to adjust for the lack of normality. A linear mixed model with two fixed factors (experience and approach) and two random factors (surgeon and 3D printed model) was applied to examine the differences between each approach. A P value of < 0.05 was considered as statistically significant.

3. Results

A total of 72 implants (4 insertion sites × 3 approaches × 6 practitioners = 72 implants) were placed by three experienced (12 implants per practitioner = 36 implants) and three novice practitioners (12 implants per practitioner = 36 implants). Two implant sites suffered from perforation at the apical part of lingual bone following drilling with freehand approach by experienced practitioners, while novice practitioners perforated lingual bone at two sites using surgical guide. In addition, a guide was fractured by a novice practitioner during osteotomy.

Table 1. Descriptive values (Mean ± SD, Range) categorized by surgical approach and experience

Approach	Entry/ mm	Apex(3D)/ mm	Apex(V)/ mm	Angle/ °	Time/ sec
Freehand					
Experienced	1.11±0.58 (0.29-2.34)	1.91±1.06 (0.97-3.93)	0.54±0.38 (0.1-1.2)	9.73±4.29 (4.01-17.65)	3.27±1.43 (2.12-6.67)
Novice	1.40±1.01 (0.09-3.15)	2.54±1.58 (0.85-6.33)	0.60±0.33 (0.1-1.09)	8.15±4.73 (3.37-21.28)	7.33±3.40 (3.25-13.17)
Surgical guide					
Experienced	0.83±0.65 (0.1-2.24)	1.67±0.94 (0.38-3.64)	0.48±0.34 (0.01-0.97)	7.27±3.82 (1.5-13.89)	3.62±1.78 (1.62-7.65)
Novice	0.92±0.38 (0.31-1.58)	1.66±0.64 (0.48-2.75)	0.41±0.27 (0.03-0.89)	7.07±4.38 (1.45-15.36)	7.59±2.17 (4.48-11.28)
Navigation					
Experienced	1.09±0.41 (0.37-1.67)	1.55±0.56 (0.65-2.77)	0.44±0.55 (0.04-1.96)	3.37±1.56 (1.61-6.68)	11.58±3.51 (6.77-19.03)
Novice	1.14±0.46 (0.4-2.02)	1.76±0.71 (0.81-2.75)	0.70±0.58 (0.14-2.2)	3.19±1.89 (1.25-6.54)	13.08±4.62 (5.75-20.33)

Table 1 describes the mean deviation between planned and actual implant position and time taken by each approach. In addition, the statistical significance of implant deviation, time and self-confidence

based on approach, experience, and interaction of both is presented in **Table 2**. Following verification of residual values normality in the transformed data, the linear mixed model showed that the navigation approach significantly improved angular deviation compared with freehand ($P<0.001$) and surgical guide ($P<0.001$). Furthermore, experienced practitioners showed a slightly higher angular deviation with all three approaches compared to novice practitioners without any significant difference. The differences in entry 2D, apex 3D and apex V were not significantly different based on approaches, experience or interaction of both ($P>0.05$).

Table 2. Statistical significance of implant deviation, time and self-confidence considering approach, experience, and interaction of both.

	Approach	**Experience**	**Approach* Experience**
Entry/ mm	0.67	0.28	0.88
Apex(3d)/ mm	0.15	0.19	0.78
Apex(v)/ mm	0.39	0.23	0.41
Angle/ °	**<0.001**	0.35	0.84
Time/ sec	**<0.001**	**<0.001**	**0.001**
Self-confidence	0.48	0.63	0.56

Numbers in bold refer to statistically significant values.

The surgical time with navigation approach was significantly longer than that of freehand ($P<0.001$) and surgical guide ($P<0.001$). In addition, novice practitioners showed an overall increase in surgical time compared with experienced practitioners ($P<0.001$). A significant difference in interaction was observed, which indicated that both experience and approach affected the surgical time ($P=0.001$). The time taken by novice practitioners with navigation approach was significantly longer compared to experienced practitioners.

The findings of the self-confidence questionnaire (**Table 3**) suggested no significant difference between self-confidence of both novice and experienced practitioners. However, novice practitioners considered that their performance improved using both guided approaches (**Fig. 3**), where they showed high level of confidence and lower anxiety with both guided approaches compared to the freehand approach. The scoring of novice practitioners' self-confidence with the navigation approach (median score = 26) was comparable to that of experienced ones (median score = 27). In addition, experienced practitioners reported highest self-confidence scores with static guide (median score = 29), followed by freehand (median score = 28) and navigation system (median score = 27).

Table 3. Self-confidence scoring of each practitioner.

		1. How confident were you during the procedure?	2. What was your surgical skill level during the procedure?	3. Were you worried during the procedure?	4. Were you anxious during the procedure?	5. Based on your performance today, would you have liked to have avoided this procedure altogether?	6. How comfortable were you with the independent planning and performing the procedure?	Total
Freehand	Experienced 1	4	5	5	4	5	5	28
	Experienced 2	4	4	3	3	4	3	21
	Experienced 3	5	5	5	5	5	4	29
	Novice 1	1	2	2	2	3	1	11
	Novice 2	2	3	3	3	5	3	19
	Novice 3	4	4	4	5	4	5	26
Surgical guide	Experienced 1	5	4	5	5	5	5	29
	Experienced 2	5	5	4	3	4	4	25
	Experienced 3	5	5	5	5	5	5	30
	Novice 1	3	3	3	3	5	4	21
	Novice 2	5	4	5	5	5	4	28
	Novice 3	3	3	4	5	3	5	23
Navigation	Experienced 1	4	5	5	4	5	4	27
	Experienced 2	5	5	5	4	5	5	29
	Experienced 3	3	5	3	3	4	3	21
	Novice 1	4	4	5	4	5	4	26
	Novice 2	3	4	3	4	4	4	22
	Novice 3	5	5	5	5	3	5	28

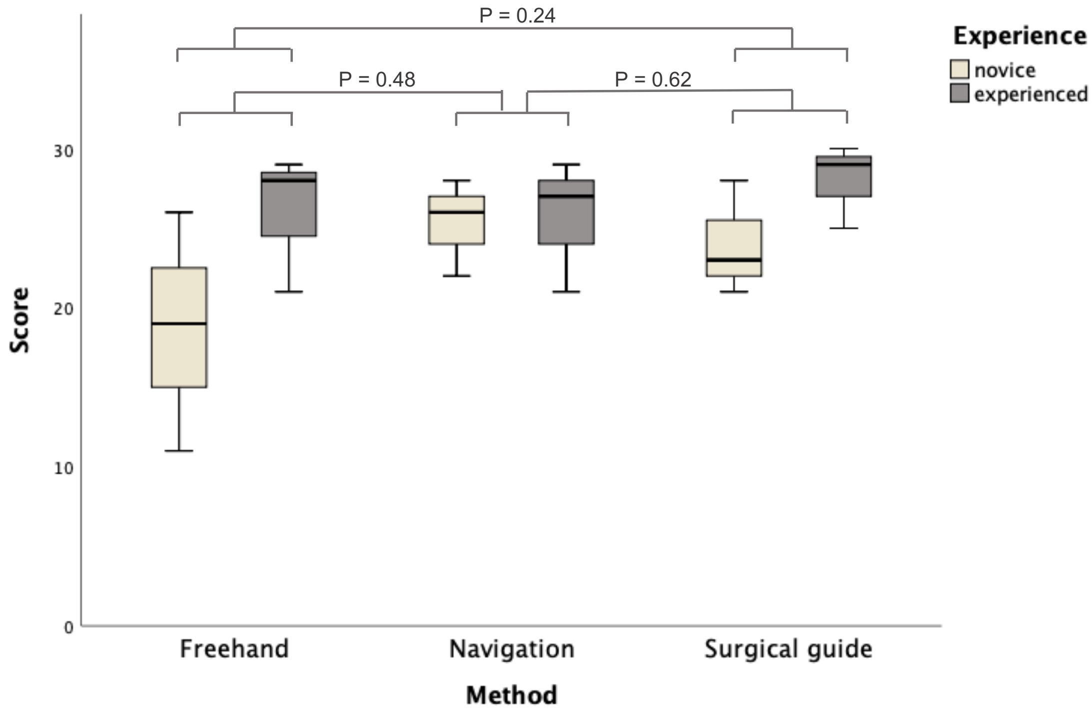

Figure 3. Median and inter-quartile range of self-confidence scores for each approach categorized by experience. Boxes comprise of 25th and 75th quartiles and median values, upper and lower whisker indicate highest and lowest values

4. Discussion

The implementation of computer-guided technologies promise a novel approach for dental implant surgery. This study investigated the accuracy, time-efficiency and self-confidence of novice practitioners compared to experienced practitioners for implant placement with freehand, static pilot drill-based guidance and navigation approaches. The findings suggested that the navigation approach could acted as a viable medium for performing implant surgery by novice practitioners with comparable accuracy, self-confidence and surgical time to that of experienced practitioners with the same level of training.

The angular deviation of implant placement was significantly better with navigation compared to freehand and surgical guided approach. As the freehand drilling mainly depends on the practitioner's theoretical and clinical skills which are often acquired over a long period of time during training; therefore, it was difficult for novice practitioners to place the implant in an ideal position. In addition, posterior implant placements are generally less accurate than anterior ones owing to difficult access and indirect visualization which might have further contributed toward lower accuracy with the freehand approach [18]. In contrast, pilot-drill guidance offered the advantage of improved implant deviation compared to the freehand approach. However, it was still prone to a large angular deviation which could have resulted due to an undesirable mechanical tolerance between the drills and sleeve or accumulative error at the data acquisition, software processing and template manufacturing steps of the digital workflow [19]. In addition, the findings suggested that experienced practitioners offered higher angular deviation compared to novice practitioners with all the approaches. However, the difference was quite minimal which is negligible from a clinical point of view and could be attributed to the small sample of practitioners. Another reason could be related to the level of attention to detail and concentration, where novice practitioners might have paid more attention to avoid any unnecessary change in angulation.

The navigation approach provided the most accurate approach for implant placement with an excellent performance by novice practitioners. These findings were consistent with previous studies, where the navigation system offered significant improvement in implant placement accuracy compared to surgical guide and freehand approach [14, 20, 21]. At the same instance, a risk of implant deviation still exists with the navigation system due to the errors generated during the workflow steps of image acquisition, tracking clip stability, registration and calibration [14]. A practitioner should be aware of these errors which is crucial for a successful treatment outcome. However, the navigation approach allowed novice practitioners to achieve similar accuracy to that of experienced ones which was in accordance with another study [13]. Similarly, Sun et al. and Wu et al. found that the experience level of practitioners did not affect the accuracy of implant placement with the navigation approach [22, 23].

The surgical time required by the navigation approach was significantly longer than the surgical guide or freehand approach which was consistent with a previous study [15]. This increased time was attributed to the necessary calibration of the drills and implant required throughout the procedure to allow for optimal tracking. In addition, reconfirmation of the correct drilling and implant placement by viewing both the screen and patient led to a further increase in time. It should be noted that the navigation system has a steep learning curve, where its more frequent usage could allow mastering the system with a higher confidence in the technology and further lower the surgical time [24, 25]. At the same instance, surgical time with the navigation system could be less compared to other approaches in complex surgical cases with limited direct access or tight interdental spaces which preclude the usage of surgical guide tubes [8, 15].

Although the dynamic navigation system offers comparable accuracy to a static guided approach, its application is limited in a clinical practice due to high costs, steep learning curve, early developmental stage and risk of inaccurate implant placement due to system error associated with either registration or calibration steps especially in completely edentulous cases [26]. Furthermore, the majority of evidence assessing the accuracy of navigation systems is based on in vitro studies and clinical studies are still scarce. Hence, further clinical studies are required to confirm whether their implant positional accuracy and time efficiency is maintained in a real clinical scenario, where different patient- and surgery-related factors could negatively impact the final outcome. In contrast, ample evidence exists justifying the satisfactory results of static guided approaches in both partial and complete edentulous cases with a relatively lower price tag [6].

In the present study, novice practitioners required more time to perform the surgery irrespective of the approach, which could be attributed to the proficiency and surgical skills of the practitioners. The self-confidence of novice practitioners was high with both guided approaches, which was partially consistent with another study, where observers showed better performance and high confidence with a static guided approach [27, 28]. Furthermore, the novice practitioners expressed a desire to use the navigation system for future implantations which was consistent with previous studies [24, 29]. Experienced practitioners were more confident with a static guided approach compared to navigation system as they preferred relying on already achieved skills rather than pursuing new innovative technologies with complex workflows [30]. Hence, their performance with static guide was more predictable and less stressful which was confirmed by a higher self-confidence score.

The study had certain limitations. First, the findings of this study should be interpreted with caution due to its in-vitro study design. Second, a lack of variability existed in relation to implant insertion sites with only involvement of posterior region. Third, the study only assessed pilot-drill guidance. Hence, further studies are required to investigate the practitioner's performance based on a static fully guided approach and with the inclusion of variable implant insertion sites.

5. Conclusions

The dynamic navigation system could act as a viable tool for dental implant placement by novice practitioners, who were able to achieve comparable accuracy and self-confidence to that of experienced practitioners. The navigation approach offered a more accurate implant placement with significant improvement in angular deviation compared to the pilot-drill surgical guide and freehand approach irrespective of practitioner's experience. Future clinical studies are required for the assessment of external validity and implant placement accuracy with navigation system in a clinical practice.

References

[1] Z. Jalbout, D.D.S.; Edgard, E. Chaar, S. Hirsch, Dental implant placement by predoctoral dental students: a pilot program, J Dent Educ. 76(2012) 1342–6.

[2] M.A. Sánchez-Garcés, E. Berástegui-Jimeno, C. Gay-Escoda, Knowledge, aptitudes, and preferences in implant dentistry teaching/training among undergraduate dental students at the university of Barcelona, Med. Oral Patol. Oral Cir. Bucal. 22 (2017) e484–e490.

[3] S. Koole, H. De Bruyn, Contemporary undergraduate implant dentistry education: A systematic review, Eur. J. Dent. Educ. 18 (2014) 11–23.

[4] M. Hultin, K.G. Svensson, M. Trulsson, Clinical advantages of computer-guided implant placement: A systematic review, Clin. Oral Implants Res. 23 (2012) 124–135.

[5] G. Pellegrino, A. Ferri, M. Del Fabbro, C. Prati, M.G. Gandolfi, C. Marchetti, Dynamic Navigation in Implant Dentistry: A Systematic Review and Meta-analysis., Int. J. Oral Maxillofac. Implants. 36 (2021;) e121–e140.

[6] B. Kunzendorf, H. Naujokat, J. Wiltfang. Indications for 3-D diagnostics and navigation in dental implantology with the focus on radiation exposure: a systematic review, Int J Implant Dent. 7 (2021) 4–11.

[7] J. D'haese, J. Ackhurst, D. Wismeijer, H. De Bruyn, A. Tahmaseb, Current state of the art of computer-guided implant surgery, Periodontol. 2000. 73 (2017) 121–133.

[8] M.S. Block, R.W. Emery, Static or Dynamic Navigation for Implant Placement - Choosing the Method of Guidance, J. Oral Maxillofac. Surg. 74 (2016) 269–277.

[9] S. Schnutenhaus, C. Edelmann, H. Rudolph. Does the macro design of an implant affect the accuracy of template-guided implantation? A prospective clinical study, Int J Implant Dent. 7 (2021) 42.

[10] C. Ilhan, M. Dikmen, E. Yüzbasioglu, Accuracy and efficiency of digital implant planning and guided implant surgery: An update and review, J. Exp. Clin. Med. 38 (2021) 148–156.

[11] N. Panchal, L. Mahmood, A. Retana, R. Emery, Dynamic Navigation for Dental Implant Surgery, Oral Maxillofac. Surg. Clin. North Am. 31 (2019) 539–547.

[12] M. Block, R. Emery, K. Lank, J. Ryan, Implant Placement Accuracy Using Dynamic Navigation, Int. J. Oral Maxillofac, Implants. 32 (2017) 92–99.

[13] C.A. Aydemir, V. Arısan, Accuracy of dental implant placement via dynamic navigation or the freehand method: A split-mouth randomized controlled clinical trial, Clin. Oral Implants Res. 31 (2020) 255–263.

[14] C.-K. Chen, D.-Y. Yuh, R.-Y. Huang, E. Fu, C.-F. Tsai, C.-Y. Chiang, Accuracy of Implant Placement with a Navigation System, a Laboratory Guide, and Freehand Drilling, Int. J. Oral Maxillofac. Implants. 33 (2018) 1213–1218.

[15] J A. Jorba-García, R. Figueiredo, A. González-Barnadas, O. Camps-Font, E. Valmaseda-Castellón, Accuracy and the role of experience in dynamic computer guided dental implant surgery: An in-vitro study, Med. Oral Patol. Oral y Cir. Bucal. 24 (2019) e76–e83.

[16] X. Wang, S. Shujaat, E. Shaheen, R. Jacobs, Quality and haptic feedback of three-dimensionally printed models for simulating dental implant surgery, J. Prosthet. Dent. (2022) 1–8.

[17] R. Geoffrion, T. Lee, J. Singer, Validating a self-confidence scale for surgical trainees, J. Obstet. Gynaecol. Canada. 35 (2013) 355–361.

[18] S. Bencharit, A. Staffen, M. Yeung, D. Whitley, D.M. Laskin, G.R. Deeb, In vivo tooth-supported implant surgical guides fabricated with desktop stereolithographic printers: fully guided surgery is more accurate than partially guided surgery, J. Oral Maxillofac. Surg. 76 (2018) 1431–1439.

[19] T. Elliott, A. Hamilton, N. Griseto, G.O. Gallucci, Additively Manufactured Surgical Implant Guides: A Review, J. Prosthodont. 31 (2022) 38–46.

[20] T.-M. Sun, H.-E. Lee, T.-H. Lan, Comparing accuracy of implant installation with a navigation system (NS), a laboratory guide (LG), NS with LG, and freehand drilling, Int J Environ Res Public Health. 17 (2020) 2107.

[21] A.M. Guzmán, E.R. Deglow, Á. Zubizarreta-Macho, R. Agustín-Panadero, S.H. Montero, Accuracy of computer-aided dynamic navigation compared to computer-aided static navigation for dental implant placement: An in vitro study, J. Clin. Med. 8 (2019).

[22] T.M. Sun, H.E. Lee, T.H. Lan, The influence of dental experience on a dental implant navigation system, BMC Oral Health. 19 (2019) 1–11.

[23] D. Wu, L. Zhou, J. Yang, B. Zhang, Y. Lin, J. Chen, Accuracy of dynamic navigation compared to static surgical guide for dental implant placement, Int J Implant Dent. 6 (2020) 78.

[24] N. Casap, S. Nadel, E. Tarazi, E.I. Weiss, Evaluation of a navigation system for dental implantation as a tool to train novice dental practitioners, J. Oral Maxillofac. Surg. 69 (2011) 2548–2556.

[25] J. Golob Deeb, S. Bencharit, C.K. Carrico, M. Lukic, D. Hawkins, K. Rener-Sitar, G.R. Deeb, Exploring training dental implant placement using computer-guided implant navigation system for predoctoral students: A pilot study, Eur. J. Dent. Educ. 23 (2019) 415–423.

[26] J. Spille, F. Jin, E. Behrens, Y. Açil, J. Lichtenstein, H. Naujokat, Comparison of implant placement accuracy in two different preoperative digital workflows: navigated vs. pilot-drill-guided surgery, Int J Implant Dent. 7 (2021)1–9.

[27] S. Prasad, N. Bansal, Predoctoral dental students' perceptions of dental implant training: Effect of preclinical simulation and clinical experience, J Dent Educ. 81 (2017) 395–403.

[28] S.D. Seitz, R.L. Zimmermann, W.D. Hendricson, Expansion of a predoctoral surgical implant selective for dental students, J. Dent. Educ. 80 (2016) 328–333.

[29] Y. Zhan, M. Wang, X. Cheng, Y. Li, X. Shi, F. Liu, Evaluation of a dynamic navigation system for training students in dental implant placement, J Dent Educ. 85 (2021) 120–127.

[30] E.M. Bucholz, G.R. Sue, H. Yeo, S.A. Roman, R.H.B. Jr, J.A. Sosa, Our Trainees' Confidence, 146 (2021) 907–914.

ARTICLE 5

Performance of novice versus experienced surgeons for dental implant placement with freehand, static guided and dynamic navigation approaches

Wang X. [1,2]
Shujaat S. [1,3]
Meeus J. [4]
Shaheen E. [1]
Legrand P. [1]
Lahoud P. [1]
Gerhardt M. [1,5]
Jacobs R. [1,6]

[1] OMFS-IMPATH Research Group, Department of Imaging & Pathology, Faculty of Medicine, KU Leuven & Oral and Maxillofacial Surgery, University Hospitals Leuven, Leuven, Belgium.

[2] Department of Oral and Maxillofacial Surgery, The First Affiliated Hospital of Harbin Medical University, Harbin, China.

[3] King Abdullah International Medical Research Centre, Department of Maxillofacial Surgery and Diagnostic Sciences, College of Dentistry, King Saud bin Abdulaziz University for Health Sciences, Ministry of National Guard Health Affairs, Riyadh, Kingdom of Saudi Arabia

[4] Department of Oral and Maxillofacial Surgery, University Hospitals Leuven, Leuven, Belgium.

[5] School of Health Sciences, Faculty of Dentistry, Pontifical Catholic University of Rio Grande do Sul, Porto Alegre, Brazil.

[6] Department of Dental Medicine, Karolinska Institutet, Huddinge, Sweden.

Published in Sci Rep. 2023 Feb;13(1):2598.

Abstract

Lack of evidence exists related to the investigation of the accuracy and efficacy of novice versus experienced practitioners for dental implant placement. Hence, the following in vitro study was conducted to assess the accuracy of implant positioning and self-efficacy of novice compared to experienced surgeons for placing implant using freehand (FH), pilot drill-based partial guidance (PPG) and dynamic navigation (DN) approaches. The findings revealed that DN significantly improved the angular accuracy of implant placement compared with FH ($P < 0.001$) and PPG approaches ($P < 0.001$). The time required with DN was significantly longer than FH and PPG ($P< 0.001$), however, it was similar for both novice and experienced practitioners. The surgeon's self-confidence questionnaire suggested that novice practitioners scored higher with both guided approaches, whereas experienced practitioners achieved higher scoring with PPG and FH compared to DN. In conclusion, implant placement executed under the guidance of DN showed high accuracy irrespective of the practitioner's experience. The application of DN could be regarded as a beneficial tool for novices who offered high confidence of using the navigation system with the same level of accuracy and surgical time as that of experienced practitioners.

Keywords: Dental Implantation; Surgery, Computer-Assisted; Surgical Navigation Systems; Dimensional Measurement Accuracy; Self Efficacy; Operative Time

1. Introduction

Dental implant surgery is a widely accepted therapeutic option for partially and fully edentulous patients. An ideal three-dimensional (3D) implant positioning and angulation is a prerequisite to ensure its long-term stable esthetic and functional outcome and to facilitate a correct prosthetic phase [1]. In contrast, non-ideal implant positioning may cause collateral damage to the vital anatomical structures within the vicinity of the placed implant and lead to certain intra-operative complications, such as maxillary sinus and/or cortical perforation, inferior alveolar nerve injury and damage to adjacent teeth [2]. Furthermore, an imprecise positioning of the implant has also been known to cause peri-implant bone loss and peri-implantitis at follow-up [2]. Hence, it is necessary that a surgeon should have a high level of experience and sufficient 3D spatial awareness to avoid complications associated with non-ideal placement of dental implants [3].

The wide adoption of cone-beam computed tomography (CBCT) coupled with computer-aided design and computer-aided manufacturing (CAD/CAM) in a dental practice has improved the implant placement accuracy compared to freehand (FH) approach and allowed delivery of predictable prosthetically-driven treatment outcomes [4]. The two main computer-assisted techniques include implant placement with either CBCT-generated static surgical guide (SG) or dynamic navigation (DN) system [5]. Implant placement by static surgical guide can be classified as fully or partially guided, where full guidance refers to the control of all steps from osteotomy till implant placement through a guide [6]. It may be beneficial in cases with irregular bone quality, where minor implant movement is associated with higher deviation [7]. On the contrary, partial guidance (pilot drill or half-guided approach) involves only the use of a pilot drill or the complete osteotomy before implant placement is guided, followed by free-handed manual drilling and implant placement. A fully-guided approach offers less implant deviation compared to its partial counterpart [8]. However, pilot drill based partial guidance (PPG) is still the most commonly employed technique in a dental practice owing to its simplistic nature, reduction in irrigation problems, allowing minor implant position adjustment if required and easier control of implant placement in patients with limited mouth opening [9,10].

Unlike SG-based approaches, DN system allows real-time guidance by tracking the optical markers fixed to the hand-piece and patient, thereby, making it possible to monitor the drills and implant to follow the planned position [7]. It offers the advantage of real-time computer-guided freehand approach, where the operator has more freedom to adjust the implant position with the possibility of flapless surgery, lower morbidity, and a predictable outcome in both normal and complex cases with limited access or poor visualization [11,12].

Recent studies have demonstrated that both SG and DN provide comparable accuracy which is higher than a FH approach for training novice surgeons, dental implant education and guiding experienced surgeons for a safe and predictable outcome [6,10,13-16]. However, to our knowledge no study exists investigating the accuracy and efficacy of novice versus experienced practitioners by comparing FH, SG and DN approaches. Therefore, the following study was conducted to quantitatively assess the accuracy of implant positioning and to qualitatively investigate the performance and self-confidence of novice surgeons compared to experienced surgeons for placing implants using FH, PPG and DN approaches.

2. Material and methods

2.1 Model fabrication

The study protocol was approved by the Ethical Review Board of the University Hospitals Leuven, Belgium (reference number: S64493). All experiments were performed in accordance with relevant guidelines and regulations. Informed consent was obtained from all participants. Inclusion criteria were CBCT dataset of lower jaw with sufficient bone quality and quantity for 3D model fabrication and implant placement, and a partial edentulous jaw with missing bilateral 1st molars. Exclusion criteria involved presence of pathological conditions or artefacts in the lower jaw.

A total of 36 identical simulation models with bilaterally missing 1st molar (72 implant placement sites) were designed in Mimics software (version 22.0, Materialise NV, Leuven, Belgium) and printed with Objet Connex 350 printer (Stratasys, Eden Prairie, MN, USA) using an acrylic-based resin (VeroDent MED670, Stratasys, Eden Prairie, MN, USA) [17].

2.2 Operators

An in-vitro study was conducted to compare three surgical protocols, which consisted of FH, PPG and DN system (Navident, ClaroNav, Toronto, Ontario, Canada). Three experienced dental practitioners with over 5-years of experience in implant surgery and three novice dental practitioners with no experience in surgical implantology participated in the study. Each participant received prior training and calibration. The training session for navigation was provided to all practitioners which consisted of theoretical knowledge and drilling simulation practice to establish minimal proficiency for implant placement (at least 10 osteotomies on simulation models) with the DN system. Both experienced and novice practitioners had no prior training of using DN systems. Furthermore, novice practitioners were also provided with a theoretical and surgical simulation training by an experienced operator for using both FH and PPG approaches to optimally place implants.

All operators were randomly assigned the task of implant placement by FH, PPG or DN approach, with random sequence generated using Excel. In order to minimize bias, there was a one-week washout period between each method. Out of the 36 printed models (72 implant placement sites), 6 models (12 implant placement sites) were allocated to each operator, where they placed implants on 2 models by each approach (2 implant placement sites per model = 4 implants per approach).

2.3 Treatment planning

The planning was performed by importing CBCT and intraoral scanned (IOS) images to an implant planning software (Blue Sky Plan 4, Blue Sky Bio LLC, Grayslake, IL, USA), where the implants were placed virtually, and surgical guides were designed following consultation with a consultant implantologist. Both the implant planning and SG were exported in standard tessellation language (STL) format. Subsequently, the surgical guide was fabricated with Objet Connex 350 printer and surgical sleeves were adhesively fixed onto the guide. Later, the CBCT dataset, IOS image and STL of virtual implant planning were imported to the user-interface of the DN system where virtual implants oriented identical to the planned position.

2.4 Surgical Procedure

The surgical procedure was standardized beforehand, and the drilling sequence was prepared with irrigation following the manufacturer's protocol utilizing customized experimental In-Hex implants (3.8mm x 9mm, Wego, China). Implants were inserted using a motor unit (OsseoSet, Nobel Biocare AB, Goteborg, Sweden) at a speed of 15 rpm and a maximum torque of 50 N.cm. The drilling order was as follows: 2.2-mm-round drill followed by 2-mm pilot drill, 3.3-mm form drill, and 3.8-mm final drill.

Each printed model was placed in a dental phantom head to mimic a real clinical setting. During surgery with the FH approach, osteotomy drilling and implant placement were performed in accordance to the virtual surgical plan (**Fig. 1a**). For the PPG, a tooth-supported guide was placed, and a single pilot drill was used for the initial drill, followed by FH drilling (**Fig. 1b**).

The DN approach involved firm attachment of the tracking tag to the anterior teeth of the jaw using silicone material (**Fig. 2a**). A tracking tag is a device which helps to maintain the registration between the jaw and its CBCT image and continuously tracks the patient's jaw pose throughout the procedure. For guaranteeing a standard protocol, each operator used the same landmarks for the trace registration step. The registration accuracy was assessed to ensure optimal tracking prior to the surgical procedure. Each drill and implant required calibration before their insertion into the bone. The real-time visual feedback on a screen was used to guide the osteotomy preparation and the implant was placed according to the planned implant position. The location, angle and depth of drilling in relation to the predetermined treatment plan on the monitor were used to assist the practitioners (**Fig. 2b**).

(a) (b)

Figure 1 Surgical photos. (a) Freehand surgery; (b) Surgical guide surgery. Surgical guide fitted intraorally.

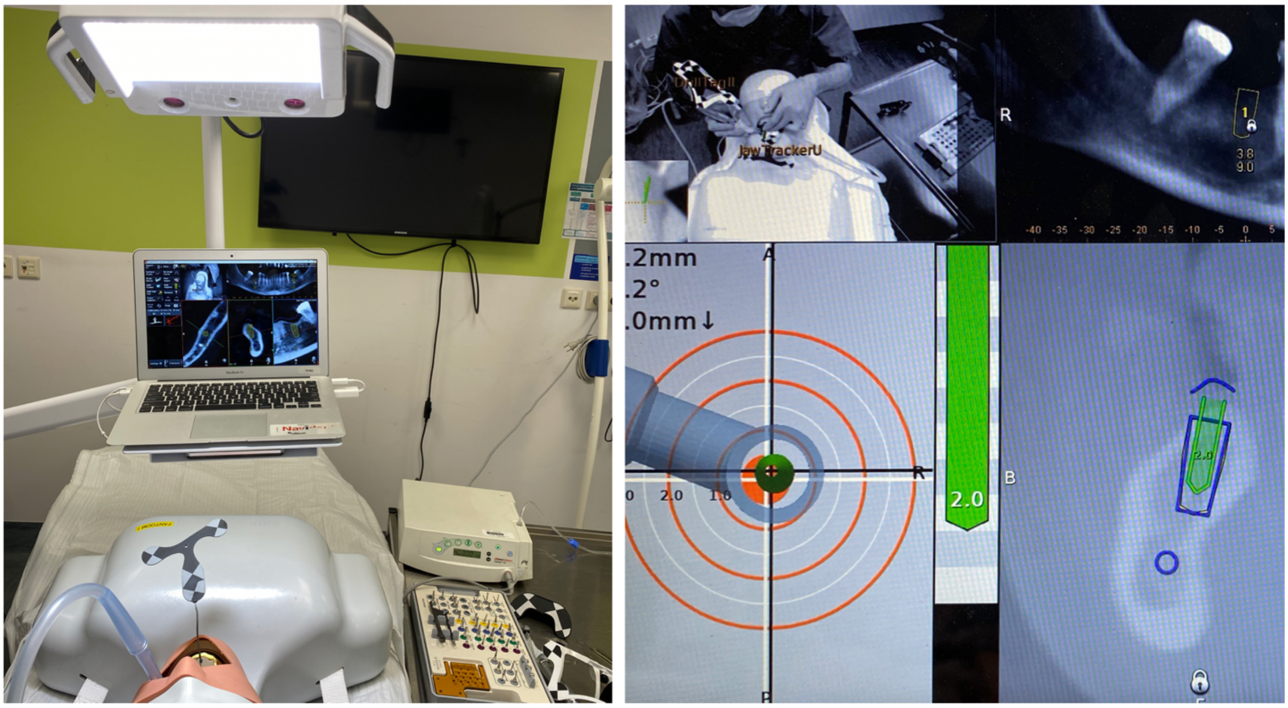

(a) (b)

Figure 2. Navigation surgery. (a) Overview of navigation system; (b) Operation screen.

2.5 Performance evaluation

A validated self-confidence questionnaire was provided to all the practitioners, where they scored their performance with each approach on a combined scale of 1 to 30 (1=least confident, 30=most confident) based on six questions (supplementary Table 1) [18]. This self-confidence scoring provided the "perceived self-efficacy" of the practitioners. In addition, time required for the procedure was also recorded.

2.6 Accuracy assessment

Following implant placement, all models were scanned with a CBCT device (Accuitomo, J. Morita, Kyoto, Japan) using a standard CBCT scanning protocol (90 kV, 5 mA, 360° full-scan mode with Hi-Fi, 0.125 mm voxel size and 8 × 8 cm field of view). The pre-operative CBCT scan with virtual implant position and the post-operative CBCT scan with actual position were superimposed using EvaluNav software (ClaroNav Technology Inc., Toronto, Canada) as shown in **Fig. 4**. Thereafter, the planned and actual implant positions were compared automatically in the software by measuring the following variables: entry two-dimensional (2D) deviation (horizontal coronal deviation), apex 3D deviation (3D apical deviation), apex (V) deviation (vertical depth deviation) and angular deviation.

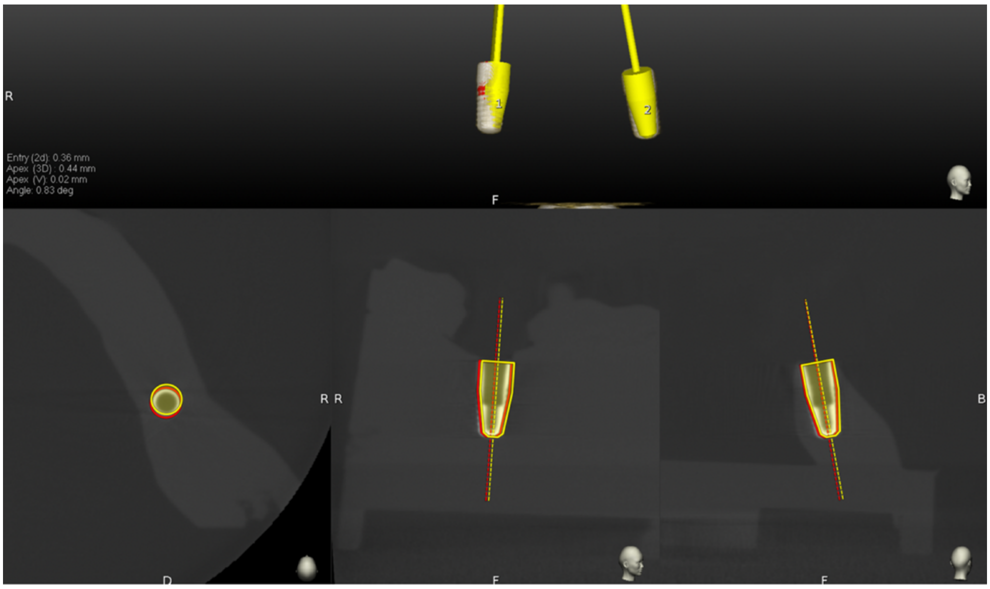

Figure 4. Superimposition of planned and actual placed implant positions.

2.7 Statistical analysis

Data were analyzed using IBM SPSS Statistics for Windows, version 21.0 (IBM Corp., Armonk, NY, USA). Descriptive statistics were calculated and presented as mean and standard deviation for entry 2D, apex 3D, apex V, angulation and surgical time. Self-confidence scores were examined by median and interquartile range. Normal distribution was assessed by means of normal quantile plots and data transformation was applied for achieving normal distributed data. The log-transformation was too strong, as confirmed by the points of the normal quantile plot which curved downward. Hence, a square-root transformation was applied for achieving normal distribution of the residual data. A linear mixed model with two crossed fixed factors (experience and method) and two random factors (surgeon and 3D printed model) were applied to evaluate the discrepancies amongst the three methods and the role of experience. Based on experience, as there were 3 novice and 3 experienced practitioners who inserted implants in two models, hence these were regarded as random factors. When the interaction was significant, a comparison was performed for methods per experience level and the experience level per method. Significance level was set at 5%.

3. Results

Out of the total 72 implant placements, perforation of the lingual wall was observed at four implant sites (2 sites by experienced practitioners with FH approach; two sites by novice practitioners with PPG approach). Furthermore, a surgical guide was fractured by a novice practitioner during surgical drilling.

According to the self-confidence questionnaire's scoring, overall navigation system scored significantly lower compared to freehand and surgical guided approaches (P=0.007 and P<0.001, respectively). Significant differences were observed based on the interaction of experience and approaches (P=0.013). Experienced operators showed a high self-confidence score in favor of PPG, followed by FH and DN. However, overall novice practitioners perceived that their performance improved when using PPG and DN approaches as shown in **Fig. 5**.

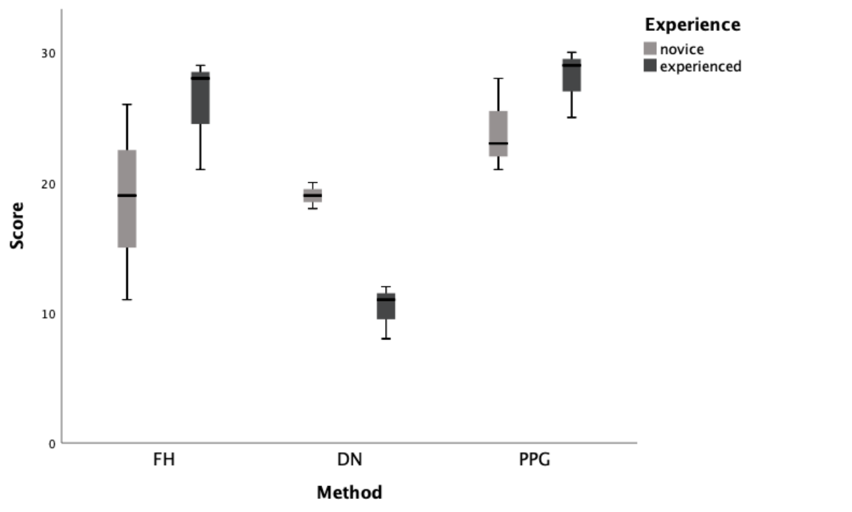

Figure 5. Median and inter-quartile range of the scoring of self-confidence assessment achieved with each method categorized by experience. Boxes comprise of 25th and 75th quartiles and median values, upper and lower whisker indicate highest and lowest values. FH: freehand, PPG: pilot drill based partial guidance, DN: dynamic navigation

Table 1 describes the mean deviation between planned and actual implant position and time consumption with each approach, where lower values indicate towards better implant positioning. The findings suggested that entry 2D deviation was lowest with the PPG approach, irrespective of operator's experience. In addition, novice operators showed the highest apex 3D deviation using FH approach. The angular deviation was lowest with the DN, followed by PPG and FH approaches. Based on timing, implant placement using DN was most time-consuming and FH technique offered the least time consumption.

Table 1. Descriptive values (Mean±SD) by surgery method and experience.

Method	Entry(2D)/ mm	Apex(3D)/ mm	Apex(V)/ mm	Angle/ °	Time/ second
FH					
Experienced	1.11±0.58	1.91±1.06	0.54±0.38	9.73±4.29	196.25±85.56
Novice	1.40±1.01	2.54±1.58	0.60±0.33	8.15±4.73	439.67±203.97
PPG					
Experienced	0.83±0.65	1.67±0.94	0.48±0.34	7.27±3.82	217.25±107.00
Novice	0.92±0.38	1.66±0.64	0.41±0.27	7.07±4.38	455.42±130.34
DN					
Experienced	1.28±0.55	1.70±0.77	0.41±0.25	4.03±1.53	934.75±773.24
Novice	1.07±0.52	1.54±0.94	0.70±0.71	2.88±2.51	900.58±379.23

FH: freehand, PPG: pilot drill based partial guidance, DN: dynamic navigation

Based on linear mixed model analysis in **Table 2**, the angular deviation differed significantly amongst different surgical approaches ($P < 0.001$), where DN significantly improved the angular accuracy compared with FH ($P < 0.001$) and PPG approaches ($P < 0.001$). No significant differences were observed between experience of the operators ($P=0.10$) or interaction of methods and experience ($P=0.57$). In addition, the platform deviations (entry 2D, apex 3D and apex V) were similar irrespective of surgical approach, experience or interaction of both ($P > 0.05$).

Table 2. Statistical significance of implant deviation and time considering approach, experience, and interaction of both.

	Method	Experience	Method * Experience
Entry/ mm	0.05	0.64	0.38
Apex(3d)/ mm	0.07	0.59	0.31
Apex(v)/ mm	0.47	0.45	0.61
Angle/ °	**<0.001**	0.10	0.57
Time/ sec	**<0.001**	**<0.001**	**0.017**

Numbers in bold indicate to statistically significant values.

The DN time was significantly longer (P< 0.001) compared with FH and PPG approaches (**Table 2**). A significant difference for interaction was observed (P=0.017), which indicated that both experience and method affected the surgical time. Time required by experienced practitioners with the FH and PPG approaches was significantly faster than that of novice practitioners. However, the time required for DN was almost similar independent of the practitioner's experience.

4. Discussion

The present study evaluated the accuracy and performance of novice versus experienced practitioners for performing implant surgery using FH, PPG and DN approaches, which has not been thoroughly investigated in the prior available literature. The recorded parameters included accuracy of implant placement by assessing its deviation compared with the virtual plan, scores of self-confidence and operation time. The findings suggested that the overall navigation approach provided more accurate implant placement and offered equal time-consumption independent of the experience. Novice practitioners reported more confident with the DN approach compared to experienced practitioners. Furthermore, perforations in the lingual cortical region by FH and PPG were observed due to difficult access and the need for indirect visualization at the posterior region of the phantom. This issue did not exist with the DN approach as the practitioners could track the real-time drilling and implant positioning on a screen. A novice practitioner also fractured a SG during drilling. As the short inter-arch distance at the posterior region makes it difficult to appropriately place the drill in the sleeve of the surgical guide if a surgeon is not optimally trained, hence causing the guide to fracture.

Although the PPG offers the advantage of reducing the implant deviation in comparison with the FH method, there is still a risk of inaccurate implant positioning due to the difficulty of inserting the drills through the sleeves of the guide and keeping them in a centric position. The deviation for surgical guide might result from the tolerance between the sleeve and drill in surgical guide and the steps of digital workflow from data acquisition, software processing and template manufacturing [19]. In contrast, implant placements executed under the guidance of the DN system showed better accuracy, which was consistent with previous studies [20, 21]. However, the cumulative error of navigation system might generate from the workflow of image processing, planning calibration, registration and surgical proficiency [16].

The time required for FH and PPG was significantly faster than the DN approach. This was consistent with previous results that DN increased surgical time compared with FH [15, 22]. The difference was due to the involvement of the necessary calibration steps for navigation throughout the surgical procedure. Another reasoning could be related to the competency of the technique related to hand-eye coordination, where the frequent use of navigation and mastering the approach might lower the surgical time. In contrast, the implant position with PPG, is completely dictated by the guide for the pilot drill and therefore the operators can quickly perform the drilling through the guide without strict monitor. Although DN requires a relatively longer surgical time compared to the FH or PPG, the potential time-efficiency in relation to planning or changing the surgical plan and delivery of the treatment on the same visit cannot be denied. In contrast, SG planning and manufacturing requires more time, especially in cases where third party companies are given the responsibility of guide preparation [11]. The surgical timing was significantly lower for experienced practitioners with FH and PPG, which could be due to their higher surgical proficiency. At the same instance, novice practitioners took longer as they required more time to orient and angulate drills. However, the DN approach led to almost similar timing irrespective of the experience.

The novice practitioners showed increased satisfaction with the assistance of guided approaches, which was consistent with previous studies [15, 23]. This implies that novice practitioners tend to adapt to the guided technologies that help decrease the fear of surgical complications by conventional FH protocol. Furthermore, a high self-evaluation scoring was also confirmed by the improved accuracy.

Amongst the guided approaches, PPG received higher self-confidence scoring compared to DN by both novice and experienced practitioners. Due to the guidance by pilot-drill orientation, the later FH drilling offers more self-control to the practitioner, where a surgeon’s personal fine motor control allows determination of the correct implant positioning by manually inspecting each step. For navigation, the practitioners could self-control the motor depend on the guidance displayed by the tracking system. The low confidence reported in the application of navigation could be explained by that it requires a certain level of technical skills, manual dexterity and hand-eye coordination to perform the surgery while looking at the screen and avoiding any visual blockage of the tracking path. In spite of that, the novice practitioners believed that their performance improved with the navigation approach during the short training time compared with FH, which enables visualization of the osteotomy in real-time with minimal stress or risk of complications. On the other hand, experienced operators scored their self-satisfaction with DN even lower than novices because the experienced surgeons prefer the approach with well-documented higher success rate and are less prone to change by challenging an innovative treatment modality into practice [24]. However, it should be kept in mind that the ability of dynamic navigation to permit correction of implant positioning by displaying immediate feedback of the actual versus planned positioning of the drills and implant reduces the risk of harming patients compared to other approaches [14].

The study had certain limitations. Firstly, the study was only limited to implant surgery at the site of lower mandibular 1st molar with small sample size, further studies should expand sample size and include other sites in both maxilla and mandible to assess its accuracy and performance of operators. Secondly, the simulated model lacked soft tissue and the factor of flap elevation was not assessed. Thirdly, the results of this in vitro study need to be interpreted with caution which might not be applied to patients in a real clinical setting. However, the applied approach could still act as an in vitro teaching model for improving novice surgeons' dexterity and their skills before they perform the procedure on real patients. Finally, a PPG protocol was applied in the current study which is a more commonly used approach in a dental practice. However, future studies should also investigate the impact of half-guided and fully-guided approaches to reach a better conclusion.

5. Conclusion

The dynamic navigation assisted implant placement technique significantly improved the angular accuracy of the implant placement compared with both FH and PPG approaches irrespective of the practitioner's experience. The application of DN could be regarded as a more beneficial approach for novices who were more confident of using the navigation system for implant placement and were able to perform the procedure at the same level of accuracy and time as that of experienced practitioners.

References

[1] C. ILHAN, M. DIKMEN, E. YÜZBASIOGLU, Accuracy and efficiency of digital implant planning and guided implant surgery: An update and review, J. Exp. Clin. Med. 38 (2021) 148–156.

[2] M. Hultin, K.G. Svensson, M. Trulsson, Clinical advantages of computer-guided implant placement: A systematic review, Clin. Oral Implants Res. 23 (2012) 124–135.

[3] S. Ivanovski, N. Mattheos, S. Scholz, L. Heitz-Mayfield, University postgraduate training in implant dentistry for the general dental practitioner, Aust. Dent. J. 55 (2010) 339–345.

[4] A.M. Greenberg, Digital Technologies for Dental Implant Treatment Planning and Guided Surgery, Oral Maxillofac. Surg. Clin. North Am. 27 (2015) 319–340.

[5] M. Vercruyssen, T. Fortin, G. Widmann, R. Jacobs, M. Quirynen, Different techniques of static/dynamic guided implant surgery: Modalities and indications, Periodontol. 2000. 66 (2014) 214–227. https://doi.org/10.1111/prd.12056.

[6] F. Younes, A. Eghbali, T. De Bruyckere, R. Cleymaet, J. Cosyn, A randomized controlled trial on the efficiency of free-handed, pilot-drill guided and fully guided implant surgery in partially edentulous patients, Clin. Oral Implants Res. 30 (2019) 131–138.

[7] J. Gargallo-Albiol, S. Barootchi, O. Salomó-Coll, H. lay Wang, Advantages and disadvantages of implant navigation surgery. A systematic review, Ann. Anat. 225 (2019) 1–10.

[8] M.C. Schulz, F. Hofmann, U. Range, G. Lauer, D. Haim, Pilot-drill guided vs. full-guided implant insertion in artificial mandibles—a prospective laboratory study in fifth-year dental students, Int. J. Implant Dent. 5 (2019).

[9] J. Abduo, D. Lau, Duration, deviation and operator's perception of static computer assisted implant placements by inexperienced clinicians, Eur J Dent Educ. 00 (2021) 1–11.

[10] J. Abduo, D. Lau, Accuracy of static computer-assisted implant placement in anterior and posterior sites by clinicians new to implant dentistry: in vitro comparison of fully guided, pilot-guided, and freehand protocols, Int. J. Implant Dent. 6 (2020).

[11] M.S. Block, R.W. Emery, Static or Dynamic Navigation for Implant Placement - Choosing the Method of Guidance, J. Oral Maxillofac. Surg. 74 (2016) 269–277.

[12] G. Gasparini, R. Boniello, A. Laforì, P. De Angelis, V. Del Deo, A. Moro, G. Saponaro, S. Pelo, Navigation system approach in zygomatic implant technique, J. Craniofac. Surg. 28 (2017) 250–251.

[13] M.C. Schulz, L. Rittmann, U. Range, G. Lauer, D. Haim, The use of orientation templates and free-hand implant insertion in artificial mandibles-an experimental laboratory examination in fifth-year dental students, Dent. J. 6 (2018).

[14] Y. Zhan, M. Wang, X. Cheng, Y. Li, X. Shi, F. Liu, Evaluation of a dynamic navigation system for training students in dental implant placement, (2020).

[15] N. Casap, S. Nadel, E. Tarazi, E.I. Weiss, Evaluation of a navigation system for dental implantation as a tool to train novice dental practitioners, J. Oral Maxillofac. Surg. 69 (2011) 2548–2556.

[16] S.M. Wei, Y. Zhu, J.X. Wei, C.N. Zhang, J.Y. Shi, H.C. Lai, Accuracy of dynamic navigation in implant surgery: A systematic review and meta-analysis, Clin. Oral Implants Res. 32 (2021) 383–393.

[17] X. Wang, S. Shujaat, E. Shaheen, R. Jacobs, Quality and haptic feedback of three-dimensionally printed models for simulating dental implant surgery, J. Prosthet. Dent. (2022) 1–8.

[18] R. Geoffrion, T. Lee, J. Singer, Validating a Self-Confidence Scale for Surgical Trainees, J. Obstet. Gynaecol. Canada. 35 (2013) 355–361.

[19] O. Schubert, J. Schweiger, M. Stimmelmayr, E. Nold, J.F. Güth, Digital implant planning and guided implant surgery – workflow and reliability, Br. Dent. J. 226 (2019) 101–108.

[20] C.-K. Chen, D.-Y. Yuh, R.-Y. Huang, E. Fu, C.-F. Tsai, C.-Y. Chiang, Accuracy of Implant Placement with a Navigation System, a Laboratory Guide, and Freehand Drilling, Int. J. Oral Maxillofac. Implants. 33 (2018) 1213–1218.

[21] T.-M. Sun, H.-E. Lee, T.-H. Lan, Comparing Accuracy of Implant Installation with a Navigation System (NS), a Laboratory Guide (LG), NS with LG, and Freehand Drilling, Int J Environ Res Public Health. 17 (2020) 2107.

[22] A. Jorba-García, R. Figueiredo, A. González-Barnadas, O. Camps-Font, E. Valmaseda-Castellón, Accuracy and the role of experience in dynamic computer guided dental implant surgery: An in-vitro study, Med. Oral Patol. Oral y Cir. Bucal. 24 (2019) e76–e83.

[23] S. Prasad, N. Bansal, Predoctoral Dental Students' Perceptions of Dental Implant Training: Effect of Preclinical Simulation and Clinical Experience, J. Dent. Educ. 81 (2017) 395–403.

[24] G. Orentlicher, A. Horowitz, M. Abboud, What's Hindering Dentistry From the Widespread Adoption of CT-Guided Surgery?, Compend. Contin. Educ. Dent. 36 (2015) 2–5.

Part III

ARTIFICIAL INTELLIGENCE

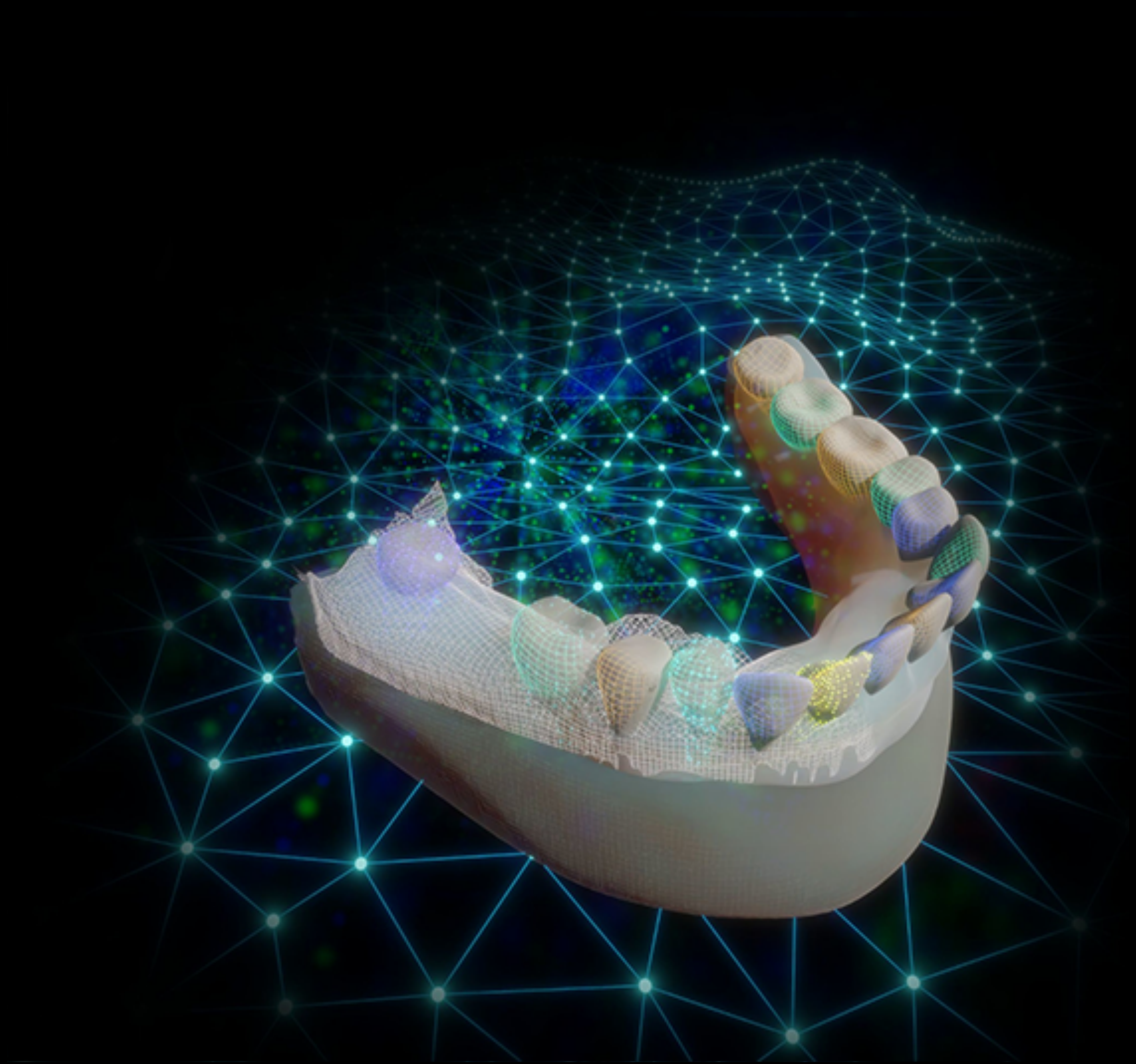

ARTICLE 6

Convolutional neural network for automated tooth segmentation on intraoral scans

Wang X. [1,2]
Alqahtani K. [1,3]
Bogaert T. [1]
Shujaat S. [1,4]
Jacobs R. [1,5]
Shaheen E. [1]

[1] OMFS-IMPATH Research Group, Department of Imaging & Pathology, Faculty of Medicine, KU Leuven & Oral and Maxillofacial Surgery, University Hospitals Leuven, Leuven, Belgium.

[2] Department of Oral and Maxillofacial Surgery, The First Affiliated Hospital of Harbin Medical University, Harbin, China.

[3] Department of Oral and Maxillofacial Surgery and Diagnostic Sciences, College of Dentistry, Sattam Bin Abdulaziz University, Al-Kharj, Saudi Arabia

[4] King Abdullah International Medical Research Centre, Department of Maxillofacial Surgery and Diagnostic Sciences, College of Dentistry, King Saud bin Abdulaziz University for Health Sciences, Ministry of National Guard Health Affairs, Riyadh, Kingdom of Saudi Arabia.

[5] Department of Dental Medicine, Karolinska Institutet, Huddinge, Sweden.

Accepted in Clinical Oral Investigations

Abstract

Objectives: To propose and evaluate the performance of a deep learning-based convolutional neural network (CNN) model for automatic tooth segmentation on intraoral scanned (IOS) images.

Material and methods: A dataset of 761 IOS images (380 upper jaws, 381 lower jaws) was acquired by intraoral scanner. Inclusion criteria consisted of a full set of permanent teeth, teeth with orthodontic brackets and partially edentulous dentition. A multi-step 3D U-Net pipeline was designed for automated tooth segmentation on IOS images. The model performance was assessed in terms of time and accuracy. Furthermore, the model was deployed on an online cloud-based platform, where a separate subsample of 18 IOS images was used to test the clinical applicability of the model by comparing three modes of segmentation i.e., automated artificial intelligence-driven (A-AI), refined (R-AI) and semi-automatic (SA) segmentation.

Results: The average time required for automated segmentation was 31.7±8.1 s per jaw. The CNN model showed an intersection over union (IoU) score of 91%, where a full set of teeth achieved the highest performance metrics and partially edentulous group scored the lowest. In terms of clinical applicability, SA took on average 860.4 s per case compared to R-AI which showed a 2.6-fold decrease in time (328.5 s). Furthermore, R-AI offered higher performance and reliability compared to SA irrespective of the dentition group.

Conclusions: 3D U-Net pipeline was found to be accurate, efficient and consistent for automatic tooth segmentation on IOS images.

Clinical relevance: The online cloud-based platform could act as a viable alternative for IOS segmentation.

Keywords: Artificial intelligence; Machine learning; Neural networks, computer; Optical imaging; Dentition; Dentistry

1. Introduction

The conventional dental impression techniques have been widely replaced by digital intraoral scanning, which is more precise, non-invasive, harmless and offers more comfortability to the patient [1]. In addition, integration of intraoral scanned (IOS) data into the digital workflows of prosthodontics, orthodontics, implant dentistry, and orthognathic surgery has improved the efficiency of treatment planning and simplified clinical procedures by eliminating labor-intensive and time-consuming steps associated with conventional physical impressions [2].

A crucial step in digital dental workflows is the three-dimensional (3D) segmentation or delineation of teeth from the IOS dataset. The acquisition of an accurate and efficient tooth segmentation is a prerequisite for clinical applications requiring tooth realignment for treatment simulation or follow-up evaluation, such as in orthodontics or implantology [3-5]. This could in turn aid in achieving a predictable and stable treatment outcome [6].

Currently semi-automatically assisted segmentation algorithms integrated in imaging software programs remain the method of choice for segmenting teeth on IOS images. These algorithms are generally designed by extracting geometric feature regions such as surface contour lines, surface curvature and harmonic field from the IOS data [7-9]. Even though semi-automatic segmentation tools have been widely employed in digital dental workflows, these are prone to certain limitations, such as lack of robustness, requirement of manual correction, labor intensiveness, expertise-dependence, and excessive time consumption. To overcome these limitations, a considerable amount of effort has been put into developing automatic segmentation tools. However, it still remains a challenging task owing to the substantial variability of the IOS data amongst different patients due to the presence of large-scale morphological and geometric variations of different teeth, missing or disarranged teeth and abnormal dental conditions, such as supernumerary teeth. Additionally, the presence of teeth rotation and crowding also makes it difficult for the segmentation algorithms to delineate the margins of each individual tooth separately. This difficulty is exacerbated in orthodontic patients with dental braces or in cases with indistinguishable gingival boundaries [5].

Recently, artificial intelligence (AI) has sporadically evolved and gained traction in the field of medicine mainly due to its potential to automate tasks in a manner that mimics human intelligence [10]. Deep-learning based convolutional neural networks (CNNs), a subcategory of AI, has been considered as the most suitable method for medical image analysis [11, 12]. Several studies have been conducted where CNNs have been successfully employed with satisfactory performance to segment teeth from IOS datasets [13]. However, the main limitation associated with these studies have been either relying on a small sample size or failure to investigate the robustness of the networks to handle deviations from a natural dentition and variability in dental status such as missing teeth, crowding or orthodontic brackets [4, 5, 14-17].

Therefore, the aim of the current study was to propose and validate the performance of CNN model to automatically segment teeth on IOS images with a full set of natural teeth, orthodontic brackets and partially edentulous dentition.

2. Materials and Methods

The World Medical Association's Declaration of Helsinki on medical research was followed in conducting this study. Ethics approval was acquired from the University Hospitals Leuven's Ethics Committee Research (reference number: S65188), which provided informed consent for the work. This study followed the Artificial intelligence in dental research checklist (Appendix Table 1) [18].

2.1 Dataset

The dataset consisted of 761 IOS images (380 upper jaws, 381 lower jaw) acquired by Trios 3Shape intraoral scanner (Copenhagen, Denmark) between June 2020 and April 2021, from LORTHOG Register, Department of Oral & Maxillofacial Surgery, University Hospitals Leuven. All data were retrospectively collected and anonymized. Inclusion criteria were complete scans of jaws consisting of a full set of permanent teeth, orthodontic patients with braces and prosthodontic patients with partially edentulous dentition. Presence of any local pathological condition was excluded. Afterwards, the total dataset was randomly divided into three subsets for training (n=609), validation (n=76) and testing (n=76).

The ground truth datasets were labeled by human experts. IOS data were prepared by semi-automatic segmentation (SA) in OrthoAnalyzer software (3Shape A/S, Copenhagen, Denmark) and exported in standard tessellation language (STL) format. The segmentation task was randomly performed by three individual dental practitioners following initial training and calibration. The IOS image was firstly preprocessed by preparing a model set then assigned to the segmentation field. Thereafter, missing teeth were deselected, followed by manual indication of distal and mesial points for creating a cut spline which outlined the tooth contour. A sculpt was created and toolkit for addition or removal was used for minor correction of segmentations with over- or under-estimation. Extra correction was applied for cases with brackets by removing the connecting wire and isolating the teeth. Finally, the segmented teeth were correctly labeled according to the FDI notation using 3-matic 14.0 software (Materialise, Leuven, Belgium). All segmentations and labeling were checked by a second observer for quality control and alterations were carried out if necessary.

2.2 AI model architecture

A multi-step 3D U-Net pipeline was designed for automated tooth segmentation on IOS images [19]. The proposed multi-step approach using U-Net models aims to refine the tooth segmentation at each step by improving the data quality, and increasing the size of the training dataset via data augmentation (**Fig. 1**). This approach leads to a more accurate and robust segmentation result. Here is a more detailed explanation of each stage:

1. Preprocessing the raw STL data:

a. Region of interest (ROI) extraction: ROI was extracted from the raw STL data, which corresponds to the tooth structure. This is typically done by manually selecting the tooth region or automatically segmenting it using thresholding or other segmentation techniques.

b. Smoothing: To improve the quality of the ROI, the data is smoothed using various techniques such as smoothing filters, morphological operations, or level set methods. The purpose of smoothing is to reduce noise and artifacts in the data, which can improve the performance of the segmentation model.

2. Data augmentation: To increase the size and variability of the training dataset, data augmentation techniques are applied to the preprocessed ROI data. This includes operations such as scaling, rotation, flipping, and deformations, which create new training samples from the original data. Data augmentation can improve the generalization performance of the model by making it more robust to variations and artifacts in the input data. The Adam optimizer, an adaptive learning rate optimization algorithm, was employed for training the U-Net networks.

To apply U-Net to mesh data, we used several procedures to pre-process the data for creating a suitable input for the neural network. Here are the steps followed:

1. STL mesh file was converted into a volumetric representation via voxelization.

2. Volumetric representation was divided into smaller sub volumes, called patches. Each patch was used as input to the network.

3. For each patch, features were extracted using convolutional layers. In U-Net, the encoder part consists of a series of convolutional layers with pooling operations to extract high-level features from the input.

4. A symmetric decoder architecture was used to reconstruct the output segmentation. The decoder part of the U-Net consists of a series of up convolutional layers with skip connections from the encoder part to reconstruct the segmentation.

5. Binary cross-entropy was used as loss function to train the U-Net on labeled mesh data. The labels for each patch were obtained by applying a labeling process to the mesh.

Once trained, the U-Net can be used to predict the segmentation for new patches of mesh data.

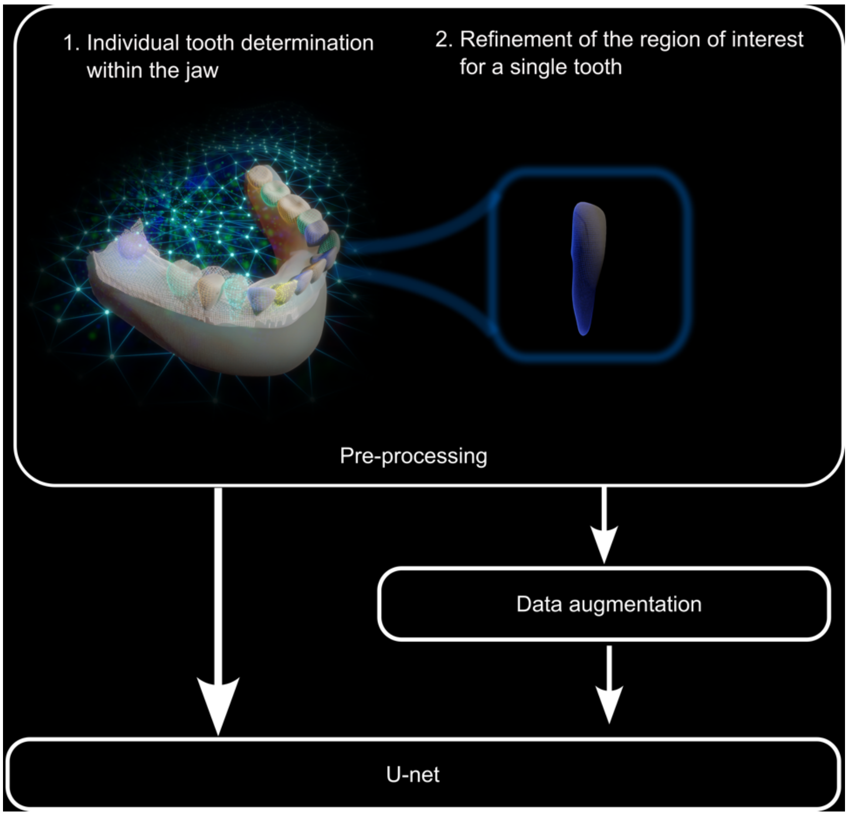

Figure 1. The multi-step approach using U-Net models

2.3 Validation metrics

The following metrics were used to evaluate the performance of CNN model:

- Intersection over union (IoU):

$$IoU = \frac{TP}{(TP + FP + FN)}$$

- Timing: The runtime of the AI was recorded in seconds for each segmentation.
- Dice similarity coefficient (DSC):

$$DSC = \frac{2 \times TP}{(TP + FP) + (TP + FN)}$$

TP = true positives; TN = true negatives; FP = false positives; FN = false negatives.

When applied to mesh data, IOU and DSC were used to compare the overlap between two sets of triangles or polygons. To calculate these metrics, the labeled area of interest was compared to the ground truth or reference data. The mesh data had been represented as a collection of vertices and faces. To apply IOU or DSC, the labeled regions on the mesh were converted into a binary mask, where each vertex was either labeled as "inside" or "outside" the labeled region. Specifically, in this case, this was done by projecting the 3D model onto a 2D plane and creating a binary image mask using traditional image segmentation methods. In the case of a crown surface dataset, typically only the visible or labeled side of the crown was analyzed and evaluated. The un-labeled side was ignored during the calculation of IOU and DSC since it was not part of the labeled area of interest. When calculating the metrics, only the labeled regions were taken into account. The unlabeled regions were ignored, and their contribution to the final metric score was treated as if they were correctly segmented. It is important to note that the accuracy of the evaluation metrics can be affected by the quality of the labeling and segmentation process, as well as the specific characteristics of the mesh data being analyzed.

2.4 Clinical applicability of the CNN model

The CNN model was transferred to an online cloud-based platform (Virtual Patient Creator, Relu Inc, Leuven, Belgium), allowing users to upload STL files of IOS data and generate automated AI-driven segmentation (A-AI). The platform also provides users with tools for correction and generating a refined AI-driven segmentation (R-AI). Hence, a test was also conducted to evaluate the clinical applicability of the tool with an additional subsample of 18 IOS images, which included IOS images of cases with a full set of permanent teeth (n=6), teeth with orthodontic brackets (n=6) and partially edentulous dentition (n=6). Timing, accuracy and consistency of the A-AI and R-AI segmentations were compared to the SA method. The time required by SA was calculated starting from STL data import into OrthoAnalyzer till the generation of a segmented model. The time for A-AI was calculated automatically by the algorithm, and the time for R-AI was computed by adding the time needed for A-AI and refinements. Two independent observers performed SA and R-AI based segmentations to assess the inter-observer reliability. For intra-observer variability, one observer repeated the same segmentations at an interval of two weeks. Furthermore, accuracy of A-AI and R-AI was evaluated by comparison with SA-based segmentation.

2.5 Statistical analyses

IBM SPSS Statistics for Windows, version 21.0 (IBM Corp., Armonk, NY, USA) was used to evaluate the data. Descriptive statistics were calculated for each evaluation metric. Normality was assessed by means of normal quantile plots and log-transformation was applied for normal distributed data. Intra-class correlation coefficient (ICC) was applied for calculating the inter and intra-observer reliability. Test-retest reliability was also calculated. Timing was compared between different methods using a two-way repeated measure ANOVA [20]. A p-value of <0.05 was considered statistically significant.

3. Results

3.1 AI model performance

Within the 76 scans used for validation, 3 groups of cases were identified: full set of teeth (n= 41), teeth with brackets (n=13) and partially edentulous dentition (n= 22). **Table 1** provides an overall segmentation performance of the CNN model compared to the ground-truth and results obtained for each individual group. The time required by CNN model for segmentation was 31.7±8.1 seconds per jaw irrespective of the dentition group. An IoU of 91.0±5.5% and DSC of 94.6±4.8% was observed which indicated towards an optimal overlap compared to the ground truth. Based on each individual dentition group, the full set of teeth achieved the highest performance metrics, whereas the partially edentulous group scored the lowest.

Table 1. AI model segmentation performance (Mean±SD) compared to ground-truth.

Dentition group	IoU (%)	DSC (%)	Timing* (s)
Full teeth	92.2±3.8	95.5±3.2	33.0±7.4
Partially edentulous	89.3±8.0	93.0±7.5	31.2±10.6
Brackets	90.0±3.4	94.6±2.0	28.8±2.5
Average	91.0±5.5	94.6±4.8	31.7±8.1

Note: * Timing for AI segmentation per upper jaw or lower jaw. DSC, Dice coefficient score; IoU, Intersection over union; SD, standard deviation

Fig. 2 illustrates a few examples of automated segmentations of different types of dentition. The CNN model effectively generated dentition with lingual fixed retainers, brackets and partially erupted, crowded or missing teeth. Although crowded teeth exhibited optimal segmentation, further improvements need to be applied to the CNN model for distinguishing boundaries in cases with extreme crowding.

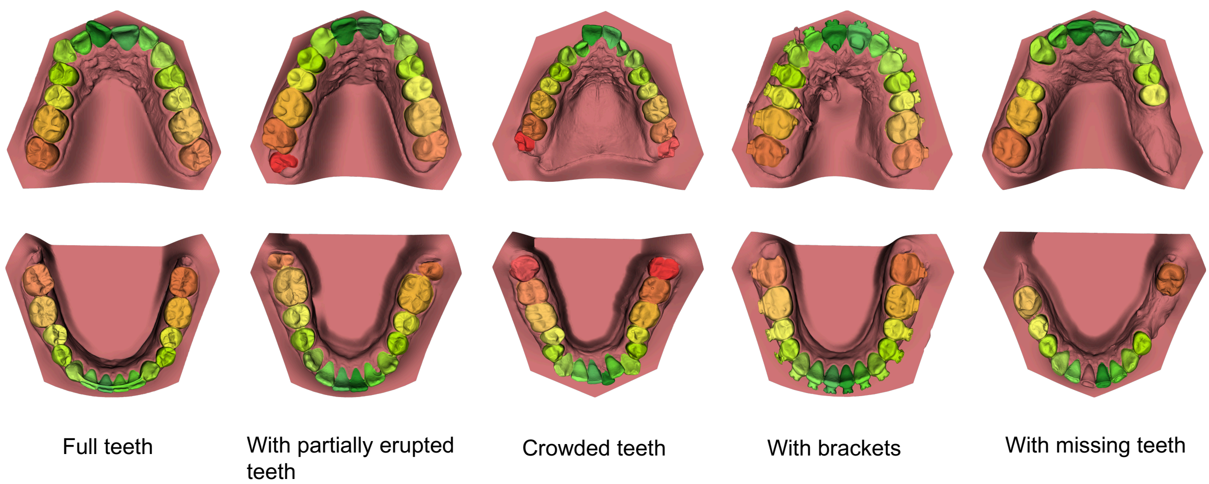

Figure 2. Example of AI segmentation results of upper and lower jaws for the different dentition groups

3.2 Clinical applicability

The average timing based on each segmentation approach is presented in **Table 2**. Time required by the A-AI method was 66.7 s for one case (both upper and lower jaw), whereas the SA approach took on average 860.4 s (14.3 min). R-AI segmentation took 328.5 s, with a 2.6-fold decrease compared to the SA approach. The two-way repeated measures ANOVA demonstrated a significant interaction between the applied method and operator (*p=0.02*). A significant difference was observed in timing between methods (SA vs R-AI) for both operators (*p<.001*). The timing of R-AI showed a significant difference between observers (*p=0.04*), whereas no significant difference existed with the SA approach (*p=0.13*).

Table 2. Timing of segmentation methods.

Method	Mean (s)	SD (s)	Min (s)	Max (s)
SA	860.4	211.4	551.0	1348.0
A-AI	66.7	8.5	55.3	79.5
R-AI	328.3	181.1	101.6	739.5

Abbreviations: A-AI, automated artificial intelligence-driven segmentation; R-AI, refined artificial intelligence-driven segmentation; SA,semi-automatic method; Max, maximal value; Min, minimal value; SD, standard deviation; s, seconds

The test-retest reliability pointed to a high correlation (r=0.873) [21]. Both intra- and inter-operator reliability of SA and R-AI were excellent, suggesting a high consistency of the training dataset. As shown in **Table 3**, R-AI had a higher observer reliability compared to SA irrespective of the dentition group, which further verified the effectiveness of the tool in performing reproducible and superior segmentation compared to a conventional SA approach.

Table 3. Inter and intra-observer assessment based on ICC values in terms of IoU (%) for SA and R-AI methods

Intra-operator consistency		
	SA	**R-AI**
Full teeth	93.7	98.2
Partially edentulous	95.4	95.5
Brackets	90.9	98.9
Inter-operator consistency		
	SA	**R-AI**
Full teeth	92.9	98.3
Partially edentulous	94.2	97.1

Brackets	91.9	98.2

Abbreviations: A-AI, automated artificial intelligence-driven segmentation; R-AI, refined artificial intelligence-driven segmentation; SA,semi-automatic method; ICC, Intra-class correlation coefficient; IoU, Intersection over union

An overview of the accuracy assessment of A-AI and R-AI compared to SA for all subgroups is displayed in **Table 4**. Both A-AI and R-AI had a high IoU of 90.5% and 92.5% respectively. The study demonstrated that R-AI had better performance than A-AI in terms of the 95th percentile of the Hausdorff Distance (HD), which represents the maximum distance between the predicted model and ground truth. The results showed that the brackets group had the highest 95% HD, followed by the full teeth group and partially edentulous group, respectively. A visual illustration of AI segmentation with and without manual refinement is presented in **Fig. 3**. The online platform allowed users to define the boundaries under lingual fixed retainers and between interdental areas which the AI failed to capture.

Table 4. Accuracy assessment of A-AI and R-AI vs SA methods (Mean±SD)

Metric	Dentition	A-AI vs SA	R-AI vs SA
IoU (%)	Full teeth	91.3±1.0	94.4±0.8
	Partially edentulous	91.3±3.5	91.8±6.2
	Brackets	88.7±5.4	91.1±6.4
	Average	90.5±4.0	92.5±5.4
DSC (%)	Full teeth	95.4±0.5	97.1±0.4
	Partially edentulous	95.4±2.0	95.6±3.6
	Brackets	93.9±3.1	95.2±3.6
	Average	94.9±2.2	96.0±3.1
95% HD (mm)	Full teeth	0.0030±0.0032	0.0029±0.0033
	Partially edentulous	0.0001±0.0001	0.00006±0.0001
	Brackets	0.7619±1.1795	0.7609±1.1778
	Average	0.2549±0.7384	0.2546±0.7373

Abbreviations: A-AI, automated artificial intelligence-driven segmentation; R-AI, refined artificial intelligence-driven segmentation; SA, semi-automatic method; DSC, Dice coefficient score; IoU, Intersection over union; SD, standard deviation; 95% HD, 95th percentile of the Hausdorff Distance.

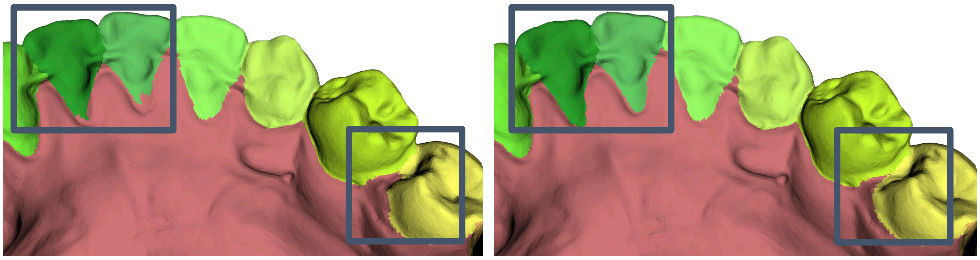

(a) A-AI (b) R-AI

Figure 3. Visual comparison of tooth segmentation with (a) A-AI (automated AI-driven segmentation) and (b) R-AI (refined AI-driven segmentation). R-AI allowed refinement for the accurate tooth segmentation boundary as highlighted in the boxes

4. Discussion

In digital dentistry, detection of teeth on IOS images aids in treatment planning and follow-up evaluation. In light of the recent technological advancements, the current study developed a robust fully automated CNN model and provided an easy-to-use interactive tool for IOS tooth segmentation using the Virtual Patient Creator platform. This model provided a time-efficient segmentation while ensuring accuracy and consistency. In addition, the performance of the CNN model was verified for clinical applications by deploying it into an online cloud-based platform where manual corrections could be performed, which further facilitates its integration into a clinical practice.

Previous studies did not explore the robustness of their proposed automated IOS segmentation algorithms for segmenting teeth with brackets or partially edentulous dentition [5, 14-17]. Therefore, the current study included a variety of normal (full set of teeth) and abnormal cases (partially edentulous group and bracket group) to assess the generalizability of the AI model across a dataset with heterogeneous geometry. The AI model not only showed a high performance for segmenting normal dentition but also its accuracy was confirmed in complex cases such as crowded or misaligned teeth which are normally difficult to detect considering the overlapped regions with adjacent teeth [17]. Unlike a previous study, the presented model was able to accurately segment teeth with brackets and partially edentulous jaws [16]. Furthermore, it also outperformed other competing methods for recognizing the boundary between noisy gingiva and partially erupted teeth [22].

Up till now, different deep learning models have been proposed for tooth segmentation on IOS images with variable performances and these have been primarily applied for the segmentation of a full set of normal teeth. Zanjani et al. proposed a Mask-MCNet framework and showed an IoU value of 98% which might have resulted due to a small dataset of 120 IOS images and the variability amongst cases was not specified [14]. Lian et al. evaluated MeshSegNet and demonstrated a DSC value of 95.2% with a dataset of 30 upper-jaw cases, however, failed to properly handle missing teeth and brackets [16]. The TS-MDL model proposed by Wu et al. reached a DSC value of 95.3% based on a relatively small sample of 36 upper IOS images, with reduction of performance in malocclusion cases [17]. Zhang et al. proposed TSGCNet which had a low IoU of 89% for segmenting incisors [23]. In comparison to the aforementioned studies, our model showed a high performance with a DSC score of more than or equal to that of other proposed models [5, 14-17, 23]. Only one study reported a superior performance of a CNN model (TSegNet) compared to our findings for segmenting both normal and abnormal cases with a DSC of 98%. However, the authors failed to specify a separate DSC scoring for both types of cases and did not identify the number of abnormal cases. Furthermore, their model also yielded incomplete segmentation of wisdom and rudimentary teeth [22]. In contrast, the 3D U-Net pipeline presented in this study showed an average DSC of 94.6% amongst different groups of cases, which confirms its ability to handle both regular and complicated dental morphologies. More importantly, the integration of the CNN model into an online cloud-based platform allows user refinements (R-AI method) with interactive tools, which is important for segmentation of complex malformations of teeth, thus further confirming its suitability for clinical applications.

Although the presented model showed high performance for automated tooth segmentation, there is still room for improvement in cases with low scanning quality and extremely crowded teeth. The differences in 95% HD results between the dentation groups may be attributed to the complexity and characteristics of the dental cases in each group. For instance, the Brackets group may have had more complicated dental cases, such as those with severe malocclusion and indistinct boundaries between braces and swollen gingiva. In contrast, the full teeth group may have had simpler cases, including those with minor alignment issues or no malocclusion, resulting in fewer deviations from the ground truth. The partially edentulous group may have had the simplest cases, with only a few missing teeth, resulting in the lowest deviations from the ground truth. As the improvement in model performance followed by R-AI was minimal, this implies that fewer corrections are required. The R-AI substantially eliminates labor-intensive steps with a 2.6-fold decrease in time consumption and higher consistency compared to SA method. The Virtual Patient Creator platform could serve as useful tool for planning and follow-up assessment in a clinical practice with the integration of an IOS image segmentation model. The platform has also integrated automated segmentation of other computed tomography-derived anatomical structures, such as teeth, maxillary complex, mandible, mandibular canals and pharynx [20, 24, 25], which could further optimize the digital workflows. As this study describes training of the model based on data derived from a single intraoral scanner, further strengthening of the algorithm is planned in the near future by introducing scans from different devices.

5. Conclusion

The proposed 3D U-Net pipeline outperformed state-of-the-art methods for automated tooth segmentation on IOS images with accurate, efficient and consistent results. Its clinically applicability is strengthened by the use of an online cloud-based platform for automated segmentation and interactive refinement.

References

[1] O. Erten, B.N. Yılmaz, Three-dimensional imaging in orthodontics, Turkish J. Orthod. 31 (2018) 86–94.

[2] F. Mangano, A. Gandolfi, G. Luongo, S. Logozzo, Intraoral scanners in dentistry: A review of the current literature, BMC Oral Health. 17 (2017) 1–11.

[3] T. Kondo, S.H. Ong, K.W.C. Foong, Tooth segmentation of dental study models using range images, IEEE Trans Med Imaging, 23 (2004) 350–362.

[4] S. Tian, N. Dai, B. Zhang, F. Yuan, Q. Yu, X. Cheng, Automatic classification and segmentation of teeth on 3D dental model using hierarchical deep learning networks, IEEE Access. 7 (2019) 84817–84828.

[5] J. Hao, W. Liao, Y.L. Zhang, J. Peng, Z. Zhao, Z. Chen, B.W. Zhou, Y. Feng, B. Fang, Z.Z. Liu, Z.H. Zhao, Toward Clinically Applicable 3-Dimensional Tooth Segmentation via Deep Learning, J. Dent. Res. (2021) 002203452110404.

[6] F. Baan, O. de Waard, R. Bruggink, T. Xi, E.M. Ongkosuwito, T.J.J. Maal, Virtual setup in orthodontics: planning and evaluation, Clin. Oral Investig. 24 (2020) 2385–2393.

[7] Y. Kumar, R. Janardan, B. Larson, J. Moon, Improved segmentation of teeth in dental models, Comput. Aided. Des. Appl. 8 (2011) 211–224.

[8] B. ji Zou, S. jian Liu, S. hui Liao, X. Ding, Y. Liang, Interactive tooth partition of dental mesh base on tooth-target harmonic field, Comput. Biol. Med. 56 (2015) 132–144.

[9] Z. Li, H. Wang, Interactive Tooth separation from dental model using segmentation field, PLoS One. 11 (2016) 1–16.

[10] D. Tandon, J. Rajawat, Present and future of artificial intelligence in dentistry, J. Oral Biol. Craniofacial Res. 10 (2020) 391–396.

[11] G. Litjens, T. Kooi, B.E. Bejnordi, A.A.A. Setio, F. Ciompi, M. Ghafoorian, J.A.W.M. van der Laak, B. van Ginneken, C.I. Sánchez, A survey on deep learning in medical image analysis, Med. Image Anal. 42 (2017) 60–88.

[12] S.B. Khanagar, A. Al-ehaideb, P.C. Maganur, S. Vishwanathaiah, S. Patil, H.A. Baeshen, S.C. Sarode, S. Bhandi, Developments, application, and performance of artificial intelligence in dentistry – A systematic review, J. Dent. Sci. 16 (2021) 508–522.

[13] K. Hung, A.W.K. Yeung, R. Tanaka, M.M. Bornstein, Current applications, opportunities, and limitations of AI for 3D imaging in dental research and practice, Int. J. Environ. Res. Public Health. 17 (2020) 1–18.

[14] F.G. Zanjani, A. Pourtaherian, S. Zinger, D.A. Moin, F. Claessen, T. Cherici, S. Parinussa, P.H.N.

de With, Mask-MCNet: Tooth instance segmentation in 3D point clouds of intra-oral scans, Neurocomputing. 453 (2021) 286–298.

[15] X. He, Unsupervised Pre-training Improves Tooth Segmentation in 3-Dimensional Intraoral Mesh Scans, 1 (2022) 1–15.

[16] C. Lian, L. Wang, T.H. Wu, F. Wang, P.T. Yap, C.C. Ko, D. Shen, Deep Multi-Scale Mesh Feature Learning for Automated Labeling of Raw Dental Surfaces from 3D Intraoral Scanners, IEEE Trans. Med. Imaging. 39 (2020) 2440–2450.

[17] T.-H. Wu, C. Lian, S. Lee, M. Pastewait, C. Piers, J. Liu, F. Wang, L. Wang, C. Jackson, W.-L. Chao, D. Shen, C.-C. Ko, Two-Stage Mesh Deep Learning for Automated Tooth Segmentation and Landmark Localization on 3D Intraoral Scans, IEEE Trans Med Imaging (2022) 1–8.

[18] F. Schwendicke, T. Singh, J.H. Lee, R. Gaudin, A. Chaurasia, T. Wiegand, S. Uribe, J. Krois, Artificial intelligence in dental research: Checklist for authors, reviewers, readers, J. Dent. 107 (2021).

[19] O. Ronneberger, P. Fischer, T. Brox, U-net: Convolutional networks for biomedical image segmentation. . In: Navab N, Hornegger J, Wells WM, Frangi AF (ed) Medical image computing and computer- assisted intervention – MICCAI 2015, 1st edn. Springer International Publishing, Cham, (2015) 234–241.

[20] P.J. Verhelst, A. Smolders, T. Beznik, J. Meewis, A. Vandemeulebroucke, E. Shaheen, A. Van Gerven, H. Willems, C. Politis, R. Jacobs, Layered deep learning for automatic mandibular segmentation in cone-beam computed tomography, J. Dent. 114 (2021) 103786.

[21] G.J. Matheson, We need to talk about reliability: Making better use of test-retest studies for study design and interpretation, PeerJ. 7 (2019) e6918.

[22] Z. Cui, C. Li, N. Chen, G. Wei, R. Chen, Y. Zhou, W. Wang, TSegNet: An efficient and accurate tooth segmentation network on 3D dental model, Med. Image Anal. 69 (2021) 101949.

[23] L. Zhang, Y. Zhao, D. Meng, Z. Cui, C. Gao, X. Gao, C. Lian, D. Shen, TSGCNet: Discriminative Geometric Feature Learning with Two-Stream GraphConvolutional Network for 3D Dental Model Segmentation, (2022).

[24] E. Shaheen, A. Leite, K.A. Alqahtani, A. Smolders, A. Van Gerven, H. Willems, R. Jacobs, A novel deep learning system for multi-class tooth segmentation and classification on cone beam computed tomography. A validation study: Deep learning for teeth segmentation and classification, J. Dent. 115 (2021).

[25] S. Shujaat, O. Jazil, H. Willems, A. Van Gerven, E. Shaheen, Automatic segmentation of the pharyngeal airway space with convolutional neural network, J. Dent. 111 (2021) 103705.

General Discussion, conclusions & future perspectives

Discussion

Digital technology is an important development direction in dentistry and an inevitable trend. The use of digital technologies in the practice of dentistry can improve the accuracy and efficiency of dental procedures, and lead to better outcomes for patients. It allows for more precise and efficient treatment, better communication and collaboration between dentists, improved patient education and can be cost effective. Digital dentistry can include 3D printing, computer-assisted surgery, and artificial intelligence [1]. The main objectives of this doctoral thesis were to provide clear view on how these digital technologies simplify the workflow in dental practice. It's important to weigh the potential benefits and drawbacks of digital dentistry before implementing it in a practice, and to consider the specific needs and resources of the practice and its patients.

3D printing has the potential to revolutionize the field of dentistry. However, the high price of 3D printing technology has hindered its widespread use. Therefore, in **article 1**, we systematically analyzed the accuracy of maxillofacial skeletal model generated from desktop and professional 3D printers. Based on the meta-analysis results, desktop printed models offered comparable mean absolute error (MAE) (0.12 mm) to professional printed models (0.10 mm). Regardless of printer type between desktop and professional printer, it was discovered that the printing technology and layer resolution might have an impact on the accuracy of the model. Considering the printing technology, MJ (0.09 mm) and SLS (0.09 mm) offered the lowest MAE, followed by BJ (0.11 mm), SLA (0.11 mm) and DLP (0.13 mm), and the highest deviation was observed with the fused deposition modeling (0.22 mm). Different printing technologies have varying printing protocols and different levels of precision. Models printed with a layer resolution of 0.15 mm or less were found to be more accurate than those printed with a resolution of ≥0.2 mm. The accuracy of 3D printed maxillofacial models is a complex issue that depends on various factors, including data acquisition, computer data processing, model fabrication, and post-processing. It has been suggested that a dimensional deviation of up to 2% discrepancy has been identified as the clinically acceptable accuracy for 3D printed skeletal models [2]. The application of a model, however, should determine how accurate it is. For instance, the contouring of the osteosynthesis or reconstruction plates and the creation of surgical guides require a higher level of accuracy than models used for educational purposes [3, 4]. On the basis of these findings, we hypothesized that the accuracy of skull models fabricated by 3D printers at low-, medium-, and high-cost would be similar. **In article 2**, we were the first to assess the efficacy and accuracy of CBCT-derived skull models fabricated by 3D printers at different cost levels using the 3D evaluation analysis. As in previous research on the accuracy of 3D-printed skulls, only 2D evaluations using linear measurements, which are prone to human error, are taken into account [5]. At the same instance, literature evaluating the accuracy of low-cost printed models using 3D evaluation approaches only included the mandible but left out the maxillofacial complex. Therefore, both maxillofacial complex and mandible were assessed in this study. Our findings revealed that while low-cost FFF printers had the highest discrepancy in terms of overall mean absolute error ($1.33 \pm 0.24\,\mathrm{mm}$), medium-cost SLA and high-cost MJ-based printers were able to replicate the skeletal anatomy with optimal accuracy ($0.07 \pm 0.03\,\mathrm{mm}$ and $0.07 \pm 0.01\,\mathrm{mm}$, respectively). Additionally, the longer printing time of desktop printers, up to 5 times longer than the medium- and high-cost printer, can further influence its efficiency in a 3D workflow, thereby, confirming its inapplicability for clinical applications. However, it still provides a practical and cost-effective solution for simulating procedures and anatomical education.

This suggests that the medium-cost SLA and high-cost MJ printers may be more suitable for clinical applications, while desktop FFF 3D printers may not be suitable for clinical use due to their lower accuracy and longer printing time, they can still serve as a cost-effective solution for simulating procedures and anatomical education. It is important to note that the study was limited to a small sample of three printers with different technologies and materials, and therefore cannot be generalized to all printers. The accuracy of 3D printed maxillofacial models is a complex issue that depends on various factors including data acquisition, computer data processing, model fabrication, and post-processing. Further investigation should be done to objectively assess the amount of error contributed at each stage of the printing process and determine how to optimize printing of skeletal models in a healthcare setting by standardizing printer settings. Choosing the right kind of desktop 3D printer for medical use is particularly essential because technology for high-quality desktop printers is constantly evolving, which may soon lead to an increase in accuracy.

The advancement of 3D printing technology has greatly improved the accuracy and realism of patient-specific skeletal models; however, it is uncertain if these models provide optimal haptic feedback for dental implant hands-on training. Therefore, an investigation into the haptic feedback of different 3D-printed models in **article 3** is crucial to determine their effectiveness in preparing dental professionals for real-world procedures. This study was the first to print trabecular mandibular bone from patient's CBCT, and 6 different printers and materials were used for model fabrication. Based on the surgeon's subjective evaluation, model MJ (acrylic-based resin) offered the highest score, followed by model SLA (acrylic-based resin), model FFF1 (polycarbonate filament), model DLP (acrylic-based resin), model FFF2 (polylactic acid filament), whereas model SLS (polyamide filament) scored the lowest. The results have shown that the haptic feedback of the printed model is highly dependent on the mechanical properties of the material, 3D printer, and printer settings, highlighting the importance of understanding the relationship between the 3D-printed models and the haptic feedback. The mechanical properties of the 3D printed material, such as tensile strength and elastic modulus, must be in accordance with the biomechanical characteristics of the tissue in order to accurately replicate the haptic feedback and mechanical characteristics of cortical bone and trabecular bone [6, 7]. Bioprinting materials, such as hydrogels and bioinks, have shown to be promising in replicating the mechanical and structural characteristics of the targeted tissue. This research may assist in identifying materials that can be used to create products for anatomical teaching or surgical simulation [8]. However, considering the haptic feedback of 3D printed models for training, the selection of materials corresponding to the tissue properties during 3D printing is required. The MJ-based model made with acrylic-based resin provided the best haptic feedback, which might be used as a standard for simulating dental implant surgery even though none of the models in this study were able to perfectly recreate the haptic perception of real bone.

In **article 4** and **article 5,** we utilized the protocol outlined in article 3 to design training models for training novice surgeons using computer-assisted surgery. It is believed that computer-assisted technologies, such as navigation and surgical guides, can help to improve the accuracy of procedures for surgeons of varying experience levels [9, 10]. Following this, our study was the first to evaluate whether navigation systems and static surgical guides can reduce the learning curve for novice surgeons, allowing them to perform implant surgery with comparable accuracy and confidence to experienced surgeons. There are various types of navigation systems utilized in dental implant surgery. Specifically, article 4 and article 5 examine the use of two different systems, the X-Guide (X-Nav technologies, LLC, Lansdale, PA) and Navident (ClaroNav, Toronto, Ontario, Canada). Different navigation systems use different hardware and software, which can affect their ease of use. While the goal of the study is not to determine a superior navigation system, the selection of the appropriate system should take into consideration factors such as the specific needs of the practice, the level of accuracy required, and the budget available.

We have conducted a pilot study to compare the accuracy of pilot-guided and half-guided surgical guide in dental implant placement. The results indicated that both techniques are effective options for implant placement, but that novice surgeons may require additional training to achieve optimal results and reduced surgical time. As pilot-drill partial guidance is the most commonly used technique in dental practice due to its ease of use [11], it offers more surgeon control compared to half-guided and fully-guided surgical guides which rely heavily on the guide itself and require less monitoring. Therefore, in our following study, we compared pilot-drill surgical guide with dynamic navigation and freehand methods to further investigate whether guided approaches can enhance novice surgeons' surgical performance, where the performance of experienced surgeons serve as a clinical reference.

The results showed that both navigation systems significantly improved angular deviation compared with freehand and pilot-guided surgical guide approaches, regardless of the surgeon’s level of experience. This improvement in accuracy can be attributed to the real-time, visual guidance provided by the navigation systems during the entire procedure. These findings are consistent with previous studies that have shown a significant improvement in implant placement accuracy with the use of navigation systems compared to surgical guides and freehand techniques [12, 13]. However, it was also observed that the surgical time using navigation systems was significantly longer than freehand or surgical guide methods. This additional time can be attributed to the need for calibration of the navigation systems, which can prolong the surgical time. Despite the longer surgical time, the benefits of navigation systems, such as increased precision and accuracy, reduction of errors, and the ability to make real-time adjustments, can outweigh the additional time required for calibration. Additionally, navigation systems can lead to reduced thermal damage and mouth opening requirements [14]. To minimize the additional time required for calibration and improve surgical proficiency, it is important to provide adequate training and support for the surgical team [15]. In contrast to navigation systems, surgical guides necessitate additional time for fabrication, which can be completed prior to the surgical procedure. Conversely, navigation systems offer the ability to deliver treatment in a single visit. The results showed that novice practitioners, in particular, may require more time to perform the surgery, regardless of the approach used, highlighting the importance of surgical skills and proficiency.

It was also found that novice surgeons had higher self-confidence with both guided approaches, while experienced surgeons were more confident with static guides. The use of navigation systems may be more beneficial for novice surgeons as it can provide them with an additional tool to learn and practice, and increase their confidence in performing dental implant procedures. Novice surgeons may also find it easier to learn the navigation system, as it can provide them with visual cues and real-time feedback, which can be more intuitive than traditional methods of training. However, experienced surgeons may prefer to continue using traditional methods, as they may not find the navigation systems necessary for their level of expertise, or may not feel comfortable with the additional time required for calibration. Additionally, it is important to note that navigation systems rely on technology and may fail or malfunction during the procedure, which can cause delays and increase the risk of errors. Improving the technology to make the tracking method even faster, robust and user-friendly could be an important step to enhance the application of navigation systems in dental implant surgery.

Surgical guides can be an effective tool in training novice surgeons for implant surgery by providing visual guidance, increasing precision and accuracy, and reducing potential errors. These guides offer the opportunity for novice surgeons to practice procedures in a controlled environment before performing them in real-life settings. However, it is important to note that surgical guides may not be suitable for all implant surgery procedures, particularly those with limited direct access or tight interdental spaces.

Overall, while both guided methods have their advantages and disadvantages, they should be used in conjunction with traditional surgical education methods to enhance the training process for novice surgeons. While guided techniques provide an additional tool for novice surgeons to learn and practice, traditional dental implant training methods remain essential for a comprehensive understanding and mastery of dental implant procedures.

AI has the potential to revolutionize the field of dentistry by improving the accuracy and efficiency of the segmentation process of CBCT and IOS data. Previous studies have demonstrated the ability of AI to accurately and efficiently identify regions of interest from CBCT data [16, 17]. The use of AI in the segmentation process has the potential to greatly optimize this process, particularly in the context of 3D printing. By automating the segmentation process, AI can save a significant amount of time compared to manual or semi-automated segmentation by human operators, where the segmentation process can be a very cumbersome and time-consuming task in the workflow of articles 2 to 5. AI algorithms can be trained to identify and segment specific structures with a high degree of accuracy and consistency. This can reduce the potential for human error and variability, which can be a significant problem in manual or semi-automated segmentation. Building an online platform that integrates data from multiple imaging modalities has the potential to create a digital virtual patient, which can aid in automatic anatomy detection, treatment planning, and surgical simulation. Tooth segmentation on IOS data is a crucial step in clinical applications such as implant planning, orthodontics, treatment monitoring, and diagnosis [18]. However, current state-of-the-art methods lack the robustness to handle human variability. **Article 6** aimed to design and validate the performance of a deep learning-based CNN model for automated tooth segmentation on IOS images. Our study was first to include a full set of permanent teeth, teeth with orthodontic brackets and partially edentulous dentition. A multi-step 3D U-Net pipeline was designed for automated tooth segmentation on IOS images and the 3D U-Net model was also deployed on an online cloud-based platform, where surgeons can refine the segmentation results of AI. The average time required for automated segmentation was 31.7±8.1s per jaw, which is significantly faster compared to manual segmentation on the software. The CNN model showed high performance of IOS segmentation with an IoU score of 91%. Additionally, the online cloud-based platform offers dental practitioners accurate, consistent and efficient segmentation results and provides tools for refinement if the AI segmentation results are not satisfactory. The presented CNN model for automated tooth segmentation showed high performance overall, but there are still challenges to be addressed, particularly with crowded teeth. To improve the algorithm, the plan is to introduce scans from different devices, as a way to increase the diversity of the data [19]. A robust AI platform can be achieved by utilizing a large and diverse dataset for training the model, while also protecting patient privacy through the implementation of encryption methods and federated learning. Encryption of patient medical data ensures confidentiality and security, while federated learning allows for the training of the model locally on devices, with only updates being shared to a central server [20, 21].

Conclusions

According to the report of a systematic review and meta-analysis presented in **article 1**, the accuracy of the maxillofacial skeletal models printed with desktop printers was comparable with that of professional printers. However, regardless of printer type, it was found that the printing technology, material, and layer resolution had an impact on the accuracy of the model. However, due to the results being based on a small number of investigations using various imaging and printing devices with varied settings, these findings should be interpreted with caution. As mentioned in **article 2,** we found that stereolithography and multi-jetting were able to replicate the skeletal anatomy on a medium- and high-cost printer, respectively, with the least amount of error, thereby confirming their applicability for clinical application, such as pre-bending plates and fabricating implants. Desktop/consumer grade FFF printer offered the highest discrepancy which might not be optimal for clinical applications, however, it could serve as a cost-effective alternative for surgical simulation, anatomical education, and/or patient communication. Based on the findings of **article 3**, the MJ-based model made with acrylic-based resin provided the best haptic feedback, which might be used as a standard for simulating dental implant surgery even though none of the models in this study were able to perfectly recreate the haptic perception of real bone. According to **article 4**, we have found that using a dynamic navigation system, novice surgeons were able to place dental implants with comparable accuracy and self-confidence to that of experienced surgeons. Regardless of the practitioner's level of experience, the navigation method provided a more accurate implant placement with a significant improvement in angular deviation compared to the pilot-drill surgical guide and freehand approach. **Article 5** showed that implant placement executed under the guidance of dynamic navigation showed high accuracy irrespective of the practitioner’s experience. The application of dynamic navigation could be regarded as a more beneficial approach for novices who were more confident of using the navigation system for implant placement and were able to perform the procedure at the same level of accuracy and time as that of experienced practitioners. **Article 6** of this thesis proposed 3D U-Net pipeline for automated tooth segmentation on IOS images and it outperformed the state-of-the-art methods with accurate, efficient and consistent results. Its clinically applicability is strengthened by the use of an online cloud-based platform for automated segmentation and interactive refinement.

Future perspectives

- The imaging and printing parameters need to be optimized, and the amount of error introduced at each stage of the printing process need to be assessed before the print can be qualified for medical-surgical applications.
- To print real bone-like structures, it is necessary to quantitatively analyze the mechanical characteristics of the printing material and the printer's capabilities. Future research should evaluate the capabilities of 3D printers for producing bone structures with various densities and evaluating the haptic feedback.
- Future clinical studies are required for the assessment of implant placement accuracy and efficacy for novice surgeons using navigation system in a clinical practice. There is a need to expand sample size and include other sites in both maxilla and mandible to assess its accuracy and performance of operators. Investigating the impact of half-guided and fully-guided approaches is essential in order to reach a better conclusion.
- Introducing a large and varied dataset via encryption or federated learning can help to strengthen the AI algorithm.

References

[1] E.D. Rekow, Digital dentistry: The new state of the art — Is it disruptive or destructive?, Dent. Mater. 36 (2020) 9–24.

[2] J. Asaumi, N. Kawai, Y. Honda, H. Shigehara, T. Wakasa, K. Kishi, Comparison of three-dimensional computed tomography with rapid prototype models in the management of coronoid hyperplasia, Dentomaxillofacial Radiol. 30 (2001) 330–335.

[3] R. Olszewski, Three-dimensional rapid prototyping models in cranio-maxillofacial surgery: systematic review and new clinical applications, 2013.

[4] M. Meglioli, A. Naveau, G.M. Macaluso, S. Catros, Correction to: 3D printed bone models in oral and craniomaxillofacial surgery: a systematic review, 3D Print. Med. 6 (2020) 1–19.

[5] S. Shujaat, E. Shaheen, F. Novillo, C. Politis, R. Jacobs, Accuracy of cone beam computed tomography–derived casts: A comparative study, J. Prosthet. Dent. (2020) 1–8.

[6] R. Ratinam, M. Quayle, J. Crock, M. Lazarus, Q. Fogg, P. McMenamin, Challenges in creating dissectible anatomical 3D prints for surgical teaching, J. Anat. 234 (2019) 419–437.

[7] T.S. Kashikar, T.F. Kerwin, A.C. Moberly, G.J. Wiet, A review of simulation applications in temporal bone surgery, Laryngoscope Investig. Otolaryngol. 4 (2019) 420–424.

[8] Z. Jin, Y. Li, K. Yu, L. Liu, J. Fu, X. Yao, A. Zhang, Y. He, 3D Printing of Physical Organ Models: Recent Developments and Challenges, Adv. Sci. 8 (2021).

[9] G. Pellegrino, A. Ferri, M. Del Fabbro, C. Prati, M.G. Gandolfi, C. Marchetti, Dynamic Navigation in Implant Dentistry: A Systematic Review and Meta-analysis., Int. J. Oral Maxillofac. Implants. 36 (2021) e121–e140.

[10] C. ILHAN, M. DIKMEN, E. YÜZBASIOGLU, Accuracy and efficiency of digital implant planning and guided implant surgery: An update and review, J. Exp. Clin. Med. 38 (2021) 148–156.

[11] J. Abduo, D. Lau, Duration, deviation and operator's perception of static computer assisted implant placements by inexperienced clinicians, Eur J Dent Educ. 00 (2021) 1–11.

[12] C.-K. Chen, D.-Y. Yuh, R.-Y. Huang, E. Fu, C.-F. Tsai, C.-Y. Chiang, Accuracy of Implant Placement with a Navigation System, a Laboratory Guide, and Freehand Drilling, Int. J. Oral Maxillofac. Implants. 33 (2018) 1213–1218.

[13] T.-M. Sun, H.-E. Lee, T.-H. Lan, Comparing Accuracy of Implant Installation with a Navigation System (NS), a Laboratory Guide (LG), NS with LG, and Freehand Drilling, Int J Environ Res Public Health. 17(2020) 2107.

[14] J. Golob Deeb, S. Bencharit, C.K. Carrico, M. Lukic, D. Hawkins, K. Rener-Sitar, G.R. Deeb, Exploring training dental implant placement using computer-guided implant navigation system for predoctoral students: A pilot study, Eur. J. Dent. Educ. 23 (2019) 415–423.

[15] N. Casap, S. Nadel, E. Tarazi, E.I. Weiss, Evaluation of a navigation system for dental implantation as a tool to train novice dental practitioners, J. Oral Maxillofac. Surg. 69 (2011) 2548–2556.

[16] F. Preda, N. Morgan, A. Van Gerven, F. Nogueira-reis, A. Smolders, X. Wang, S. Nomidis, E. Shaheen, H. Willems, Deep convolutional neural network-based automated segmentation of the

maxillofacial complex from cone-beam computed tomography: A validation study, J. Dent. 124 (2022) 104238.

[17] P.J. Verhelst, A. Smolders, T. Beznik, J. Meewis, A. Vandemeulebroucke, E. Shaheen, A. Van Gerven, H. Willems, C. Politis, R. Jacobs, Layered deep learning for automatic mandibular segmentation in cone-beam computed tomography, J. Dent. (2021).

[18] F. Mangano, A. Gandolfi, G. Luongo, S. Logozzo, Intraoral scanners in dentistry: A review of the current literature, BMC Oral Health. 17 (2017) 1–11.

[19] S. Kulkarni, N. Seneviratne, M.S. Baig, A.H.A. Khan, Artificial Intelligence in Medicine: Where Are We Now?, Acad. Radiol. 27 (2020) 62–70.

[20] Q. Yang, Y. Liu, T. Chen, Y. Tong, Federated Machine Learning: Concept and Applications, 10 (2019) 1–19.

[21] R. Rischke, L. Schneider, K. Müller, W. Samek, F. Schwendicke, J. Krois, Federated Learning in Dentistry: Chances and Challenges, J Dent Res. 101(2022) 1269-1273.

Summary

The use of digital technologies in the practice of dentistry can improve the accuracy and efficiency of dental procedures, and lead to better outcomes for patients. It allows for more precise and efficient treatment, better communication and collaboration between dentists, improved patient education and can be cost effective. Digital dentistry can include 3D printing, computer-assisted surgery, and artificial intelligence. The main objectives of this doctoral thesis were to provide clear view on how these digital technologies simplify the workflow in dental practice. It's important to weigh the potential benefits and drawbacks of digital dentistry before implementing it in a practice, and to consider the specific needs and resources of the practice and its patients.

3D printing has the potential to revolutionize the field of dentistry. However, the high price of 3D printing technology has hindered its widespread use. Therefore, in **article 1**, we systematically analyzed the accuracy of maxillofacial skeletal model generated from desktop and professional 3D printers. Based on the meta-analysis results, desktop printed models offered comparable mean absolute error (MAE) (0.12 mm) to professional printed models (0.10 mm). Regardless of printer type between desktop and professional printer, it was discovered that the printing technology and layer resolution might have an impact on the accuracy of the model. The lowest MAE was provided by material jetting (0.09 mm) and selective laser sintering (0.09 mm), whereas fused deposition modeling showed the greatest difference (0.22 mm). In comparison to models printed with a resolution of ≥0.2 mm, models with a layer resolution of 0.15 mm or less were found to be more accurate. The accuracy of 3D printed maxillofacial models is a complex issue that depends on various factors, including data acquisition, computer data processing, model fabrication, and post-processing. A dimensional deviation of up to 2% discrepancy has been identified as the clinically acceptable accuracy for 3D printed skeletal models. However, the accuracy of a model should depend on its area of application. On the basis of these findings, **in article 2**, we were the first to assess the efficacy and accuracy of CBCT-derived skull models fabricated by 3D printers at different cost levels using the 3D evaluation analysis. We found that stereolithography and multi-jetting were able to replicate the skeletal anatomy on a medium- and high-cost printer, respectively, with the least amount of error, thereby confirming their applicability for clinical application, such as pre-bending plates and fabricating implants. Desktop/consumer grade FFF printer offered the highest discrepancy which might not be optimal for clinical applications, however, it could serve as a cost-effective alternative for surgical simulation, anatomical education, and/or patient communication. It is important to note that the study was limited to a small sample of three printers with different technologies and materials, and

therefore cannot be generalized to all printers. The advancement of 3D printing technology has greatly improved the accuracy and realism of patient-specific skeletal models; however, it is uncertain if these models provide optimal haptic feedback for dental implant hands-on training. The study in **article 3** is the first to print trabecular mandibular bone from patient's CBCT, and 6 different printers and materials were used for model fabrication. Based on the surgeon's subjective evaluation, model MJ (acrylic-based resin) offered the highest score, followed by model SLA (acrylic-based resin), model FFF1 (polycarbonate filament), model DLP (acrylic-based resin), model FFF2 (polylactic acid filament), whereas model SLS (polyamide filament) scored the lowest. However, none of the models in this study were able to perfectly recreate the haptic perception of real bone. The results have shown that the haptic feedback of the printed model is highly dependent on the mechanical properties of the material, 3D printer, and printer settings, highlighting the importance of understanding the relationship between the 3D-printed models and the haptic feedback. The MJ-based model made with acrylic-based resin provided the best haptic feedback, which might be used as a standard for simulating dental implant surgery. In **article 4** and **article 5,** we utilized the protocol outlined in article 3 to design training models for training novice surgeons using computer-assisted surgery. It is believed that computer-assisted technologies, such as navigation and surgical guides, can help to improve the accuracy of procedures for surgeons of varying experience levels. Following this, our study was the first to evaluate whether guided approaches can enhance novice surgeons' surgical performance, where the performance of experienced surgeons serve as a clinical reference. According to **article 4**, we have found that using a dynamic navigation system, novice surgeons were able to place dental implants with comparable accuracy and self-confidence to that of experienced surgeons. Regardless of the practitioner's level of experience, the navigation method provided a more accurate implant placement with a significant improvement in angular deviation compared to the pilot-drill surgical guide and freehand approach. **Article 5** showed that implant placement executed under the guidance of dynamic navigation showed high accuracy irrespective of the practitioner's experience. The application of dynamic navigation could be regarded as a more beneficial approach for novices who were more confident of using the navigation system for implant placement and were able to perform the procedure at the same level of accuracy and time as that of experienced practitioners. **Article 6** of this thesis proposed 3D U-Net pipeline for automated tooth segmentation on IOS images and it outperformed the state-of-the-art methods with accurate, efficient and consistent results. Its clinically applicability is strengthened by the use of an online cloud-based platform for automated segmentation and interactive refinement.

The integration of digital technologies in dental treatment, surgical training, and education has been shown to enhance accuracy and efficiency. However, it is crucial to carefully consider the potential benefits and drawbacks before implementing these technologies in a practice, taking into account the unique needs and resources of both the practice and its patients.

Scientific acknowledgements

The China Scholarship Council (CSC) supported the author of this thesis. This work would not successfully reach its completion without the commitment from other contributors, whom I would like to extend my gratitude.

Article 1: XW: conceptualization, formal analysis, methodology, data curation, investigation, writing - original draft, visualization. SS: conceptualization, formal analysis, methodology, investigation, writing - review & editing. ES: supervision, visualization, writing - review & editing. RJ: supervision, project administration, writing - review & editing.

Article 2: XW, SS and EF: Conceived the ideas and design of study. XW, SS and ES: Acquisition of data. XW and SS: Analysis of data. XW, SS, ES and EF: Drafting of article and/or critical revision

Article 3: XW: data collection, data and analysis tools, writing the paper. RJ: conceptualization, revision. ES: data collection, revision. SS: data and analysis tools, writing the paper.

Article 4: RJ: conceived the ideas. XW, ES, SS, JM and PL and designed the study; XW, ES, JM and PL collected the data; XW, SS, JM, PL, PL and MG contributed data; XW drafted the paper; SS, CP, RJ, ES and PL revised it.

Article 5: RJ: conceived the ideas. XW, SS, JM, ES and PL designed the study. XW, ES, JM and PL collected the data. XW, S, J M, PL, PL and MG contributed data. XW drafted the paper. SS, RJ, ES and PL revised it.

Article 6: XW: conception, design, data acquisition and interpretation, analysis, drafted and critically revised the manuscript. KA: conception, design, data acquisition and critically revised the manuscript. TB: design, data acquisition and critically revised the manuscript. SS: critically revised the manuscript. RJ, ES: conception, design, and critically revised the manuscript.

I would like to thank Prof. dr. Paul Legrand and Dr. Jan Meeus for the help to design and develop the protocols in Article 3-5, without their expertise the completion of these projects would not have been possible. Thanks to the efforts of ReLu team (Adriaan Van Gerven, Jaron Maene, and Holger Willems) for providing computing resources and aiding in the development and training of the relevant networks in Article 6. I would like to thank Ming Wu for the cover and figure design and manuscript revision in Article 2 and 6. A special thanks to Wim Coucke, who provided us help for statistical analysis. Lastly, I would like to sincerely acknowledge my Promoter Prof. dr. Reinhilde Jacobs and both my co-promoters, Dr. Eman Shaheen and Dr. Sohaib Shujaat for their scientific support and contributions throughout the duration of the PhD.

Personal contribution

The author, Xiaotong Wang, conceived the projects, collected data, performed the experiments, and wrote the research publications with the scientific support of her promoter Prof. dr. Reinhilde Jacobs and co-promotors, Dr. Eman Shaheen and Dr. Sohaib Shujaat. Xiaotong Wang is the first author of all the thesis chapters and associated research papers.

Conflict of interest

The authors declare no conflicts of interest concerning the publications of this work.

Curriculum vitae

Xiaotong Wang (王晓彤)

Born on May 9th, 1991, in Harbin, China

Education

- 2019-2023 — Ph.D candidate **OMFS-IMPATH research group, Faculty of Medicine, Katholieke Universiteit Leuven, Belgium**
- 2010-2018 — Bachelor and Master's degrees **Faculty of Dentistry, Harbin Medical University, China**

Experience

- 2018-2019 — **Resident doctor**
  First Affiliated Hospital of Harbin Medical University
  Work at department of oral and maxillofacial surgery to perform surgery, treatment in outpatient clinics and emergency.

- 2015-2018 — **Clinical postgraduate and trainee of resident doctor**
  First Affiliated Hospital of Harbin Medical University
  Conducted a three-year residency training in the Oral & Maxillofacial Surgery department.

- 2013-2015 — **Trainee**
  First Affiliated Hospital of Harbin Medical University
  Received medical practice in various departments to learn the basic operation techniques of stomatology.

Publications

Publications part of the PhD thesis:

- **Wang X**, Shujaat S, Shaheen E, Jacobs R. Accuracy of desktop versus professional 3D printers for maxillofacial model production. A systematic review and meta-analysis. J Dent. 2021 Sep;112:103741. doi: 10.1016/j.jdent.2021.103741.

- **Wang X**, Shujaat S, Shaheen E, E Ferraris, Jacobs R. Trueness of cone-beam computed tomography-derived skull models fabricated by different technology-based three-dimensional printers. BMC Oral Health. (Accepted)

- **Wang X**, Shujaat S, Shaheen E, Jacobs R. Quality and haptic feedback of three-dimensionally printed models for simulating dental implant surgery. J Prosthet Dent. 2022 May;S0022-3913(22)00201-3. doi: 10.1016/j.prosdent.2022.02.027.

- **Wang X**, Shaheen E, Shujaat S, Meeus J, Legrand P, Lahoud P, Gerhardt M, Politis C, Jacobs R. Influence of experience on dental implant placement. An in vitro comparison of freehand, static guided and dynamic navigation approaches. Int. J. Implant Dent. 2022 Oct;8(1):42. doi: 10.1186/s40729-022-00441-3.

- **Wang X**, Shujaat S, Meeus J, Shaheen E, Legrand P, Lahoud P, Gerhardt M, Jacobs R. Performance of novice versus experienced surgeons for dental implant placement with freehand, static guided and dynamic navigation approaches. Sci Rep. 2023 Feb;13(1):2598.

- **Wang X**, Alqahtani K, Bogaert T, Shujaat S, Jacobs R, Shaheen E. Convolutional neural network for automated tooth segmentation on intraoral scans. Clin. Oral Investig. (Accepted)

Other publications in the field:

- Shen Y, **Wang X**, Su L, Jiao X, Fan X, Wang D. An ulcer arising in a postoperative scar of a labial capillary malformation. Oral Dis. 2023 Mar 29(3): 859-861.
- Preda F, Morgan N, Gerven A Van, Nogueira-reis F, Smolders A, **Wang X**, Nomidis S, Shaheen E, Willems H, Jacobs R. Deep convolutional neural network-based automated segmentation of the

maxillofacial complex from cone-beam computed tomography: A validation study. J Dent; 2022 Sep;124:104238.

- Gao Y, Zang Q, Song H, Fu S, Sun W, Zhang W, **Wang X**, Li Y, Jiao X. Comprehensive analysis of differentially expressed profiles of non-coding RNAs in peripheral blood and ceRNA regulatory networks in non-syndromic orofacial clefts. Mol Med Rep. 2019 Jul; 20(1):513-528.

- Zhang W, Zhou S, Gao Y, Song H, Jiao X, **Wang X**, Li Y. Alterations in DNA methyltransferases and methyl-CpG binding domain proteins during cleft palate formation as induced by 2,3,7,8 tetrachlorodibenzo-p-dioxin in mice. Mol Med Rep. 2018 Apr;17(4):5396-5401.

- **Wang X**, Song H, Jiao X, Hao Y, Zhang W, Gao Y, Li Y, Mi N, Yan J. Association between a single-nucleotide polymorphism in the GREM1 gene and non-syndromic orofacial cleft in the Chinese population. J Oral Pathol Med. 2018. Feb;47(2):206-210.

- Song H, **Wang X**, Yan J, Mi N, Jiao X, Hao Y, Zhang W, Gao Y. Association of single-nucleotide polymorphisms of CDH1 with nonsyndromic cleft lip with or without cleft palate in a northern Chinese Han population. Medicine. 2017 Feb;96(5):e5574.

Contributions to international conferences

- **Presentation, "Efficacy of cone-beam computed tomography-derived skull models fabricated by three-dimensional printers at different cost levels", IADMFR World Tour Congress 2023**
  Brussels, Belgium - July 5th-8th 2023

- **Poster, "Deep learning-based automatic tooth segmentation on intraoral scans", 4th Digital Dentistry Society conference**
  Rhodes, Greece - Oct 14th-15th 2022

- **E-Poster, "Quality and haptic feedback of 3D printed models for simulating dental implant surgery", European Association of Osseointegration Digital Days 2021**
  Online congress - Oct 12th-14th 2021

Xiaotong Wang achieved her Bachelor and Master of dental medicine from Harbin Medical University, China (2010-2018). From June 2018 till August 2019, she worked as a resident doctor in the department of Oral and Maxillofacial Surgery at First Affiliated Hospital of Harbin Medical University. She was a PhD researcher under the supervision of Prof. Reinhilde Jacobs in the OMFS-IMPATH research group, KU Leuven, Belgium (2019-2023).

The use of digital technologies in the practice of dentistry can improve the accuracy and efficiency of dental procedures, and lead to better outcomes for patients. This doctoral thesis aimed to study the impact of digital technologies on dentistry and to explore how digital dentistry can simplify the workflow through the use of 3D modeling and AI assistance.

The outcome of this thesis could allow dental treatment, surgical training, and education with the integration of digital technologies to achieve enhanced accuracy and efficiency. However, it is crucial to carefully consider the potential benefits and drawbacks before implementing these technologies in practice, taking into account the unique needs and resources of both the practice and its patients.

OMFS IMPATH

KU LEUVEN